

GeoMEC-4P Geothermal Energy Brielle

31 January 2012

GeoMEC-4P Geothermal Energy Brielle

PanTerra G945

Authors

Annelies Bender

Reviewed by

Andrew van de Weerd

Pieter van den Heuvel

Prepared for

GeoMEC-4P

T.a.v. Mr. M. Oerlemans

Minervum 7181

4817 ZN, Breda

Prepared by

PanTerra Geoconsultants B.V.

Weversbaan 1-3

2352 BZ Leiderdorp

The Netherlands

T +31 (0)71 581 35 05

F +31 (0)71 301 08 02

info@panterra.nl

This report contains analysis opinions or interpretations which are based on observations and materials supplied by the client to whom, and for whose exclusive and confidential use, this report is made. The interpretations or opinions expressed represent the best judgement of PanTerra Geoconsultants B.V. (all errors and omissions excepted). PanTerra Geoconsultants B.V. and its officers and employees, assume no responsibility and make no warranty or representations, as to the productivity, proper operations, or profitableness of any oil, gas, water or other mineral well or sand in connection which such report is used or relied upon.

Executive summary

The geothermal exploration licenses Vierpolders and Brielle-2 have been granted to GeoMEC-4P and GeoMEC-4P has asked PanTerra Geoconsultants to investigate the geology of the Brielle area for geothermal purposes. The study area is located in the southern fringe area of the West Netherlands Basin. Target reservoir sandstones are the lower Triassic Main Buntsandstein sediments. This report is written in order to apply for the 'Subsidieregeling energie en innovatie, Risico's dekken voor Aardwarmte' of the Dutch government and is in line with the report-requirements for the application.

- **Data**

For the seismic interpretation one 3D survey and 30 2D lines have been used. In order to obtain optimal results, only migrated 2D seismic data has been used. Migration is important for the correct identification and location of faults and dipping horizons. All available wells that have been drilled into the Triassic in the southern part of the West Netherlands basin are used for this study. The HVS-01 well is located within the geothermal licenses and is of key importance for this geological study. Other important wells are RZB-01, SPKW-01, BTL-01 and MSV-01 due to their vicinity to the study area.

- **Seismic, depth and thickness**

Calibrated checkshot data and synthetic seismograms were used for reflector identification of the base Tertiary, base Chalk, Posidonia Shale, top Triassic, top Lower Detfurth sandstone and the Base Permian Unconformity. The 3D seismic was interpreted first. The solid interpretation on the 3D seismic significantly contributes to a good interpretation on the 2D seismic. Both the top of the Triassic and the base of the Permian are clearly recognised on seismic as angular unconformities. The sound interpretation of the Base Permian unconformity in combination with the mapped top of the Lower Detfurth Sandstone is important for the delineation and thickness estimate of the Main Buntsandstein reservoir.

The seismic interpretation has been converted to depth using a velocity model based on constant interval velocity maps. The depth of the top of the Main Buntsandstein reservoir within the geothermal licenses Vierpolders and Brielle-2 varies between 1975 and 2275 m. The top of the aquifer in the proposed producer is at 2191 m depth and in the proposed injector at 2045 m depth. The determined total thickness of the Main Buntsandstein in the Brielle area is 182 m. In the study area, the Houthem Formation occurs on top of the Ommelanden Chalk. The Houthem formation consists of chalk as well and is important for the casing scheme.

- **Temperature**

In order to determine a suitable temperature gradient for the Brielle area, borehole temperature data (BHT) from HVS-01, RZB-01 and SPKW-01 were corrected for circulation time. The variation between the temperature gradients in these wells is large. The preferred method is to use a combination of the corrected BHT data. This gives a gradient of $T = 0.0314 * D + 10$ (T= temperature in °C and D= depths in meters). The expected temperature in the middle of the reservoir in the proposed producer (2292 m) is expected to be 82°C. Uncertainty in the depth maps is set at 10%. Minimum temperature in the middle of the reservoir in the proposed producer is therefore 75°C and maximum temperature is 89°C.

- **Petrophysics**

Porosity, permeability and Net/Gross ratio of the reservoir have been calculated for ten wells. These wells were selected based on vicinity to the study area and availability of data necessary for petrophysical evaluation (core and wireline data). Core measurements have been used to determine porosity-permeability relations. The results of the petrophysical evaluation have been used to determine the reservoir quality in the study area. The reservoir quality is expected to be good, with a median estimated porosity of 19.8%, permeability of 730 mD and N/G of 91%.

- **Well proposal**

A geothermal doublet, with a producer (BRI-GT-01) and an injector (BRI-GT-01) has been planned. For this doublet, flow rate calculations have been performed over the Main Buntsandstein interval with use of Doublet Calculator. The resulting P50 flow rate is 282.7 m³/h resulting in a return of 9.35 MW geothermal power. The breakthrough time is modelled with the software package Petrasim. After 30 years the temperature will have decreased 0.05 °C. A preliminary well scheme has been designed by Well Engineering Partners.

- **Uncertainties**

Uncertainties with respect to depth, thickness, temperature and reservoir quality are evaluated.

- Seismic coverage by 2D lines is good and the fact that the area is close to the 3D survey L3NAM1990C allows a reliable interpretation and reduces the uncertainty of the seismic interpretation. A depth uncertainty of 10% is applied.
- The uncertainty with regard to the presence and the thickness of the sandstones in the proposed wells is considered low due to the short distance from the HVS-01 well and the continuous character of the Main Buntsandstein sediments. A thickness range of ± 15 m is applied.
- Uncertainty in the mapping of major faults is low due to the use of 3D seismic and migrated 2D seismic.
- The vicinity of the planned wells to the HVS-01 well significantly reduces the uncertainty in reservoir quality. The range of Net/Gross values is 88-93%. Uncertainty of the calculated permeability is high. A range of 210 mD to 3555 mD is used in the flow rate calculation.
- Uncertainty in the temperature estimate in the study area is related to availability of temperature data from existing wells and corrections applied to borehole temperature data. Uncertainty in the depth maps is set at 10%. Minimum temperature in the middle of the reservoir in the proposed producer is 75°C and maximum temperature is 89°C

- **Risk assessment**

The risks associated with the planned doublet have been assessed. Risk of swelling clays exists in the Tertiary and the Vlieland. Mud losses may occur in the Chalk formation. The wells are planned > 750 m from the major faults. Major faults are assumed not to be open, probably cemented and hampering fluid flow. Sub seismic faults may be present. The chance of finding a hydrocarbon accumulation is considered small and estimated at 1%. The chance of finding residual and/or dissolved gas in the formation water of the sandy intervals is large, estimated at 80%. However, the amounts are difficult to estimate. The risk of presence of oil is estimated at 1-2%. H₂S will be absent. CO₂ and N₂ may be present with amounts <1.5 % each. The formations that will be encountered by the proposed producer and injector are not expected to be overpressured.

Contents

Executive summary	v
1 Introduction	9
1.1 Introduction	9
1.2 Sequence of events	10
1.3 Geological setting	10
1.3.1 The West Netherlands Basin	10
1.3.2 The Brielle area	11
2 Available data and software	14
2.1 Coordinate system and Units system	14
2.2 Seismic data	14
2.3 Well data	16
2.4 Stratigraphy	18
2.5 Additional data	19
2.6 Database	19
3 Seismic interpretation	20
3.1 Reflector identification and seismic interpretation	20
3.2 Time maps	25
3.3 Velocity model	26
3.4 Depth maps	28
3.5 Thickness	32
4 Petrophysical interpretation	35
4.1 Core analysis	35
4.2 Log analysis	38
4.2.1 Volume of Clay	38
4.2.2 Effective porosity	39
4.2.3 Permeability	40
4.2.4 Averages	42
4.3 Salinity	43
4.4 Temperature	43
5 Geothermal doublet	46
5.1 Proposed well configuration	46
5.2 Flow rate calculation	53
5.3 Geological uncertainties	58
5.4 Risk assessment	59
6 Conclusions	62
7 References	64
8 Appendices	65
8.1 Appendix 1: Seismic surveys	65

8.2	Appendix 2: Synthetic Seismograms	68
8.3	Appendix 3: Additional Time Maps	72
8.4	Appendix 4: Petrophysics	75
8.5	Appendix 5: Temperature	76
8.6	Appendix 6: Well correlation panel	78
8.7	Appendix 7: Well configuration	79
8.8	Appendix 8: Flow rate results	81
8.9	Appendix 9: Schematic sketch of the proposed doublet by Well Engineering Partners	84

1 Introduction

1.1 Introduction

GeoMEC-4P has asked PanTerra Geoconsultants to investigate the geology of the Brielle area for the planning of a geothermal doublet. The geothermal exploration licenses Vierpolders and Brielle-2 have been granted to GeoMEC-4P. The outline of the licenses is shown in Figure 1-1. Target reservoir sandstones are part of the lower Triassic Main Buntsandstein. An overview of the geological setting and a general description of the reservoir are given in Chapter 1.3. The objective of this study is to determine the depth, thickness and temperature of the Triassic reservoir units and their petrophysical properties in the Brielle area. In addition, a geothermal doublet is planned within the exploration licenses and the expected flow rate is calculated.

This report is written in order to apply for the 'Subsidiereregeling energie en innovatie, Risico's dekken voor Aardwarmte' of the Dutch government. In line with the report-requirements for the application this report consists of the following chapters:

A) Seismic interpretation

Available seismic data is listed in Chapter 2.2 and the seismic interpretation and time-depth conversion are discussed in Chapter 3.1 to 3.3.

B) Depth maps

Depth maps are given in Chapter 3.4 and Chapter 3.5.

C) Wells

The available data for the wells that are used for this study is given in Chapter 2.3. Table 2-2 gives an overview of the data that was used for the various parts of this study. Petrophysical results are discussed in Chapter 4.

D) Doublet Calc input and results

The proposed producer and injector and the flow rate are discussed in Chapter 5.

E) Schematic sketch of the proposed wells

A schematic sketch of the proposed doublet is given in Appendix 8.9.

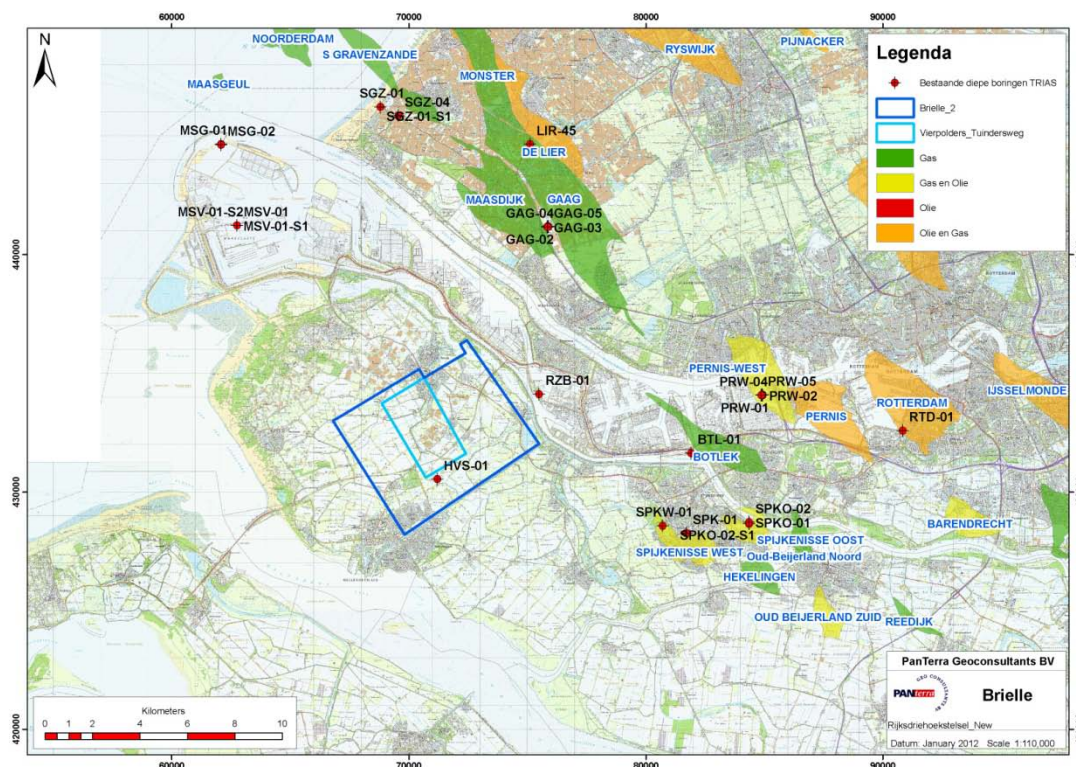


Figure 1-1 Location map of the study area. The geothermal exploration licenses Vierpolders and Brielle-2 are shown in blue. Existing wells and oil and gas fields are shown as well.

1.2 Sequence of events

- The quote for the project was issued on November 18th, 2011.
- The project was officially assigned to PanTerra Geoconsultants on December 7th, 2011.
- 2D seismic data was received from TNO on November 28th after which the 2D seismic was digitized and migrated by Fugro and received back again on December 7th, 2011.
- Draft versions of the report were sent to GeoMEC-4P on January 18th and January 23rd.
- The final report is sent to GeoMEC-4P on January 31st 2012.

1.3 Geological setting

1.3.1 The West Netherlands Basin

The deep subsurface below the area of investigation is part of the southern basin fringe area of the West Netherlands Basin (WNB). A structural cross-section of the Netherlands is shown in Figure 1-3. The age of the sediments in the basin varies between Carboniferous (>300 million years) to recent. The geological history of the basin is complex. During the Early Triassic, the basin deepened in northward direction. The northern part was later uplifted. After a minor deformation phase during Late Triassic, a period of strong subsidence followed from Jurassic to Cretaceous times. This strong subsidence stopped during deposition of the Rijnland Group (Early Cretaceous). Deposition of the Rijnland Group and the older Schieland Group sediments occurred in grabens whereas erosion took place on the structural highs. The basin was inverted during Late Cretaceous and Tertiary times. This resulted in fault reactivation with strike-slip and oblique-slip movements. Some fault blocks were uplifted and eroded.

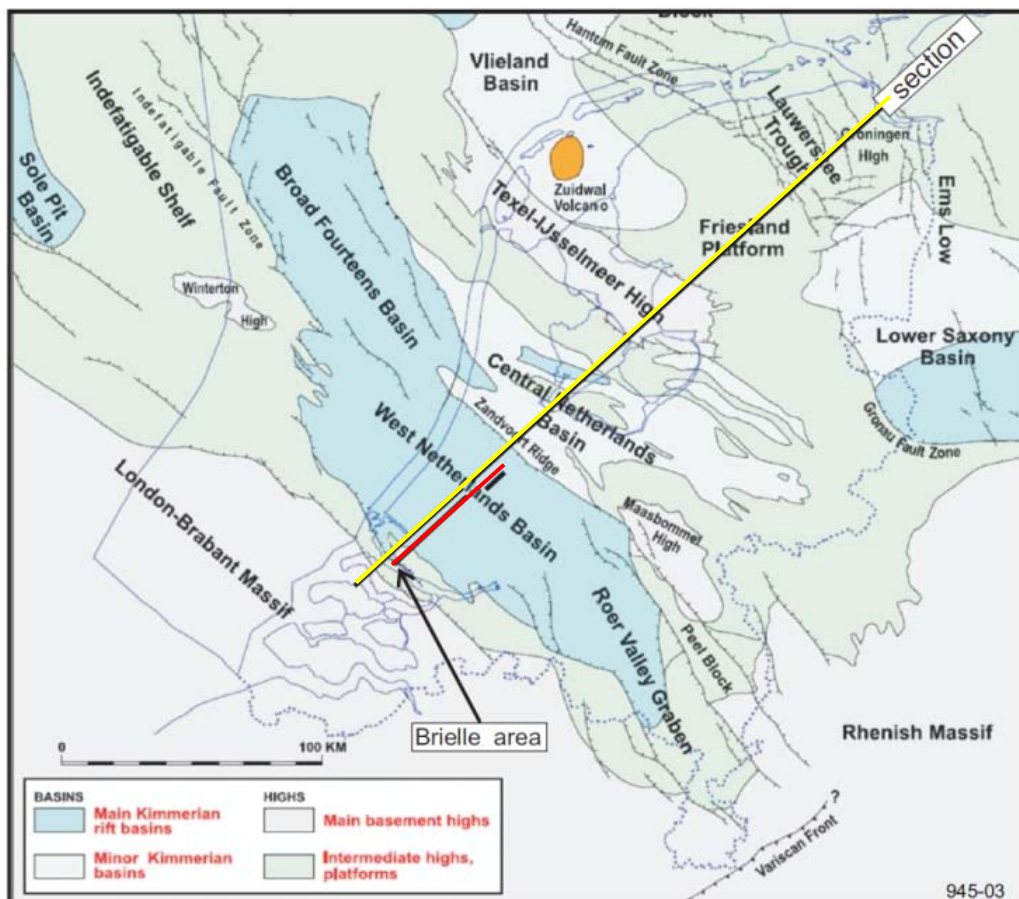


Figure 1-2 Structural map of the Netherlands. The yellow line is the cross-section in Figure 1-3 and the red line is the cross-section in Figure 1-4 (Geology of the Netherlands, 2007).

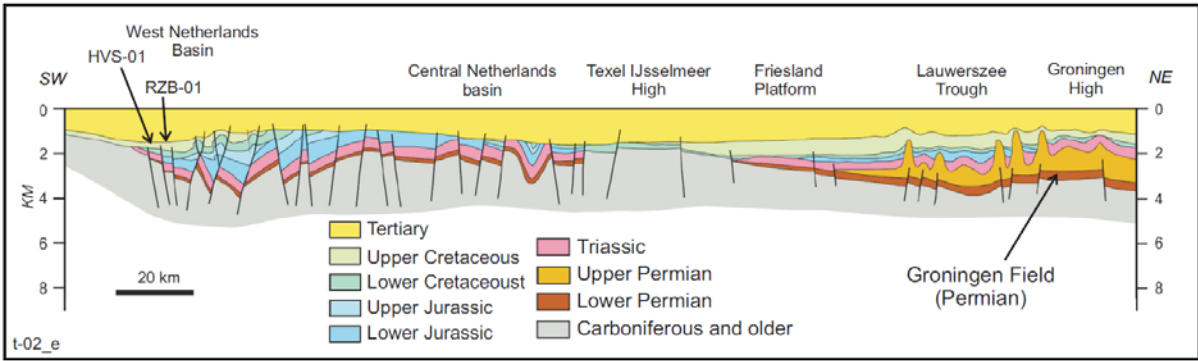


Figure 1-3 Structural cross-section of the Netherlands from southwest to northeast. The line is shown in yellow on the map in Figure 1-2. The study area is near the HVS-01 and RZB-01 wells, which are shown at the southern flank of the basin next to the London Brabant Massif (Geology of the Netherlands, 2007).

1.3.2 The Brielle area

The Brielle area is located over a fault-block (the ‘Brielle fault-block’) at the southern fringe of the WNB (Figure 1-3 and Figure 1-4). Due to its location at the southern fringe of the basin the stratigraphy is different from that of areas in the WNB to the north. Many formations are missing and formations are thinner in the ‘Brielle block’. This is illustrated in Figure 1-5, where the stratigraphy in the HVS-01 well is compared to the stratigraphy in P-18. In the fault block just to the north of HVS-01 (with the well Rozenburg-01) most of the missing formations are present (see Figure 1-4). The boundary-fault between the two blocks is below the northern tip of the Vierpolders geothermal license.

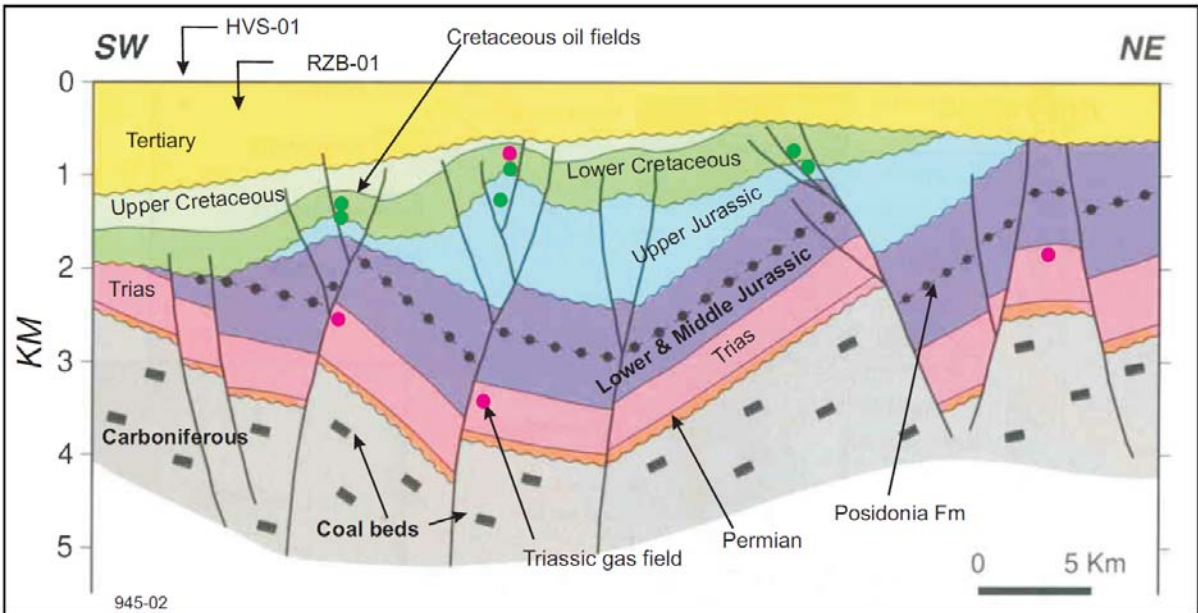


Figure 1-4 Structural cross-section through the West Netherlands Basin. The line is shown in red on the map in Figure 1-2. The fault blocks in which HVS-01 and RZB-01 were drilled are indicated by arrows. (Rondeel et al, 1996).

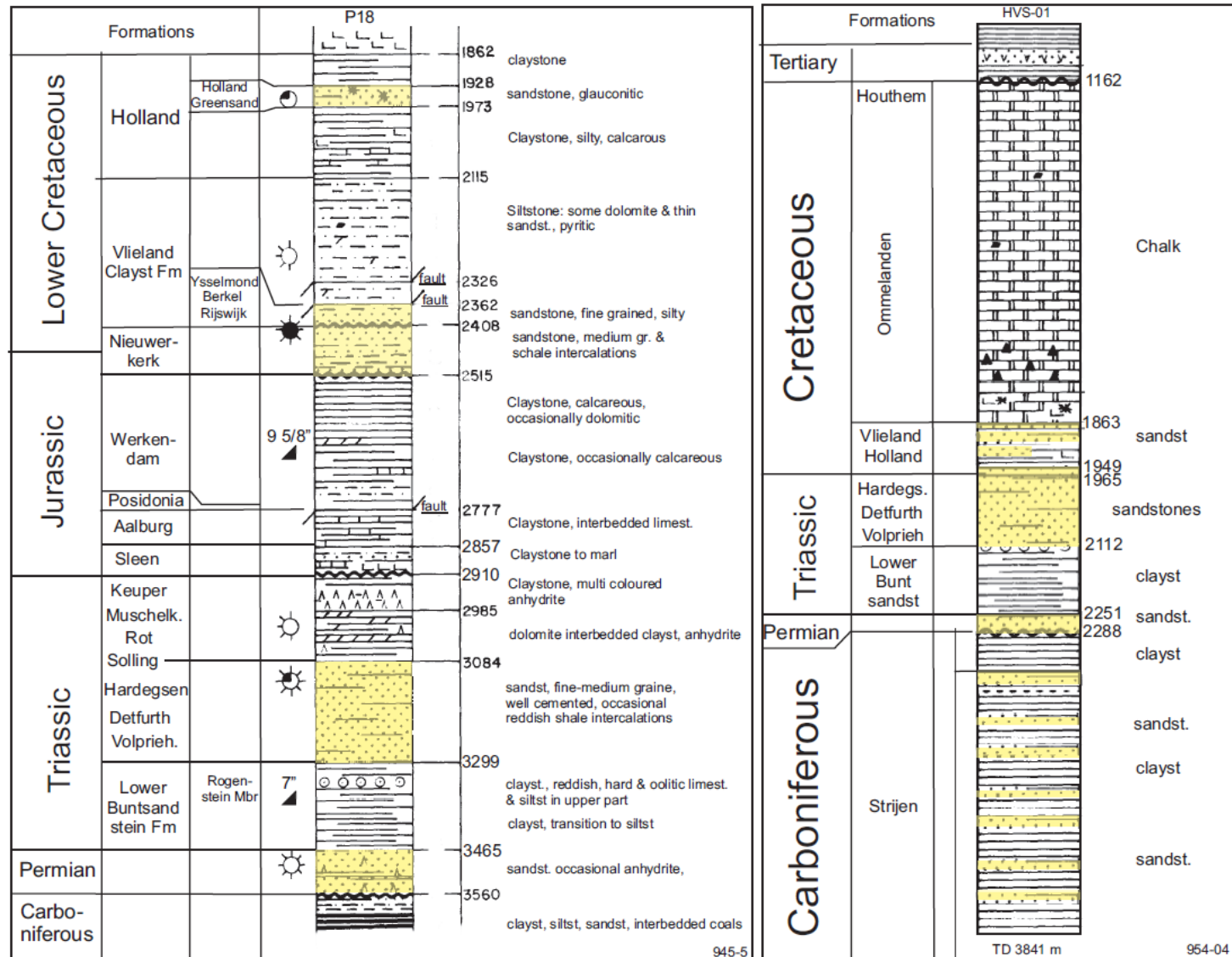


Figure 1-5 Stratigraphy of the P18 well (left) and the HVS-01 well (right). The Lower Cretaceous, the Jurassic and the upper Triassic are not present in the HVS-01 well.

The Triassic deposits lie conformably on top of Zechstein Group sediments from the Permian. The Triassic in the Netherlands is at places very thick and has been subdivided into many formations. In general the lower part is non-marine, while the upper part consists of shallow-marine and lagoonal sediments, including thick evaporates. A thick fluvial sand-rich unit (formally named the Main Buntsandstein Subgroup) is an important gas reservoir in the Netherlands. The Triassic is well described and reference is made to the 'Triassic' chapter in the *Geology of the Netherlands (2007)* and *De Ondergrond van Nederland (2003)*. Uplift and subsequent erosion before deposition of the Solling formation have strongly influenced the thickness of the Buntsandstein (Figure 1-6).

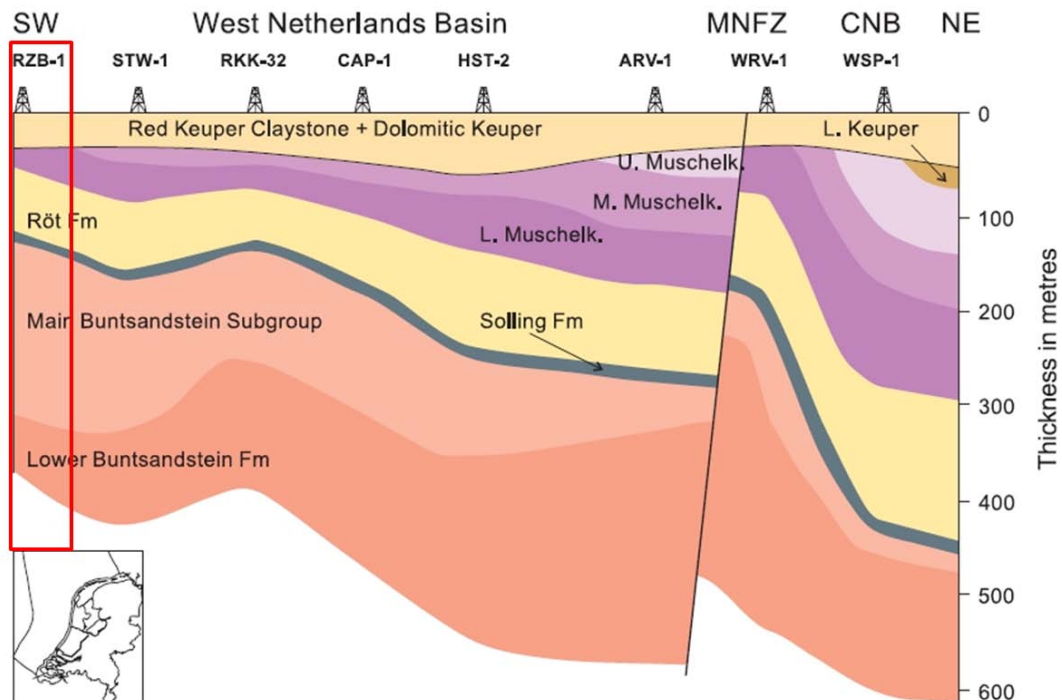


Figure 1-6 Southwest-northeast cross-section of the Triassic in the West Netherlands Basin. In northward direction the base of the Solling formation progressively cuts deeper into the Main Buntsandstein Subgroup (*Geology of the Netherlands, 2007*). The study area, indicated by the red rectangle, is located at the southern basin fringe of the West Netherlands Basin.

In Brielle the sand-rich Main Buntsandstein is well developed and consists of porous sands. Slightly to the north in the WNB in Rozenburg and further north in the Gaag and Rotterdam fields, three formations can be recognized in the Main Buntsandstein. From bottom to top these are: the Volpriehausen, Detfurth and Hardeggen Formations. The Hardeggen sandstone is of aeolian and fluvial facies, the Volpriehausen and Detfurth are fluvial deposits. In particular the Hardeggen is a good reservoir. In the Brielle area these formations consists of stacked sandstones and all three formations are good reservoirs. The upper part of the Triassic sands in the 'Brielle block' may consist of some sands in the Solling and the Röt Formations. This is followed by a major unconformity marking the top of the Triassic.

The Jurassic in the West Netherlands Basin is thick. In the Rozenburg block and further north a thick section of Lower-Middle Jurassic shales (including the Posidonia Formation) and Upper Jurassic-Lower Cretaceous shales and sands are present. The Jurassic is absent in the 'Brielle block' (Figure 1-5) and here the Triassic sands are directly overlain by the "middle" Cretaceous sands. Similar to P-18 (Figure 1-5) the Cretaceous section in the Rozenburg block is more complete with presence of Lower Cretaceous and Upper Cretaceous.

2 Available data and software

2.1 Coordinate system and Units system

The location data of most data is in the new Netherlands National Triangulation System (Rijksdriehoekstelsel). Location data of different projection systems were converted to this system.

Name:	Netherlands National System new: (Rijksdriehoekstelsel new)
Type:	Double Stereographic
Central Meridian:	5.387638889
Origin Latitude:	52.156160556
Scale Factor:	0.999907900
False Northing:	463000.000000
False Easting:	155000.000000

Units: Metres

Datum: Amersfoort

Ellipsoid: Bessel 1841

Prime Meridian: Greenwich

Transform Method: Molodensky

Delta x (m): 593

Delta y (m): 26

Delta z (m): 478

The units used in this report are based on the units used in the International System of Units (abbreviated SI from the French *Système International*). All distances are expressed in metres c.q. kilometres. Temperatures are expressed in degrees Celsius.

2.2 Seismic data

For this study one 3D seismic survey and eight 2D seismic surveys were obtained from TNO through the DINO-loket (www.nlog.nl). The eight 2D seismic surveys contain thirty 2D lines in total. Figure 2-1 shows the location of the seismic data used for this study. Eighteen lines were shot after 1970 and are shown in green and twelve lines were shot before 1970 and are shown in red. A map showing the lines and their names is given in Appendix 8.1.

The available 3D survey is L3NAM1990C. Acquisition took place in 1990 and was commissioned by the NAM. The coordinates of this survey are Rijksdriehoekstelsel coordinates, which were preloaded in the segy file. The L3NAM1990C survey has been shifted down 50 ms in vertical direction, in order to make sure that the earth's surface is set at $t = 0$ (s). The dominant frequency is about 40 Hz, which is enough to be able to distinguish important seismic markers. The quality of the 3D seismic is generally good. An overview of the processing parameters of this survey is found in Appendix 8.1. The polarity of the 3D seismic is reversed SEG. This means that an increase in impedance is recorded as an increase in pressure (hydrophone) or an upward movement (geophone) and is measured as a negative value.

An overview of the used 2D surveys and lines is shown in Table 2-1. Acquisition took place between 1957 and 1985 and was commissioned by the NAM and by Amoco. Digitisation of the tiff files and post-stack migration of the 2D seismic data has been carried out for PanTerra by Fugro. Migration is important for the correct identification and location of faults and dipping horizons. The coordinates of the lines are Rijksdriehoekstelsel coordinates. The polarity of the 2D data varies per line. The 3D survey L3NAM1990C is used as reference to apply necessary polarity and static shifts to the 2D seismic lines. Specific shifts are listed in Appendix 8.1.

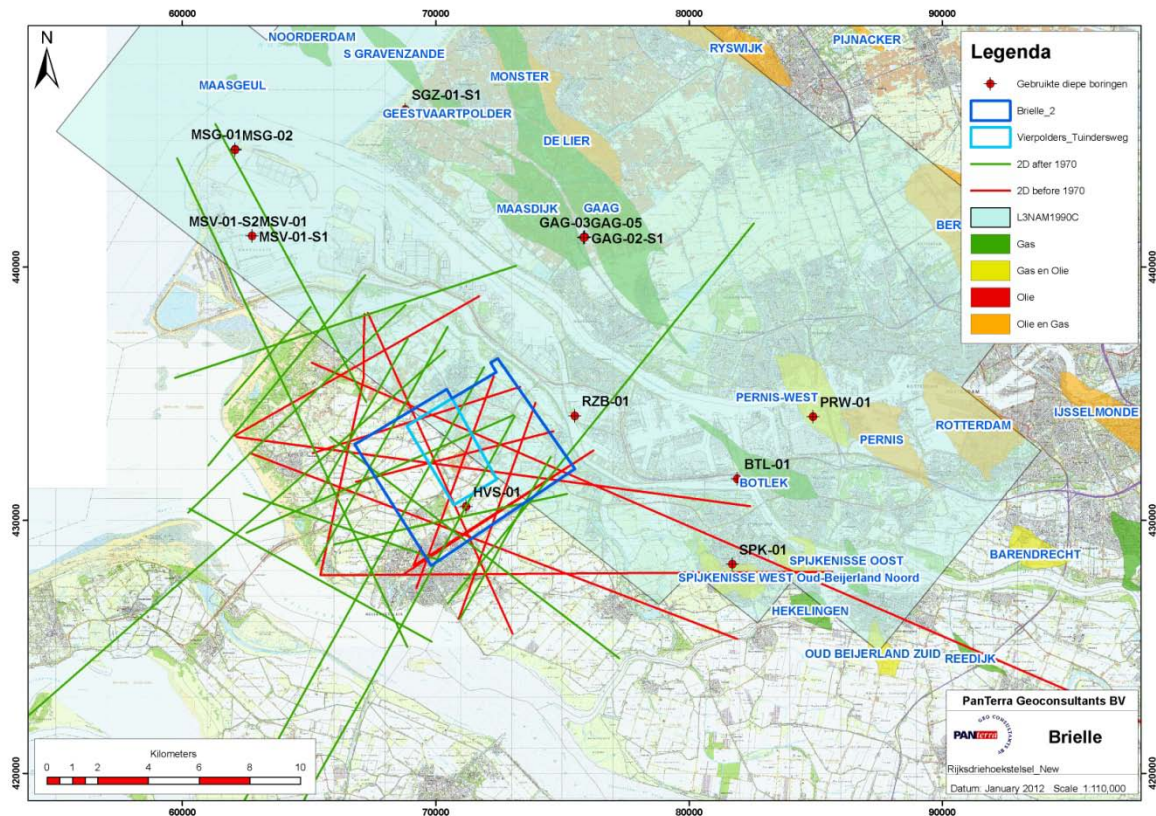


Figure 2-1 Position of the seismic and well data used for this study. Wells are shown in red. The 3D survey is shaded blue. 2D seismic lines that were shot before 1970 are shown in red, lines that were shot after 1970 are shown in green. The names of the 2D seismic lines are not shown on this map but can be found on the map in Appendix 8.1.

Table 2-1 Overview of 2D seismic lines that were used for this study.

Seismic survey	Seismic line	Length	Seismic survey	Seismic line	Length
L2AMC1981A	ANE81-300	7408	L2NAM1973H	903084B	10913
L2AMC1981A	ANE81-301	9420	L2NAM1974D	742015	7308
L2AMC1981A	ANE81-306	14384	L2NAM1974D	742017	21795
L2NAM1957A	2099	10497	L2NAM1974D	742019	21353
L2NAM1958A	2100	9060	L2NAM1974D	742021	10770
L2NAM1958A	2104	20470	L2NAM1974D	742025	5151
L2NAM1958A	2105	20208	L2NAM1984K	843429	19283
L2NAM1964A	2404	8927	L2NAM1985D	852102	12497
L2NAM1964A	2414	43365	L2NAM1985D	852104	21331
L2NAM1964A	2415	20594	L2NAM1985D	852106	8227
L2NAM1964A	2430	13905	L2NAM1985D	852109	14172
L2NAM1964A	2431	11132	L2NAM1985D	852111	9751
L2NAM1964A	2432	8601	L2NAM1985D	852113	11871
L2NAM1964A	2433	8072	L2NAM1985D	852115	26911
L2NAM1964A	2434	18163	L2NAM1985D	852117	11527

It is assumed that the seismic data is (almost) zero-phase data. After applying the time- and phase-shifts, assuming reversed SEG and zero-phase data, the top of the Chalk Group (the transition from the low-impedance North Sea Group to the high-impedance Chalk Group) will, for instance, be interpreted at the maximum value of the negative wave.

2.3 Well data

In the vicinity of the study area several wells have been drilled deep enough to encounter the Triassic sediments. Regional geological information of the West Netherlands Basin indicates that the development of the formations from the Buntsandstein is more or less continuous. Therefore all available information on the Triassic sediments from the available wells has been used for this study. The location of the selected wells used for this study is shown on the map in Figure 2-1. All open file well data have been downloaded from the TNO portal (www.nlog.nl). Table 2-2 provides an overview of available well data and for which part of the study the well data has been used.

The coordinates of the surface locations of the selected wells have been read from the composite well logs (cwl). These coordinates correspond to the Rijksdriehoekstelsel coordinate system. Of some of the older wells, the coordinates are given in a previous version of the Rijksdriehoekstelsel, which had its origin in Amersfoort. In the new coordinate system, the origin is not in Amersfoort but in Paris. Therefore, the older coordinates have been recalculated by adding 155,000 m to the x-coordinates and 463,000 m to the y-coordinates.

Wells for which time-depth data (also called checkshot data) are available can be projected onto seismic data, as the depth in the wells (in meters) can be linked to the depth of the seismic (in seconds). These wells are therefore of great importance for the seismic interpretation. For an optimal coupling between the wells and the seismic, the available checkshot data have been calibrated. In addition, synthetic seismograms have been created for three wells that are important for the seismic interpretation, namely BTL-01, RZB-01 and MSV-01 (Appendix 8.2.). Based on the calibration and synthetic seismograms the checkshot data for three wells have been shifted (see Table 2-2).

Table 2-2 Overview of available well data and what data was used for which part of the study.

Overview				Data availability					Data used in study			
Well_ID	Borehole_Name	Total Depth (TVD in meters)	Formation @ TD	Deviation data	Logs	Core data Triassic	Time-Depth data	Checkshot TWT edits (in ms, positive is down)	Seismic interpretation	Core data analysis	Wireline log analysis	Temperature analysis BHT data
BTL-01	BOTLEK-01	3015	Strijen Formation	✓	✓	✓	✓	+20	✓	✓	✓	
GAG-02-S1	GAAG-02-SIDETRACK1	3199	Rogenstein Member	✓	✓	✓	✓		✓	✓	✓	
GAG-03	GAAG-03	3069	Lower Volpriehausen Sandstone Member	✓	✓	✓				✓		
GAG-05	GAAG-05	3947	Upper Volpriehausen Sandstone Member	✓	✓	✓				✓	✓	
HVS-01	HELLEVOETSLUIS-01	3835	Ruurlo Formation	✓	✓						✓	✓
MSG-01	MAASGEUL-01	3376	Strijen Formation	✓	✓	✓	✓	+35	✓	✓	✓	
MSG-02	MAASGEUL-02	2961	Rogenstein Member	✓	✓	✓	✓		✓	✓		
MSV-01	MAASVLAKTE-01	2502	Basal Solling Sandstone Member	✓	✓	✓	From sidetrack	+62		✓		
MSV-01-S1	MAASVLAKTE-01-SIDETRACK1	2719	Rogenstein Member	✓								
MSV-01-S2	MAASVLAKTE-01-SIDETRACK2	2555	Hardeggen Formation	✓	✓		✓		✓			
PRW-01	PERNIS WEST-01	3136	Strijen Formation	✓	✓	✓	✓		✓	✓	✓	
RZB-01	ROZENBURG-01	3074	Rogenstein Member	✓	✓	✓	✓		✓	✓	✓	✓
SGZ-01-S1	'S-GRAVENZANDE-01-SIDETRACK1	3001	Rogenstein Member	✓	✓		✓		✓		✓	
SPK-01	SPIJKENISSE-01	3272	Strijen Formation	✓	✓							
SPKO-01-S1	SPIJKENISSE OOST-01-SIDETRACK1	2681	Rogenstein Member	✓	✓	✓	✓		✓	✓	✓	
SPKW-01	SPIJKENISSE WEST-01	2657	Upper Volpriehausen Sandstone Member	✓	✓	✓	✓		✓	✓		✓
STW-01	STRIJEN-WEST-01	2608	Strijen Formation	✓	✓		✓		✓		✓	

2.4 Stratigraphy

For all wells a stratigraphic overview is available through the TNO portal (www.nlog.nl). This stratigraphy corresponds to the stratigraphic nomenclature by TNO. The stratigraphy of the Triassic is shown in Figure 2-2.

Global Period	Epoch	Stage	Group	Subgroup	Formation	Basin Area Member	Basin Fringe Area Member	
Jurassic	Lias	Sinemurian	Altena (AT)		Aalburg Fm (ATAL)			
		Hettangian			Sleen Fm (ATRT)			
Triassic	Late Triassic	Rhaetian	Upper Germanic Trias (RN)		Keuper Fm (RNKP)	Upper Keuper Claystone (RNKPU)		
		Norian				Dolomitic Keuper (RNKPD)		
						Red Keuper Claystone (RNKPR)		
						Red Keuper Evaporite (RNKPE)		
	Middle Triassic	Ladinian				Middle Keuper Claystone (RNKPM)		
					Main Keuper Evaporite (RNKPS)			
		Anisian				Lower Keuper Claystone (RNKPL)		
						Upper Muschelkalk (RNMU)		
						Middle Muschelkalk Marl (RNMUA)		
						Muschelkalk Evaporite (RNMUE)		
Early Triassic	Scythian	Lower-Germanic Trias (RB)	Main Buntsandstein (RBM)		Rot Fm (RNRO)	Upper Röt Claystone (RNROU)	Upper Röt Fringe Claystone (RNROY)	
						Upper Röt Evaporite (RNRO2)	Röt Fringe Sandstone (RNROF)	
						Intermediate Röt Claystone (RNROM)	Lower Röt Fringe Claystone (RNROL)	
						Röt Claystone (RNROC)		
						Main Röt Evaporite (RNRO1)		
						Solling Fm (RNSO)	Solling Claystone member (RNSOC)	
							Basal Soling Sandstone member (RNSOB)	
							Hardegsen Fm (RBMH)	
							Detfurth Fm (RBMD)	Detfurth Claystone (RBMDC)
						Volpriehausen Fm (RBMV)	Volpriehausen Clay-Siltstone (RBMVC)	Lower Detfurth Sandstone (RBMDL)
Lower Volpriehausen Sandstone (RBMVL)	Upper Volpriehausen Sandstone (RBMVU)	Lower Volpriehausen Sandstone (RBMVL)						
Perm	Late Perm				Lower-Buntsandstein Fm (RBSH)	Rogenstein (RBSHR)	Nederweert Sandstone (RBSHN)	
						Main Claystone (RBSHM)	Rogenstein (RBSHR)	
							Main Claystone (RBSHM)	
	Lopingian							
	Guadelupian							
	Kungurian							

Figure 2-2 Stratigraphic overview of the Triassic based on the Stratigraphic Nomenclature of the Netherlands as published by TNO. The Main Buntsandstein is marked by the red rectangle.

The well tops from the Stratigraphic Nomenclature of the Netherlands have been revised by PanTerra in a regional study of the Triassic in the West Netherlands Basin (Matev, 2011). The study is based on core descriptions, core photos and well log correlation of over eighty wells. Correlation is based on sequence stratigraphic principles and provides a consistent framework for the Triassic. The revised well tops are used for the petrophysical evaluation. The applied subdivision is shown in Table 2-3.

Table 2-3 Subdivision of the Main Buntsandstein as proposed by Matev (2011). FS = Flooding Surface.

Top	Subgroup	Formation
Upper Röt FS		
Lower Röt FS		Röt Sst Member
Base Soling Formation	Main Buntsandstein	Hardegsen
		Detfurth
		Volpriehausen
Base Main Buntsandstein Subgroup		

2.5 Additional data

GIS files (shapefiles en rasters) have been downloaded from the TNO portal in order to compare results and create overview maps:

- Well locations
- Licenses
- Coastline
- Offshore blocks
- Fault maps created by TNO
- General depth and thickness maps created by TNO

All these shapefiles and raster files have been transformed from the UTM 31, ED50 to the Rijksdriehoekstelsel coordinate system in order to display the data on the cadastral maps of the Netherlands.

2.6 Database

All seismic and well data have been loaded in the software package Petrel for interpretation. Available shapefiles and final result maps have been loaded in ArcGIS in order to create the overview maps.

3 Seismic interpretation

Seismic interpretation is carried out in the Petrel interpretation software. Interpretation in the 3D seismic survey is done every 8 lines (i.e. every 160 m). All available 2D seismic lines have been used for this interpretation; except the lines 2414-P2, 742017-1, 742019-1 and 903084-P1 & P2, that are too far from the area of interest. The resulting time maps have been converted to depth using the velocity model described in Chapter 3.3.

3.1 Reflector identification and seismic interpretation

Identification of the reflectors is based on the results of synthetic seismograms and on the wells that have checkshot surveys. The synthetic seismogram shows the expected seismic response based on sonic and density log measurements in the borehole. This can subsequently be compared with the real seismic data. Synthetic seismograms created for the BTL-01, RZB-01 and MSV-01 wells are given in Appendix 8.2. Identification of the reflectors was performed first on the 3D seismic survey, as this has the best resolution. Then the interpretation was continued on the 2D seismic lines covering the study area.

The following reflectors were selected for interpretation:

- **The Base Tertiary Unconformity**

This is the top of the Ommelanden Chalk. This unconformity is characterised by an increase in impedance and therefore a negative reflection. This reflector can be traced reasonably well across the study area. In the study area, the Houthem Formation (which is part of the Chalk Group) lies on top of the Ommelanden Chalk and so strictly speaking the picked reflector is not the base of the Tertiary here (see also Chapter 3.5).

- **Base Ommelanden Chalk**

Because the Chalk group has a much higher velocity it must be treated separately in the velocity model. The actual kick on seismic is most likely due to the lithology of the underlying Texel Marl. This is a strong reflector that can be traced well across the study area. The transition from the Ommelanden Chalk to the Texel Marl is characterised by a decrease in impedance and thus a positive reflection.

- **The Posidonia Shale**

The base of the Posidonia shale is characterised by an increase in impedance, thus is a negative reflection. This reflection stands out very well in all fault blocks. Caution is of importance in locations where the Posidonia shale has been eroded and where the Delfland (Cretaceous) can cause a similar reflection.

- **Top Triassic**

The top of the Triassic is characterised by an increase in velocity and in most cases also an increase in density. This results in an increase in impedance, thus a negative reflection. The increase in impedance is often related to the transition of the Upper Keuper Claystone to the Dolomitic Keuper. This can be ~7 m deeper than the true Top Triassic. This difference falls well within the degree of uncertainty related to seismic and checkshot data. Generally the Posidonia Shale can be traced easier from one faultblock to another than the top of the Triassic. The faults that have dislocated the Posidonia shale have dislocated the Triassic in a similar manner. The Posidonia shale is therefore used as a guide for the interpretation of the Triassic in faultblocks where the Triassic is hard to recognise.

The top of the Triassic is an unconformity and the Triassic is overlain by sediments of varying age. In the target faultblock near the well HVS-01, the Upper Triassic and part of the Lower Triassic sediments have been eroded. The erosional surface is at places well visible on seismic by an angular unconformity (Figure 3-4). This unconformity has been mapped and is still named Top Triassic, as it represents the time line between the sediments that are of Triassic age and the younger overlying Cretaceous sediments.

- **Top Lower Detfurth sandstone**

In the target fault block, near HVS-01, the top of the Lower Detfurth Sandstone is recognised as a negative reflector (Figure 3-4). This is confirmed by sonic and density log response in the HVS-01 and BTL-01 wells. The HVS-01 well has only encountered the lower part of the Main Buntsandstein, as the upper part has been eroded. Further northwest however, the Main Buntsandstein sequence is expected to be more complete. The top of the Lower Detfurth Sandstone has been mapped in the target fault block in order to accurately determine the depth and thickness of the Main Buntsandstein sediments northwest of the HVS-01 well.

- **Base Permian Unconformity**

The Base Permian unconformity is a well-known unconformity. In the study area it can be clearly recognised as an angular unconformity (Figure 3-4). Projection of the HVS-01 well onto the seismic confirms the identification of the angular unconformity as the Base Permian Unconformity. The Base of the Permian is recognised as a positive reflector but as it is an unconformity, its character varies. The Base Permian unconformity has been mapped in the target fault block. It has not been mapped in the neighbouring fault blocks. The base Permian unconformity is important for the delineation of the lower part of the Triassic.

The selected seismic reflectors have been interpreted on the 3D seismic survey. Consistent interpretation between the MSV-01, RZB-01 and BTL-01 well was secured (Figure 3-3), before the interpretation was continued on the 2D seismic lines covering the study area. The availability of a solid interpretation on the 3D seismic significantly contributes to a good interpretation on the 2D seismic. Interpretation of the top of the Triassic is uncertain in the area southeast of the HVS-01 well (circled red in Figure 3-1 and Figure 3-2). There is only one seismic line over this area (dotted black in Figure 3-1), from which the geology cannot be conclusively interpreted. The interpretation in this area has no consequences for the interpretation over the target area. On the maps in following chapters, this area has been shaded grey.

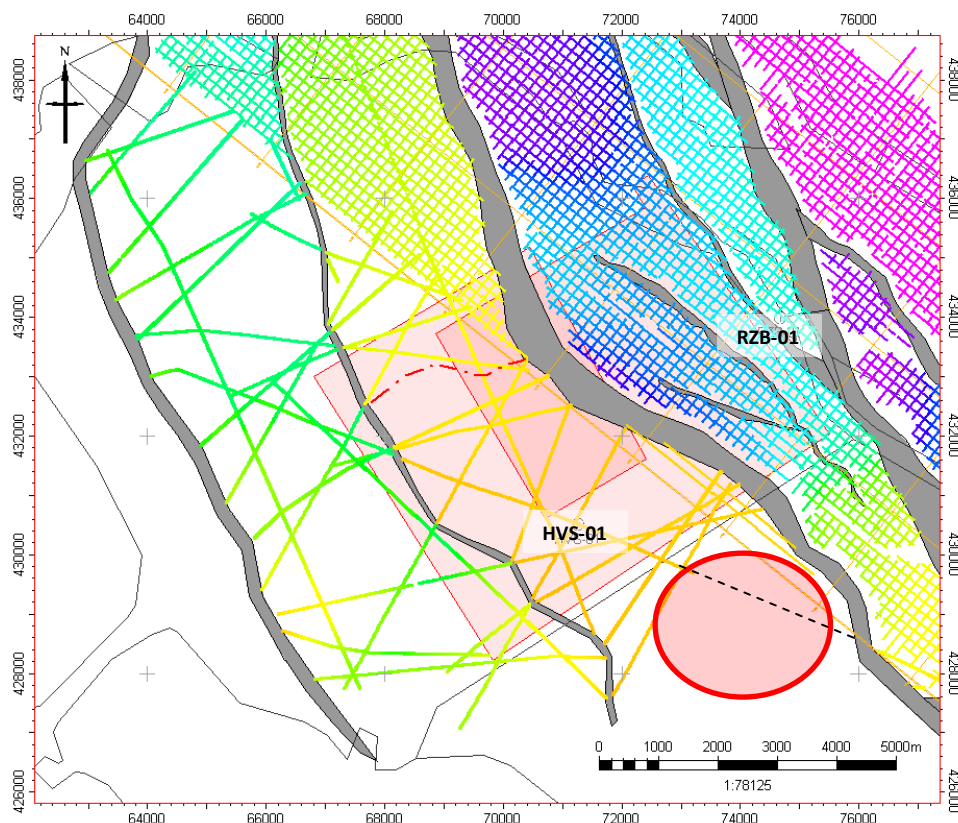


Figure 3-1 Overview of seismic interpretation of the top of the Triassic. The upper part of the Triassic is eroded past the red dotted line in the HVS-01 fault block. Past the red dotted line towards the southeast, the interpreted horizon represents the timeline (in the form of an angular unconformity) between the sediments of Triassic age and the younger overlying Cretaceous sediments. The red circle shows the area where interpretation of the top of the Triassic is inconclusive due to poor seismic coverage (see Figure 3-2). Fault polygons are shown in grey. The Vierpolders and Brielle-2 geothermal licenses are shaded red.

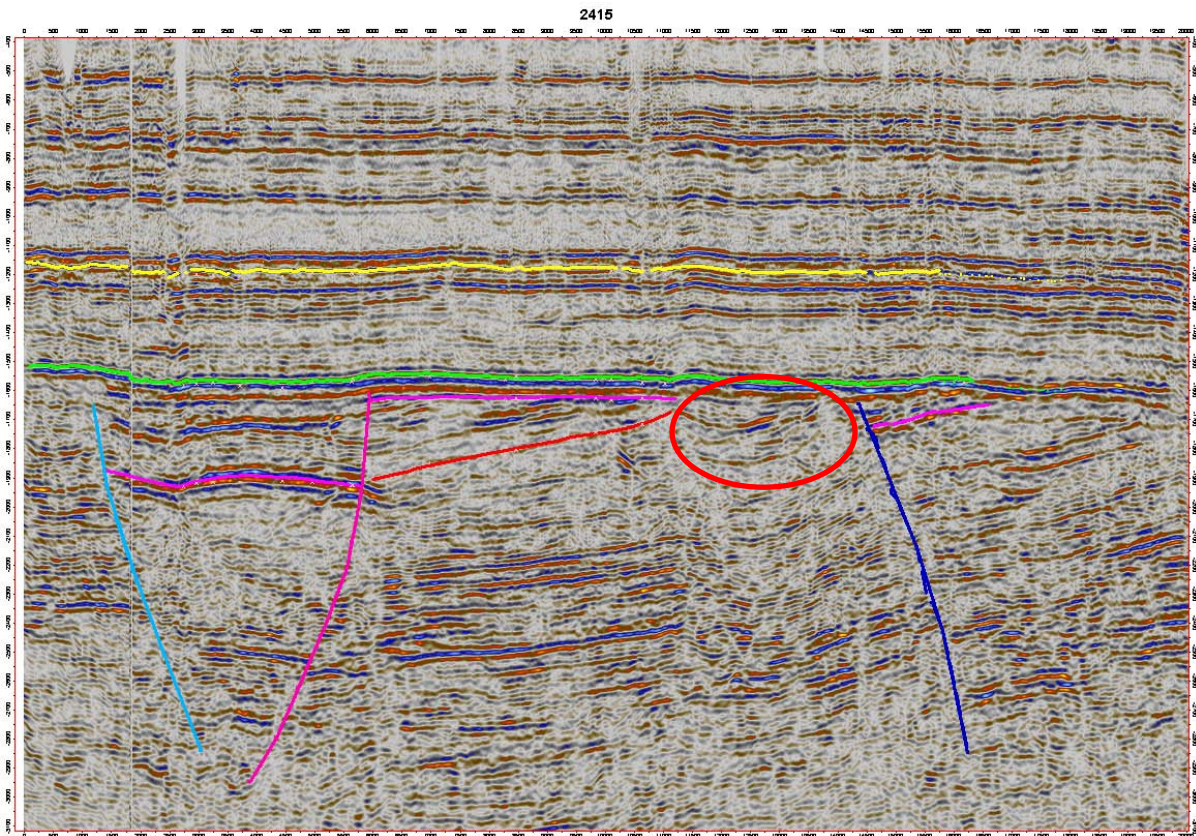


Figure 3-2 Seismic line 2415. This is the only line crossing the area that is circled red in Figure 3-1 (indicated by the black dotted line). The red circle on the seismic corresponds to the red circled area in Figure 3-1. Here, the interpretation of the top of the Triassic is difficult due to poor seismic coverage. This does not have any consequences for the interpretation over the target area.

Another observation that stands out is the character of the seismic reflectors in the Main Buntsandstein (pointed out in Figure 3-4). The seismic character of the reflections in the Main Buntsandstein changes from the HVS-01 well towards the northwest, where the target location for the proposed doublet is. The seismic character of the Main Buntsandstein sediments is very transparent in other wells like BTL-01, RZB-01 and MSV-01 where only the Upper Triassic sediments cause strong reflections. The seismic response near the HVS-01 well is in that perspective an exception.

The most likely explanation for this observation is constructive interference: the frequency content in the HVS-01 well is such that the layering in the Main Buntsandstein is picked up. Towards the northwest, the Main Buntsandstein is buried deeper and the overlying Cretaceous sequence becomes thicker. The deeper burial and the thicker Cretaceous sequence result in a lower frequency content that eventually changes the seismic character of the Main Buntsandstein layers.

The possibility of gas causing these reflections is considered unlikely for several reasons: 1) No hydrocarbons were encountered by the HVS-01 well, not even shows. 2) The reflections stop along a more or less vertical line. If gas is present near the HVS-01 well, the contact would be expected to be horizontal (Gas Water Contact). 3) There are no structural traps. The geology shows that the Main Buntsandstein layers can be followed over large distances and local stratigraphic trapping is therefore also unlikely.

L3NAM1990C arbitrary line

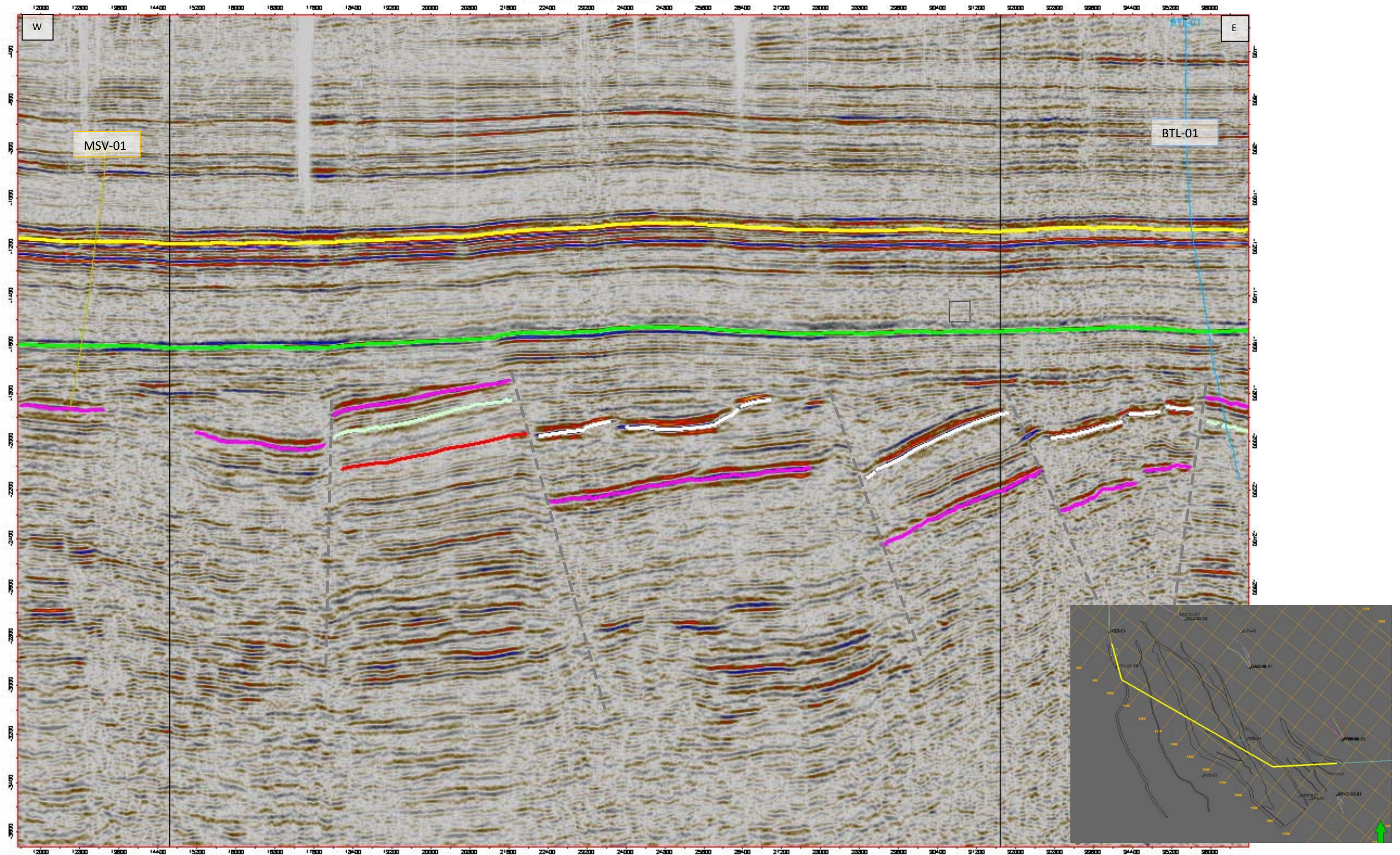


Figure 3-3 Seismic cross-section through the 3D seismic survey from MSV-01 to BTL-01. The line is shown in yellow on the map on the right. On the map, the green arrow points north and the fault polygons for the Top Triassic in the interpreted area are shown in black. The colouring of the horizons on the seismic image is as follows: Yellow = Base Tertiary, Green = Base Chalk, White = Posidonia Shale, Pink = Top Triassic, Light green = top Lower Detfurth Sandstone, Red = Base Permian. The latter two are only interpreted in the Brielle fault block.

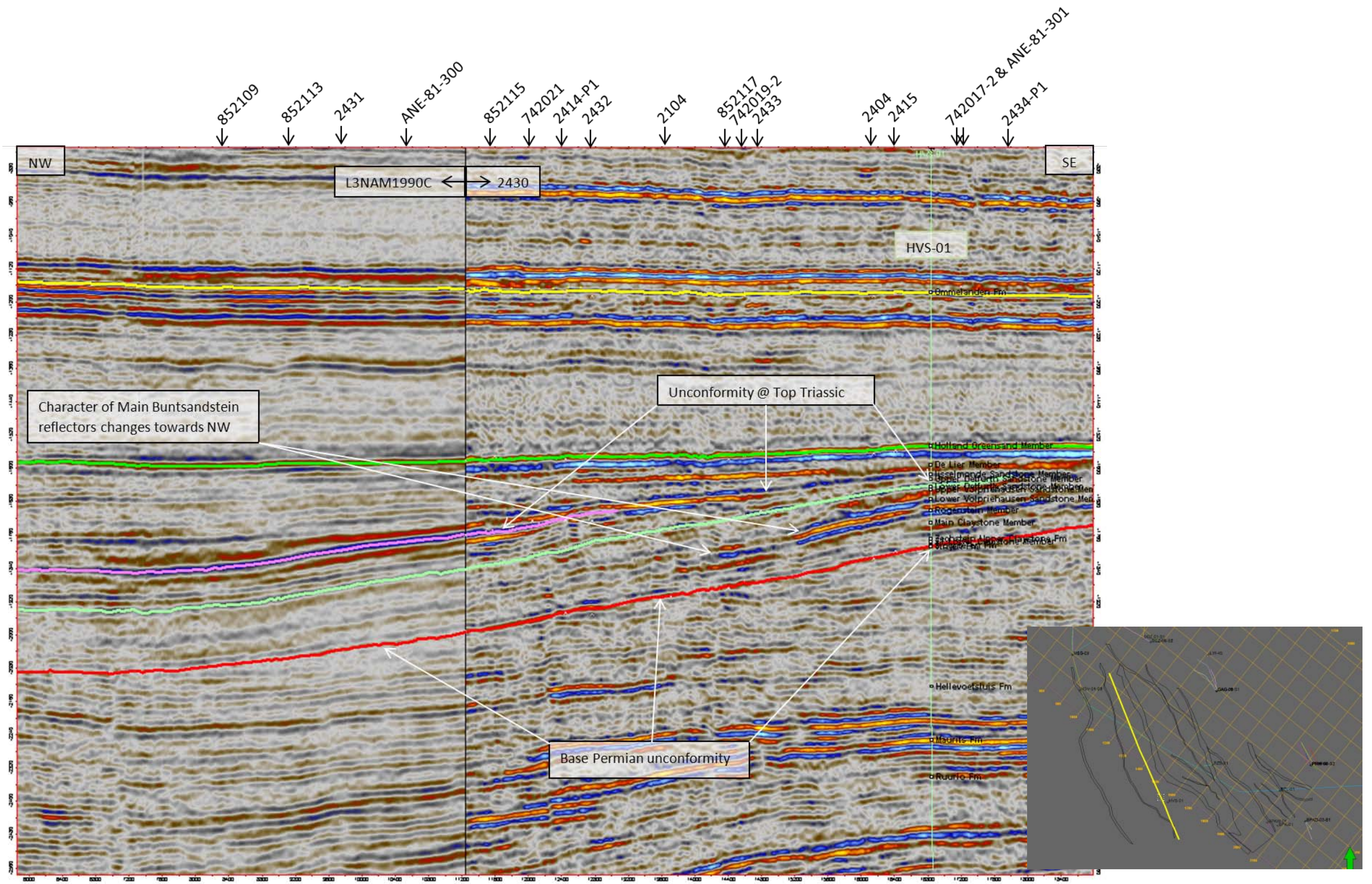


Figure 3-4 Seismic cross-section within the target fault block from the 3D survey onto the 2D line 2430, near the HVS-01 well. The line is shown in yellow on the map on the right. On the map, the green arrow points north and the fault polygons for the Top Triassic in the interpreted area are shown in black. The colouring of the horizons on the seismic image is as follows: Yellow = Base Tertiary, Green = Base Chalk, White = Posidonia Shale, Pink = Top Triassic, Light green = top Lower Detfurth Sandstone, Red = Base Permian. Both the Base Permian unconformity and the Top Triassic are clearly recognised as angular unconformities. The seismic character of the set of strong reflectors in the Main Buntsandstein near the HVS-01 well changes towards the northwest. This observation is discussed in the text. Cross sections of this line with other 2D lines are marked by the arrows at the top.

3.2 Time maps

Reflections are interpreted in time, as seismic surveys record the time of subsurface reflections from an energy source. A time map of the top of the Triassic, in Two Way Travel time in ms, is shown in Figure 3-5. Time maps of the other interpreted horizons are given in Appendix 8.3.

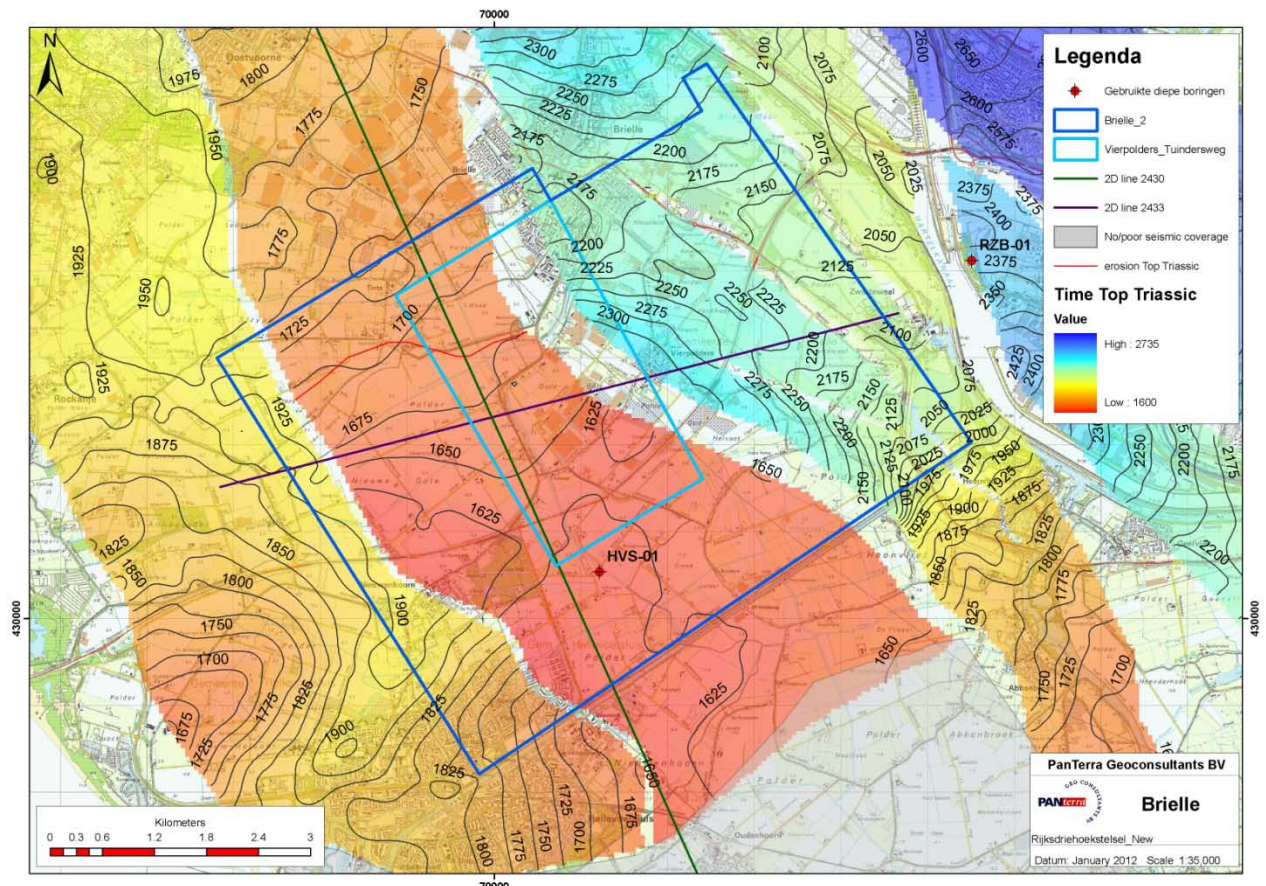


Figure 3-5 Time map of Top Triassic in two way travel time (ms). The grey shade indicates an area of no or poor seismic coverage. The outline of the Vierpolders and Brielle-2 licenses is shown in blue. The red line in the same fault block as HVS-01 indicates the erosional line of the Upper Triassic sediments in that fault block. North of this line, the entire Triassic sequence is present in that fault block. Two 2D seismic lines, 2430 and 2433, are shown for reference.

3.3 Velocity model

The contour maps in time are converted to depth maps using velocity data. The velocity model that was created is based on interval velocities. Interval velocities were obtained by dividing the depth of the layer in the well by the time value of the interpretation on seismic. The wells that were used are MSG-01, MSG-02, MSV-01, RZB-01, HVS-01, GAG-02-S1, BTL-01, SPK-01 and SPKW-01. A four-layer velocity model has been used, as shown in Figure 3-6. The interval velocity maps used for the upper three layers are shown in Figure 3-7 to Figure 3-9. For the deepest interval of the model, an interval velocity map could not be created because the deepest interpreted horizon outside the fault block in which HVS-01 was drilled is the Top Triassic. Therefore a constant velocity was chosen. This constant velocity is based on the velocity calculated from the time and depth of the Base Permian Unconformity in the HVS-01 well. This is a high velocity that may decrease away from the HVS-01 well. This increases the uncertainty of the depth of the horizons away from the HVS-01 well.

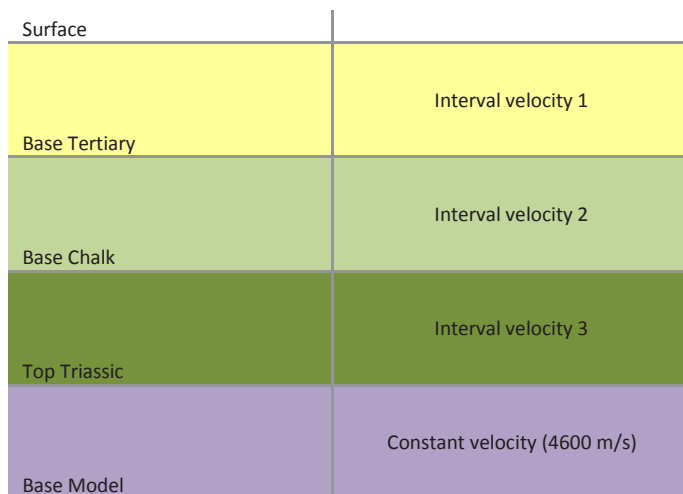


Figure 3-6 Layer cake model for the interval velocities as used in the velocity model for time-depth conversion.

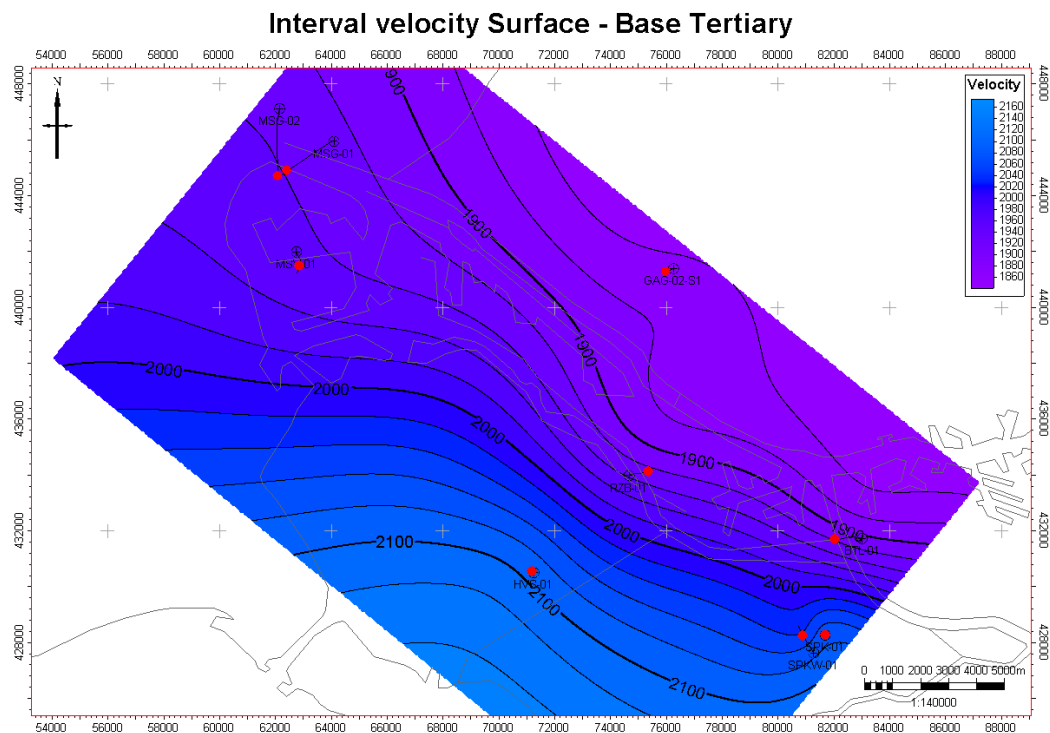


Figure 3-7 Interval velocity map for the interval between surface and base Tertiary. For reference, a rough outline of the Dutch topography is plotted in black. The interval velocity data points from which this map was created are marked red and the wells are labelled in black.

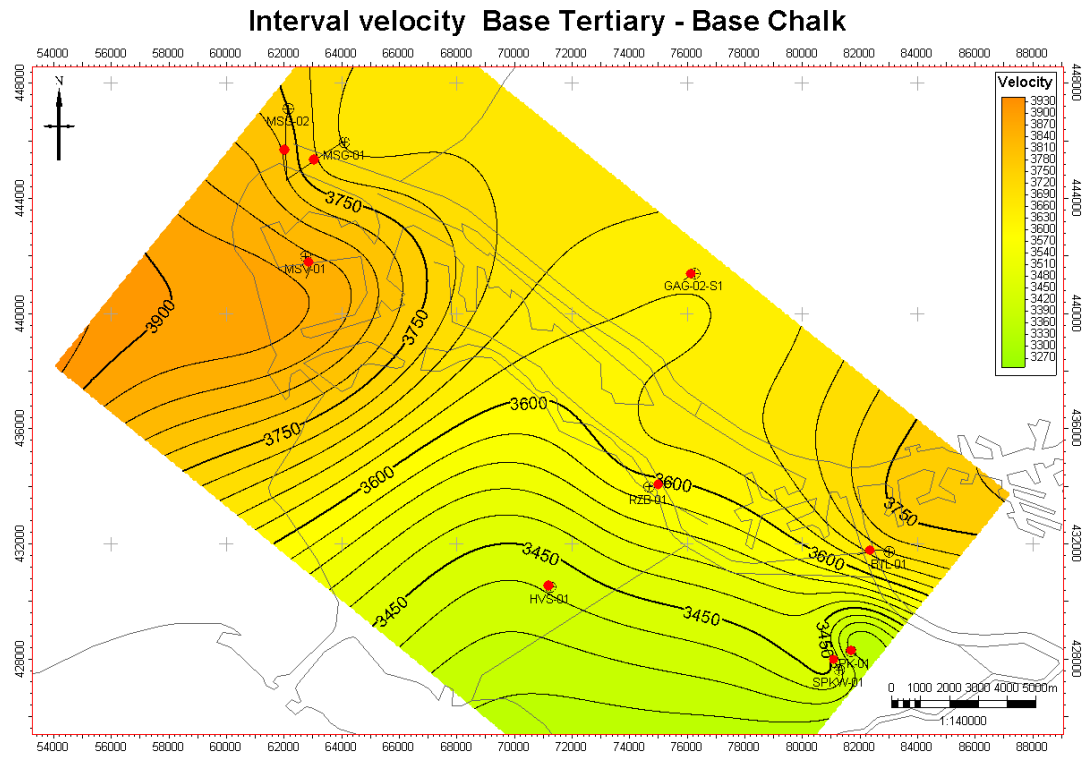


Figure 3-8 Interval velocity map for the interval between base Tertiary and base Chalk. For reference, a rough outline of the Dutch topography is plotted in black. The interval velocity data points from which this map was created are marked red and the wells are labelled in black.

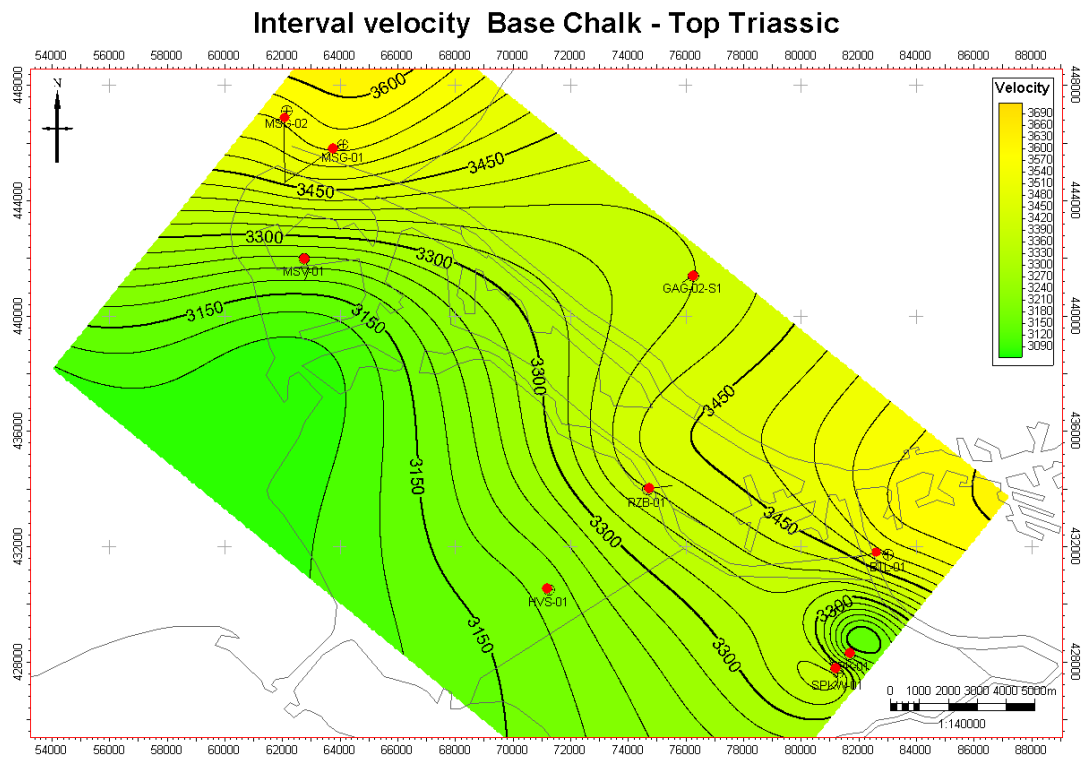


Figure 3-9 Interval velocity map of the interval between base Chalk and top Triassic. For reference, a rough outline of the Dutch topography is plotted in black. The interval velocity data points from which this map was created are marked red and the wells are labelled in black.

3.4 Depth maps

The depth maps of the interpreted horizons are shown below:

- Base Tertiary Unconformity Figure 3-10
- Base Chalk Figure 3-11
- Posidonia Shale Figure 3-12
- Top Triassic Figure 3-13
- Top Detfurth Sandstone Figure 3-14
- Base Permian Unconformity Figure 3-15

The outline of the Vierpolders and Brielle-2 licenses (shown in blue) and the location of 2D seismic lines 2430 and 2433 are shown on the maps for reference. The grey outline indicates an area of no or poor seismic coverage.

The uncertainty in the depth maps due to time-depth conversion was evaluated by comparing well tops in BTL-01, HVS-01 and RZB-01 with the depth maps that are based on the seismic interpretation. These wells are chosen because they fall within the area that was interpreted for the depth maps. The maximum error in these wells is less than 1%.

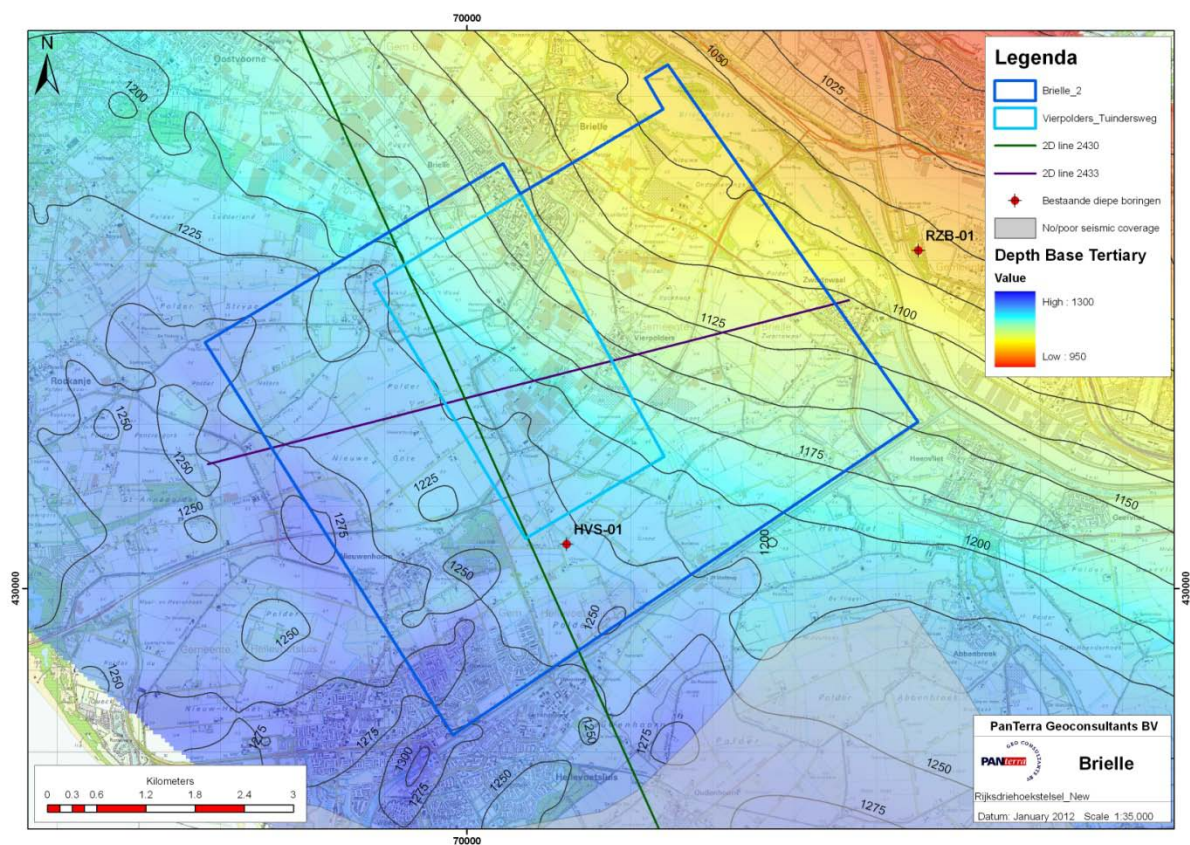


Figure 3-10 Depth map of Base Tertiary in meters.

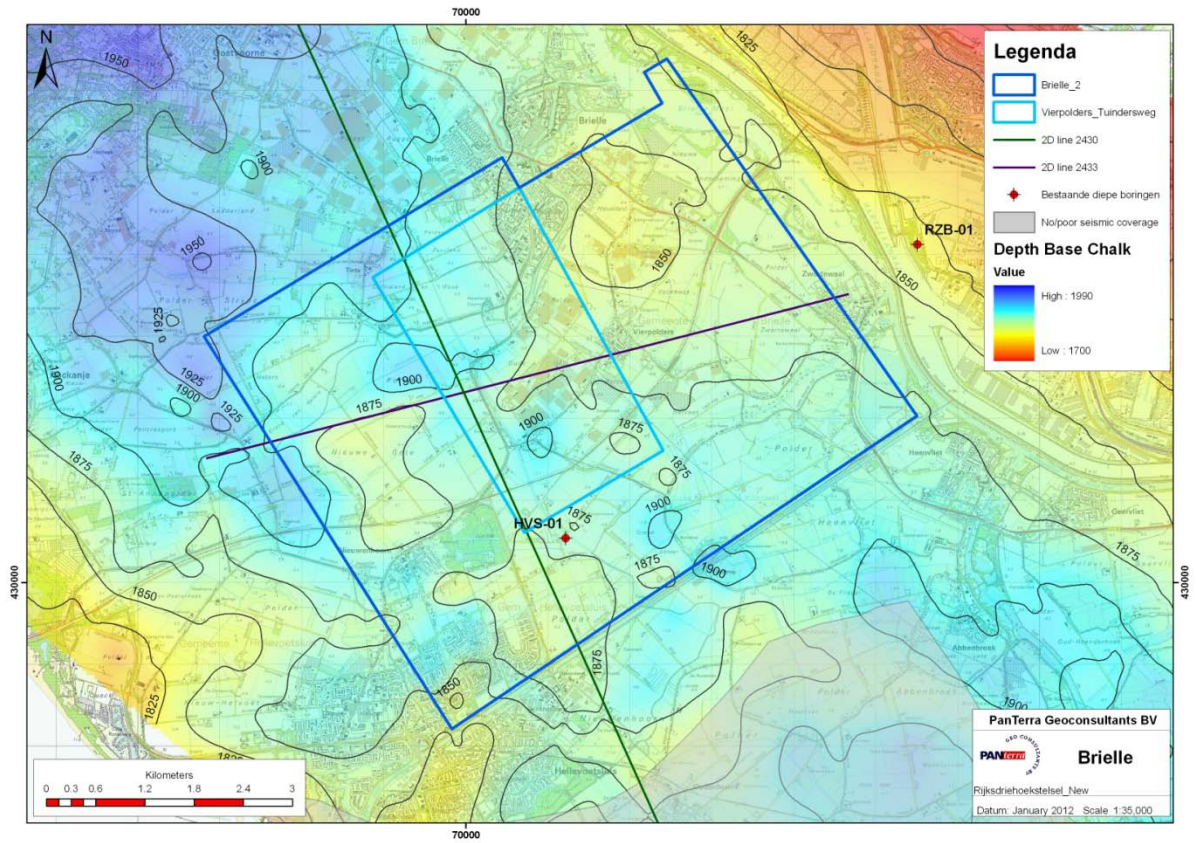


Figure 3-11 Depth map of Base Chalk in meters.

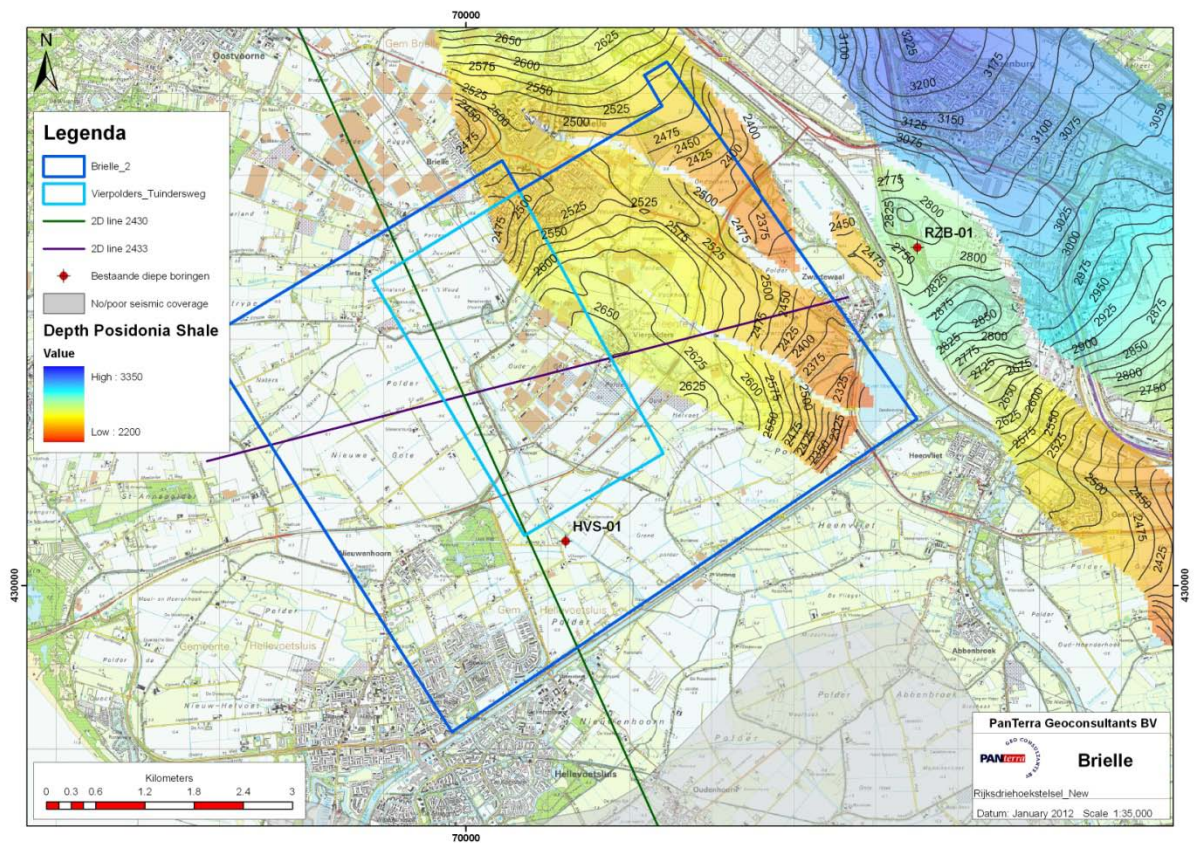


Figure 3-12 Depth map of the Posidonia Shale in meters.

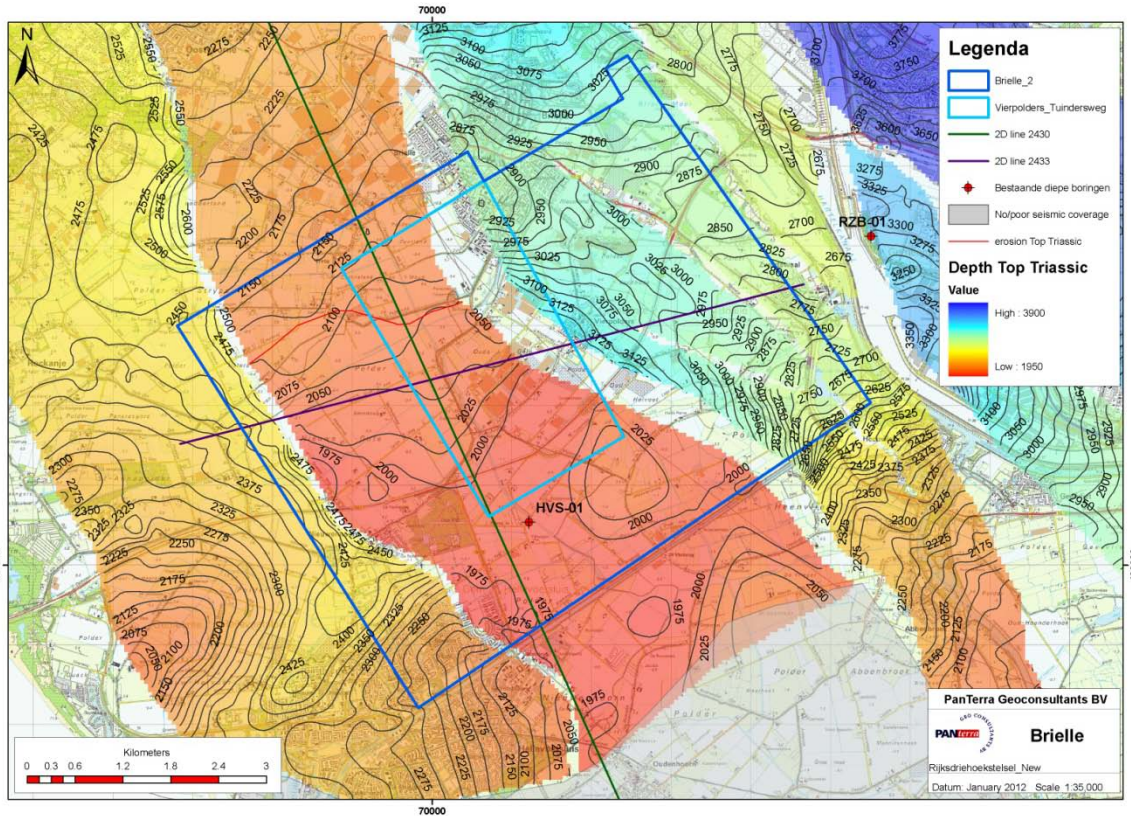


Figure 3-13 Depth map of Top Triassic in meters. The red line in the same fault block as HVS-01 indicates the erosional line of the Upper Triassic sediments in that fault block. North of this line, the entire Triassic sequence is present in the Brielle fault block.

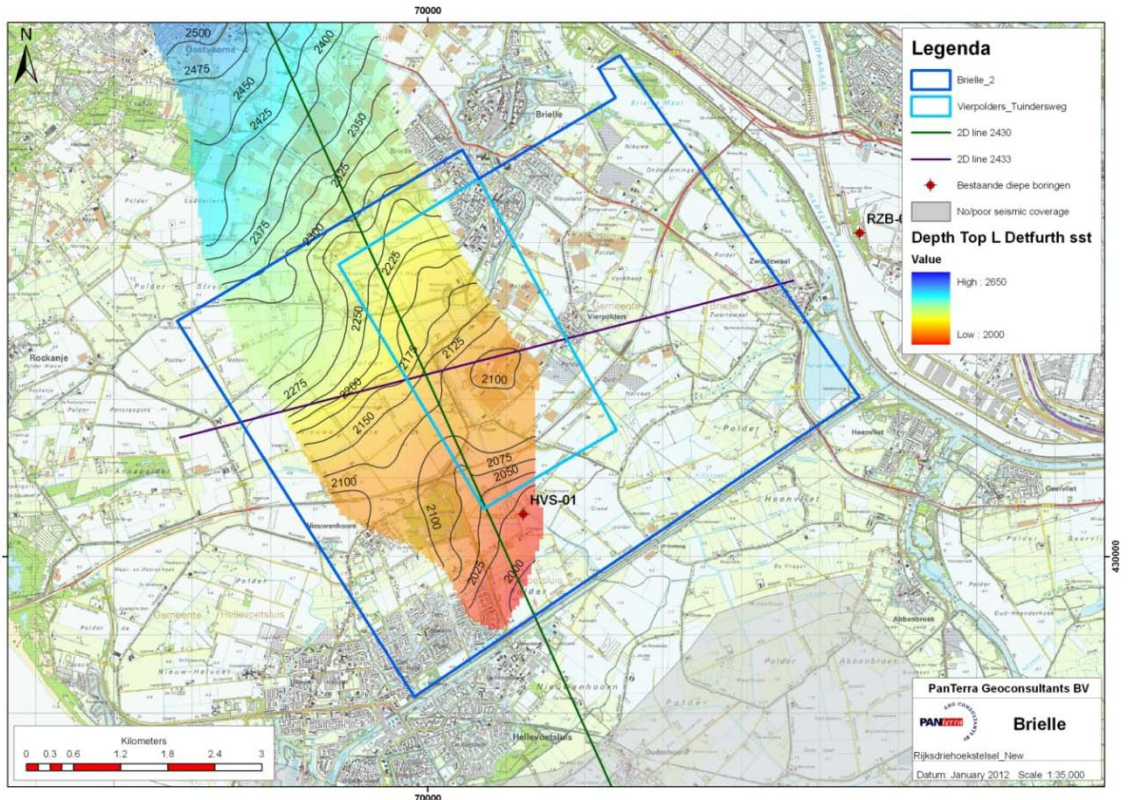


Figure 3-14 Depth map of the top of the Detfurth Sandstone in meters. This horizon has only been mapped in the target fault block.

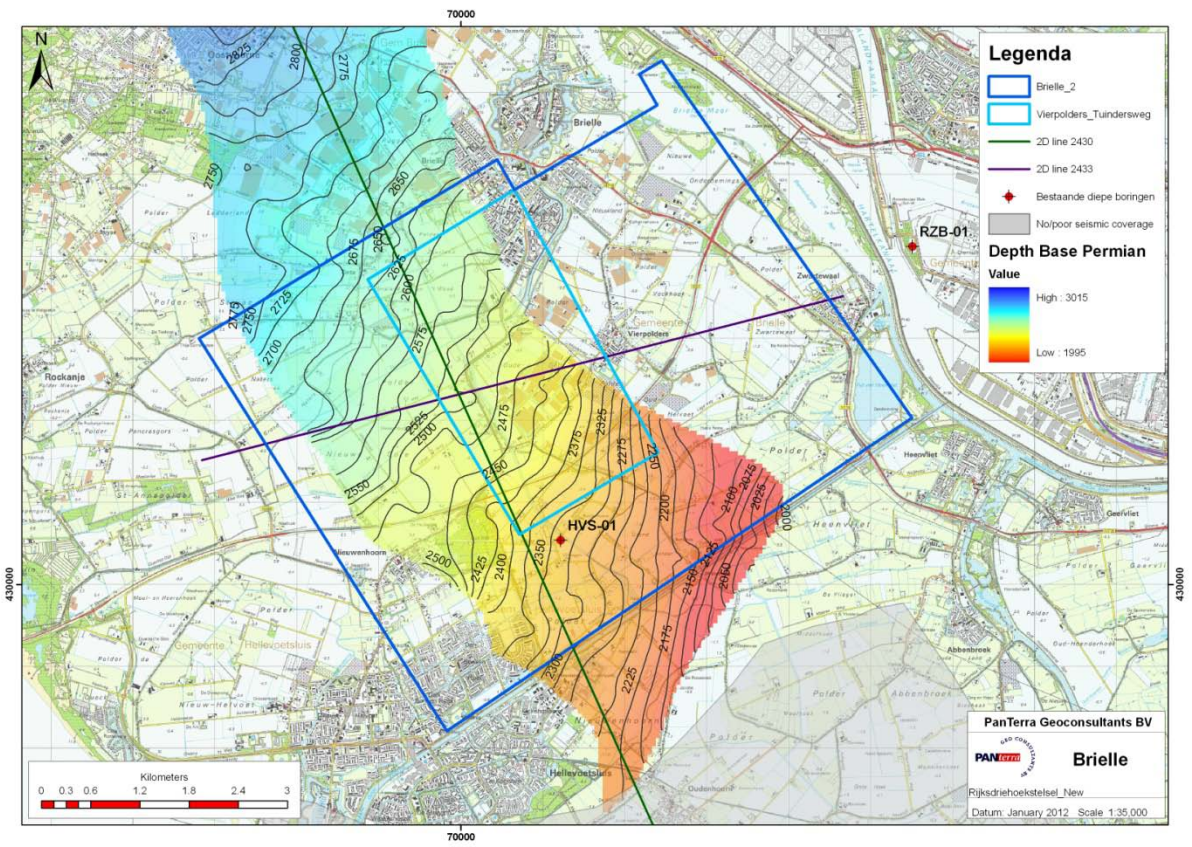


Figure 3-15 Depth map of the Base Permian Unconformity in meters. This horizon has only been mapped in the target fault block.

3.5 Thickness

The thickness of the Tertiary, the Chalk Group, the Lower Cretaceous and the Triassic-Permian sequence in the proposed wellscan be directly derived from the depth maps resulting from seismic interpretation. The established thickness of the Main Buntsandstein Subgroup, the Röt Fringe Sandstone Member and the Tertiary Houthem Formation are explained below.

- **Main Buntsandstein Subgroup**

Determining the thickness of the Triassic reservoir at the target area is complicated by the fact that the top and the base of the Main Buntsandstein Subgroup cannot be interpreted on seismic and that the youngest Triassic formation encountered by HVS-01 is the Upper Detfurth sandstone.

Thickness changes of layers of the Main Buntsandstein are not seen on seismic sections. The thickness in the HVS-01 well is therefore considered indicative of the reservoir thickness at the target area. This observation combined with the interpretation of the unconformity at the top of the Triassic and at the base of the Permian provides a solid base in determining the thickness of the Main Buntsandstein at the target area.

The thickness of the section that is missing in HVS-01 has been estimated. This has been done based on the thickness of the Upper Detfurth Sandstone Member and the Hardeggen Formation from the wells MSV-01, RZB-01 and SPKW-01.

Table 3-1 shows the expected reservoir thickness in the target area. The Main Buntsandstein sequence is expected to be complete. The total thickness of the Main Buntsandstein is 182 m. The map of the depth of the top of the Main Buntsandstein is given in Figure 3-16. The depth of the top of the Main Buntsandstein reservoir within the geothermal licenses Vierpolders and Brielle-2 varies between 1975 and 2275 m.

Table 3-1 Expected reservoir thickness at the target area. The Main Buntsandstein sequence (shaded yellow) is expected to be complete. Two horizons, the top of the Lower Detfurth Sst Member and the Base Permian Unconformity, have been interpreted on seismic.

Surface	Thickness (m)	Note
Hardeggen + Upper Detfurth Sst Mbr	70	Estimate of missing section at HVS: based on MSV, RZB, SPKW Interpreted horizon
Lower Detfurth Sst Mbr	14	From HVS
Upper Volpriehausen Sst Mbr	44	From HVS
Lower Volpriehausen Sst Mbr	54	From HVS
Lower Buntsandstein	139	From HVS
Permian	37	From HVS Interpreted horizon

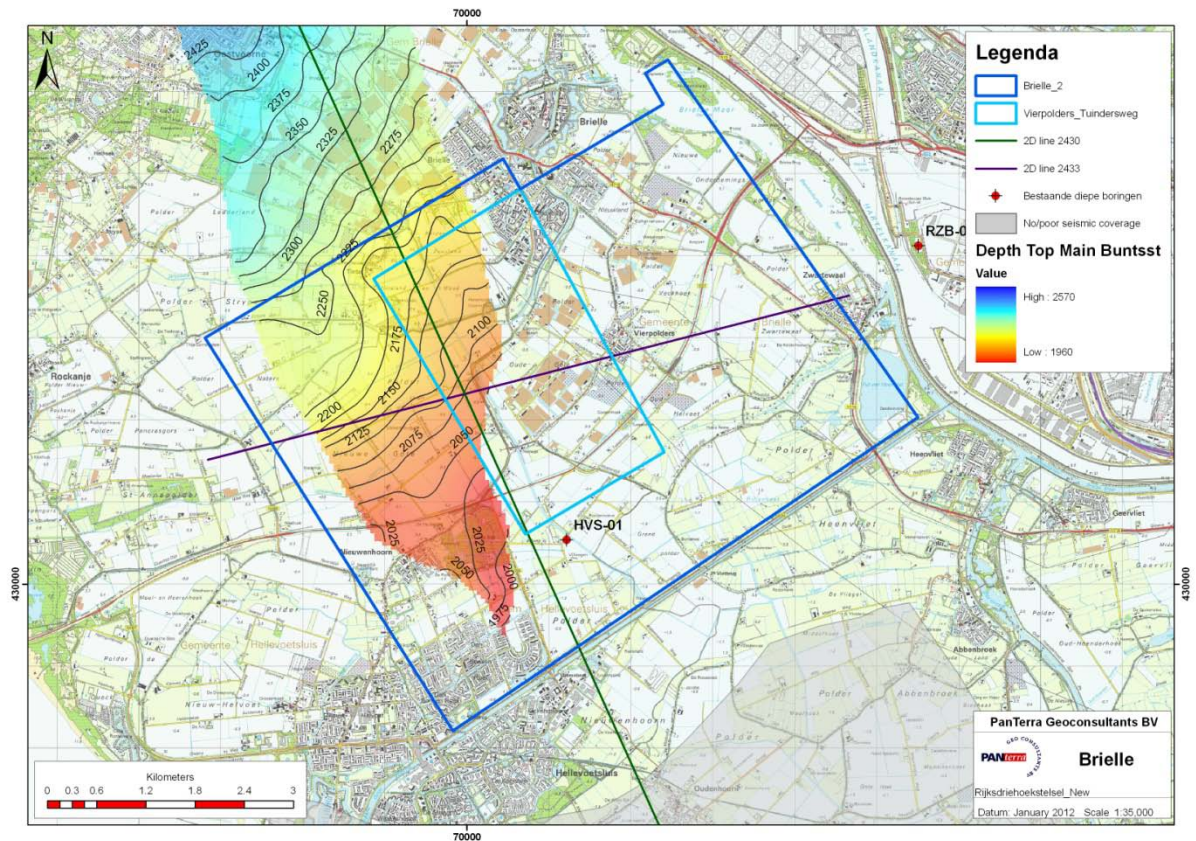


Figure 3-16 Estimated depth of the top of the Main Buntsandstein Subgroup, based on estimated thickness and the depths maps from Chapter 3.4.

- **Röt Fringe Sandstone Member**

In the fringe area of the West Netherlands Basin (where the target area lies) the Röt Fringe Sandstone Member is a good reservoir rock. The thickness of the Röt Fringe sandstone has been estimated at 22 meters, based on the thickness in MSV-01, RZB-01 and SPKW-01. The depth of top of the Röt Fringe sandstone is estimated to be 60 m shallower than the top of the Main Buntsandstein. This is based on the combined thickness of the Röt Fringe Sandstone Member, the lower Röt Fringe Claystone Member and the Solling Formation in MSV-01, RZB-01 and SPKW-01. A depth map of the top of the Röt Fringe Sandstone Member is given in Figure 3-17.

- **Houthem Formation**

The Base Tertiary horizon that has been interpreted is the top of the Ommelanden Chalk. In the study area, the Houthem Formation occurs on top of the Ommelanden Chalk. The Houthem formation consists of chalk as well and is therefore important for the casing scheme. The Houthem Chalk is about 90 m thick in the HVS-01 well. In the reflectors above the interpreted Base Tertiary horizon no thickness variation is observed (e.g. Figure 3-4). The thickness is therefore expected to be the same in the proposed producer and injector.

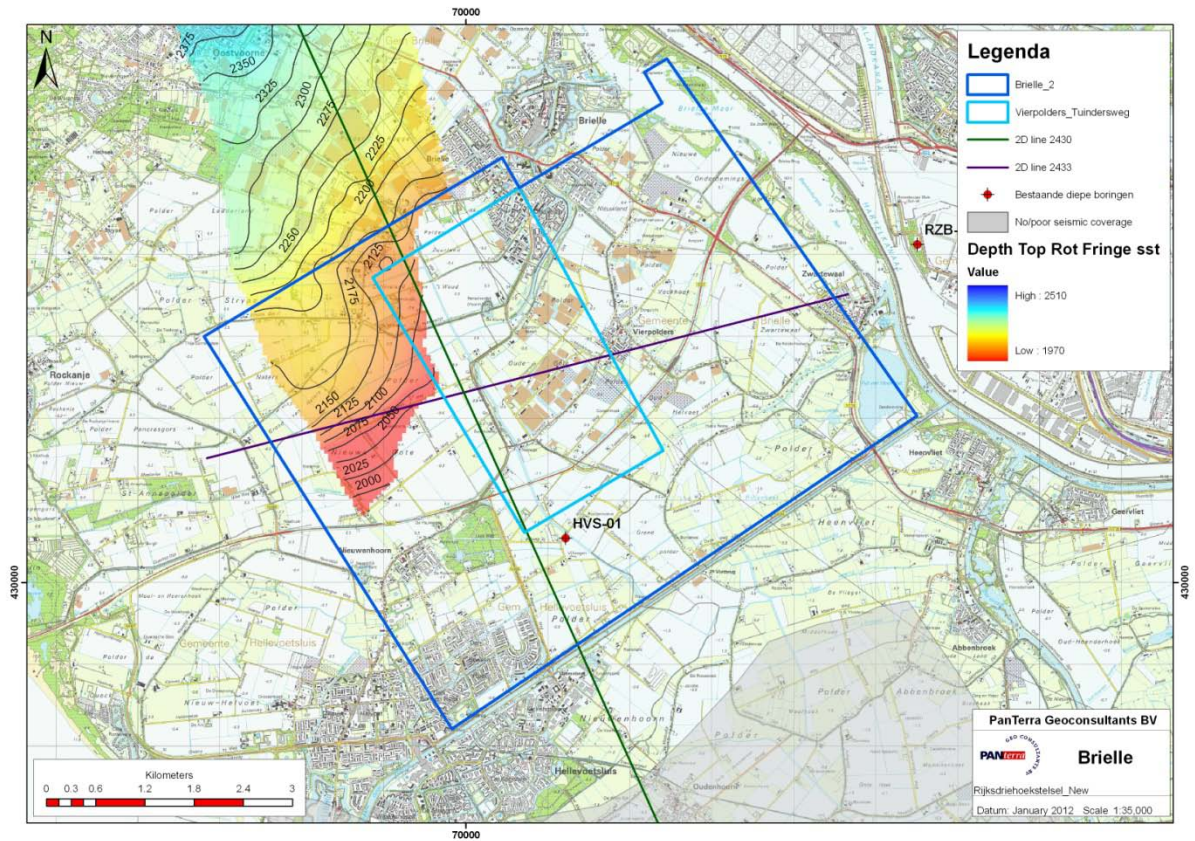


Figure 3-17 Estimated depth of the top of the Röt Fringe Sandstone Member, based on estimated thickness and the depths maps from Chapter 3.4.

4 Petrophysical interpretation

The reservoir quality of the Main Buntsandstein reservoir in the study area can be appraised with use of core data and wireline logs from existing wells in the vicinity of the target area. The wireline logs are necessary to calculate the volume of clay and the porosity of the reservoir. The core data are of importance for quality control of the log evaluation and for calculation of the permeability. We have used formation tops from a regional study for the petrophysical interpretation (Matev, 2011). These tops are given in Appendix 8.4.

4.1 Core analysis

Core data of eleven wells in the West Netherlands Basin have been studied (Table 2-2). The available core data include grain density, porosity and permeability measurements. An overview of available core plug measurement data is given in Appendix 8.4.

Log to core depth shifts were applied to all cores. Core gamma or notes on log to core shifts were not available. In order to establish reasonable depth shifts, grain density and porosity measurements were utilized to shift against the wireline logs.

Core analysis reports are not available for most wells apart from BTL-01 and MSG-01 and do not always list specifics with respect to the way the samples were cleaned and analysed. It is most likely that all available core porosity and core permeability were measured under ambient conditions. Depending on the method of cleaning and drying, the available core porosity is either the total porosity (ϕ_{total}) or the effective porosity ($\phi_{\text{effective}}$; including clay bound water). The core permeability is air permeability (K_{air}).

The core porosity and permeability need to be corrected to obtain the porosity and brine permeability (K_{brine}) at reservoir stress conditions. These corrections can be determined with special core analysis. Because no special core analysis is available for any of the wells, it has been decided not to correct the core data for stress. Also, the air permeability (K_{air}) needs to be corrected to brine permeability (K_{brine}). Corrections can be applied for low, medium and high permeability classes with use of functions as described by Yuhasz (1986). These corrections can only be applied when both the $\phi_{\text{effective}}$ and ϕ_{total} of the core are known or the Cation Exchange Capacity (or Q_v). These are also not available.

The use of the porosity-permeability relations for the calculation of permeability is discussed in Chapter 4.2.

Permeability is dependent on grain size and sorting. Depositional environment is therefore of importance and different porosity-permeability relations should be applied for each formation, especially for the Hardeggen formation which is an Aeolian deposit whereas the Detfurth and Volpriehausen are fluvial. Core porosity has been plotted against air permeability in order to determine a porosity-permeability relationship for each formation (Figure 4-1 and Figure 4-2). The resulting porosity-permeability relationships are as follows, with K = permeability in milliDarcy and ϕ = porosity in fractions:

Röt Formation:	$K = 0.002 e^{61.347 \phi}$	(Figure 4-2)
Hardeggen Formation:	$K = 0.008 e^{57.852 \phi}$	(Figure 4-2)
Detfurth Formation:	$K = 0.0003 e^{71.696 \phi}$	(Figure 4-2)
Volpriehausen Formation:	$K = 0.001 e^{64.798 \phi}$	(Figure 4-2)
Main Buntsandstein Subgroup:	$K = 0.0005 e^{71.528 \phi}$	(Figure 4-1)

Only data points with porosity higher than 8% have been used because it is assumed that no water will be produced from layers with lower porosity.

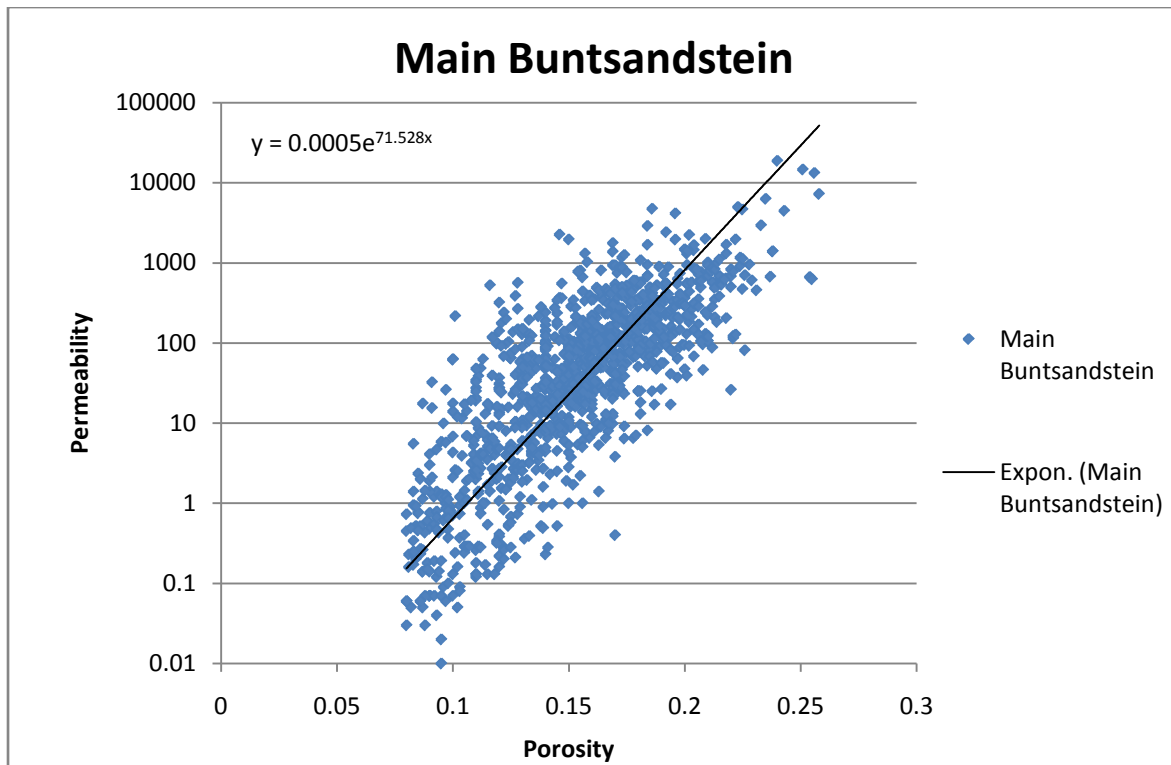


Figure 4-1 Porosity–permeability relationship of the Main Buntsandstein Subgroup. A porosity cut-off of 8% has been applied. All available data points from the Volpriehausen, Detfurth and Hardeggen formations are plotted.

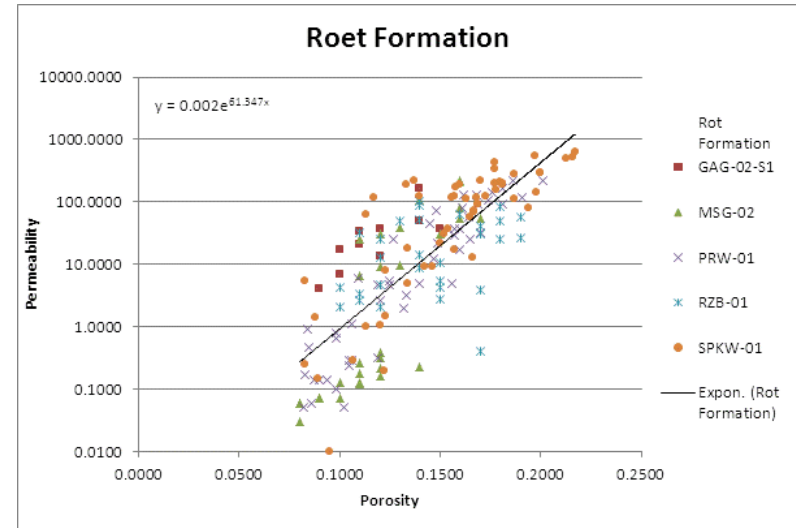
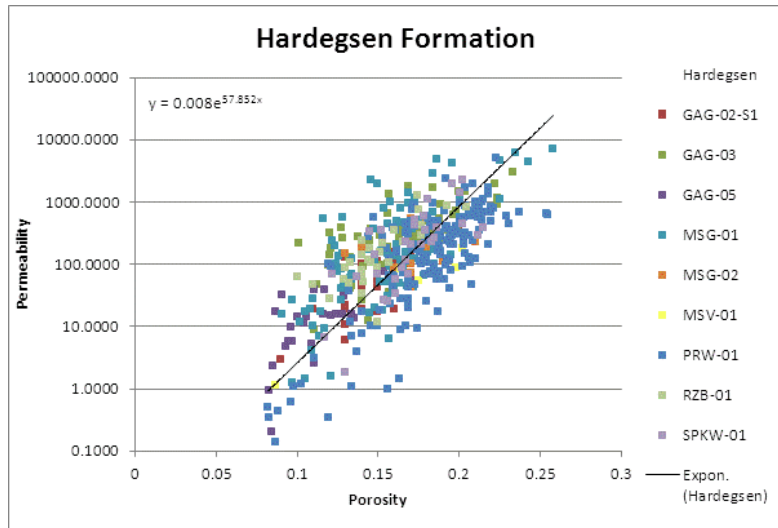
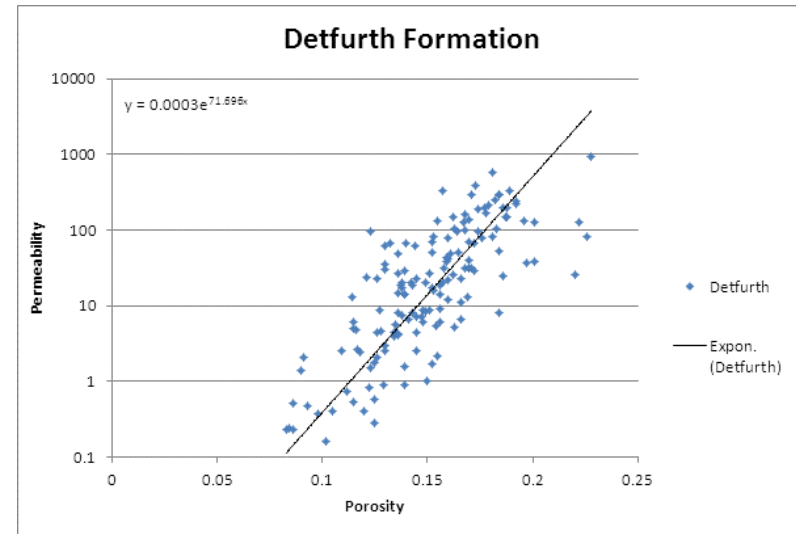
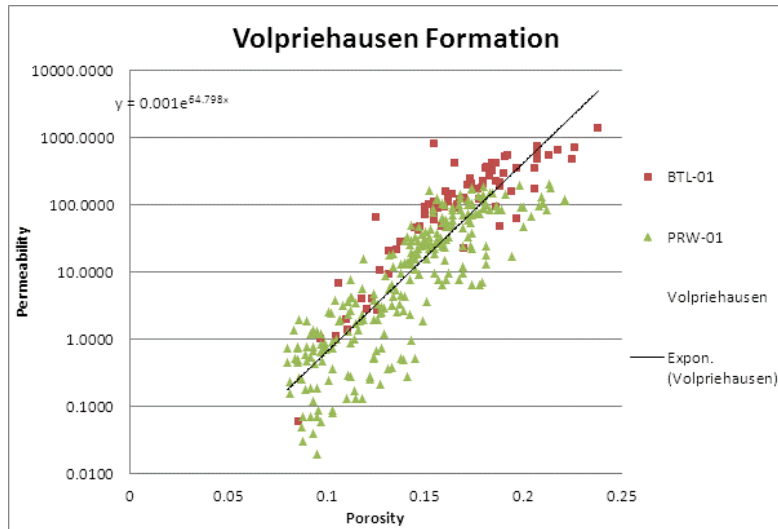


Figure 4-2 Porosity–permeability relationship of the Volpriehausen, Detfurth, Hardeggen and Röt Formation. A porosity cut-off of 8% has been applied. The Detfurth plot is based on PRW-01 data only.

4.2 Log analysis

The volume of clay and the porosity of the various sandstone layers have been calculated using wireline logs of ten wells in the vicinity of the study area (see Table 2-2). These wells were selected based on the availability of wireline logs, core data and the logged intervals. Both core data and wireline logs are available for all wells apart from HVS-01 and SGZ-01-S1.

4.2.1 Volume of Clay

The volume of clay in the intervals of interest is determined with use of the Gamma Ray (GR) method.

$$V_{Clay} = \frac{GR_{log} - GR_{min}}{GR_{max} - GR_{min}}$$

With:

- V_{cl} = Volume of clay
- GR_{log} = GR value from log
- GR_{min} = min. GR value (sand line)
- GR_{max} = max. GR value (shale line)

Appropriate GR_{min} and GR_{max} values were obtained statistically and have been adjusted per well. Histograms were used to derive a lower and an upper 5% GR cut-off (Figure 4-3). The difference between GR_{min} and GR_{max} describes the found ΔGR value. This value was found to be 65 API. The sand baselines were defined per well, supported by composite well logs. The clay baselines were found by adding the ΔGR values and comparing found V_{cl} curves with information from the CWL.

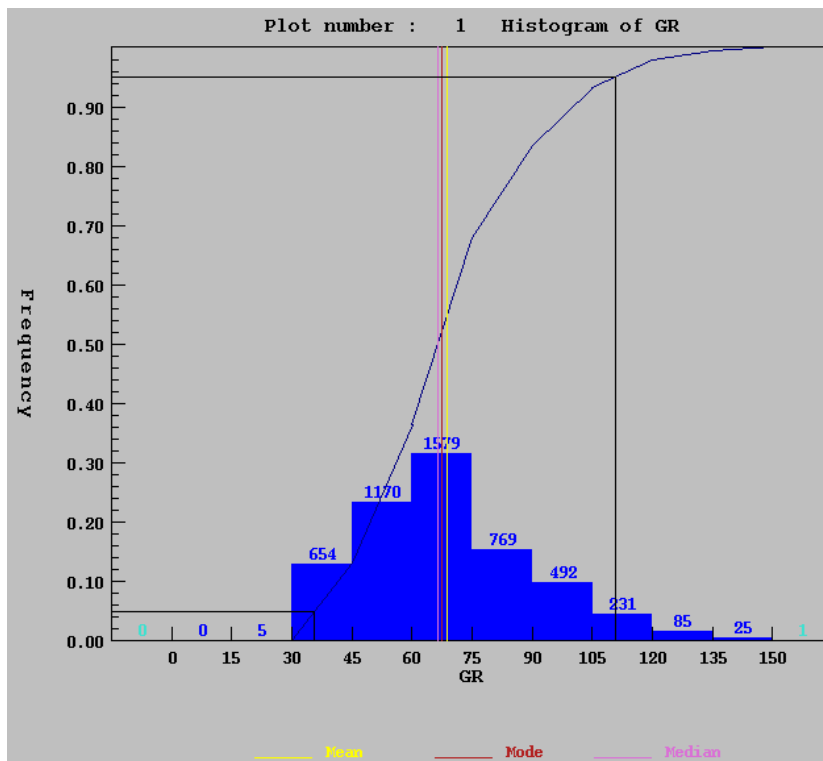


Figure 4-3 Example histogram of GR, marking the lower and upper 5% boundaries.

4.2.2 Effective porosity

The effective porosity of the Triassic sandstone intervals has been calculated with use of the density method.

$$\Phi_{density} = \frac{\rho_{ma} - \rho_{log}}{\rho_{ma} - \rho_{mf}} - V_{clay} * \left(\frac{\rho_{ma} - \rho_{cl}}{\rho_{ma} - \rho_{mf}} \right)$$

With:

- ρ_{log} = bulk density log (g/cm³)
- ρ_{ma} = matrix density
- ρ_{mf} = mud filtrate density (1.05 g/cm³)
- ρ_{cl} = clay density
- V_{cl} = volume of clay

The calculations were guided by core data where available. Clay corrections were applied using the results of the V_{cl} calculations. The matrix density is based on core plug measurements. Clay densities are determined by evaluating GR vs. RHOB plots. Calculations performed with these parameters proved valid as their results fit well to measured core porosity in all wells. The following petrophysical parameters have been applied for the various intervals:

Röt Sst Mbr:	$\rho_{ma} = 2.68 \text{ g/cm}^3, \rho_{cl} = 2.7 \text{ g/cm}^3$
Hardeggen Fm:	$\rho_{ma} = 2.66 \text{ g/cm}^3, \rho_{cl} = 2.6 \text{ g/cm}^3$
Detfurth Fm:	$\rho_{ma} = 2.69 \text{ g/cm}^3, \rho_{cl} = 2.65 \text{ g/cm}^3$
Volpriehausen Fm:	$\rho_{ma} = 2.69 \text{ g/cm}^3, \rho_{cl} = 2.65 \text{ g/cm}^3$

The calculated average effective porosity has been plotted against the depth of the middle of the Main Buntsandstein sequence (Figure 4-4).

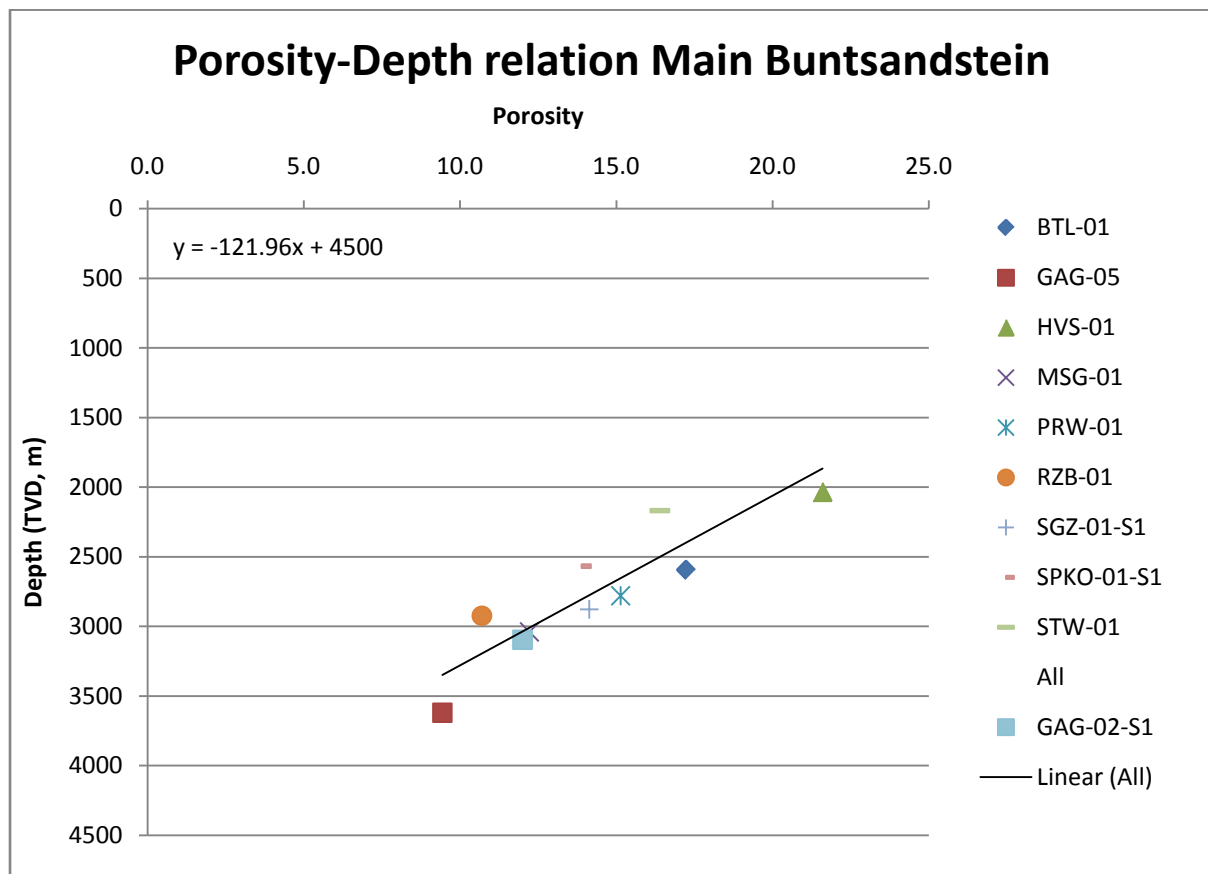


Figure 4-4 Porosity-depth relation for the Main Buntsandstein in the evaluated wells.

4.2.3 Permeability

The porosity-permeability plots shown in Chapter 4.1 are constructed using measurements made at ambient conditions. Therefore both porosity and permeability are optimistic. As explained in Chapter 4.1, no in situ corrections have been applied to the core data due to lack of special core analysis.

The method of using the porosity-permeability relations from core data to calculate the permeability from the derived effective porosity logs is considered valid based on the following considerations:

1) K_{brine} vs. K_{air}

If the rock has a high clay content, K_{brine} may be much less than K_{air} . However, the difference between K_{brine} and K_{air} becomes very small if the clay content is low. This is the case in the study area.

2) Permeability at depth

An assumption can be made that under stress porosity and permeability both reduce such that they move along the porosity-permeability line. This is still optimistic for very low permeability (less than 1-10 mD) but is considered an acceptable assumption for medium to high permeability. In this case this assumption is considered valid because the study area is an area of high permeability.

In conclusion: the low clay content of the reservoir in the study area significantly reduces the necessity of a K_{air} to K_{brine} correction and a depth correction is indirectly applied by using the porosity-permeability relations from core data with the log-derived effective porosity (i.e. the in situ porosity) as input.

The calculated permeability values are shown on the map in Figure 4-5 as well as the fault polygons over the area that is covered by available seismic data. Interpolation of the resulting permeability values is complicated by the fact that existing Triassic wells are relatively far apart and are drilled in different fault blocks. Moreover, most wells are drilled on structural highs and the GAG-05 well is the only permeability data point from a deeper fault block. An interpolated permeability map based on the available data is not considered useful for determining the permeability at the location of the proposed geothermal doublet location. Instead, the permeability range is determined by using the results for the nearby HVS-01 well and the porosity-depth relation from Figure 4-4. This is explained in more detail in Chapter 5.2.

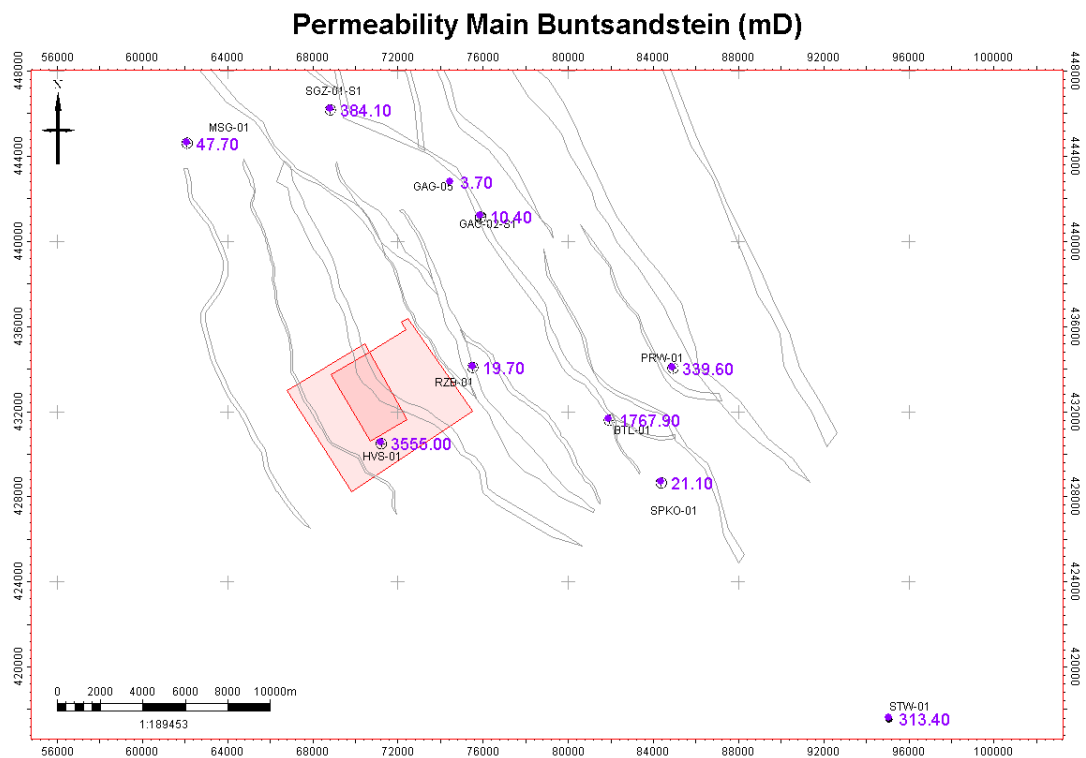


Figure 4-5 Average permeability values for the Main Buntsandstein in the evaluated wells. The geothermal exploration licenses indicating the study area are shown in red. Fault polygons at Top Triassic level are shown in black. Fault polygons are only shown over the area that is covered by available seismic data.

Figure 4-6 shows the petrophysical evaluation for the well PRW-01. This well is exceptional because cores have been taken over the entire Triassic interval. Figure 4-6 illustrates the good match between the calculated porosity and permeability logs and the porosity and permeability core measurements.

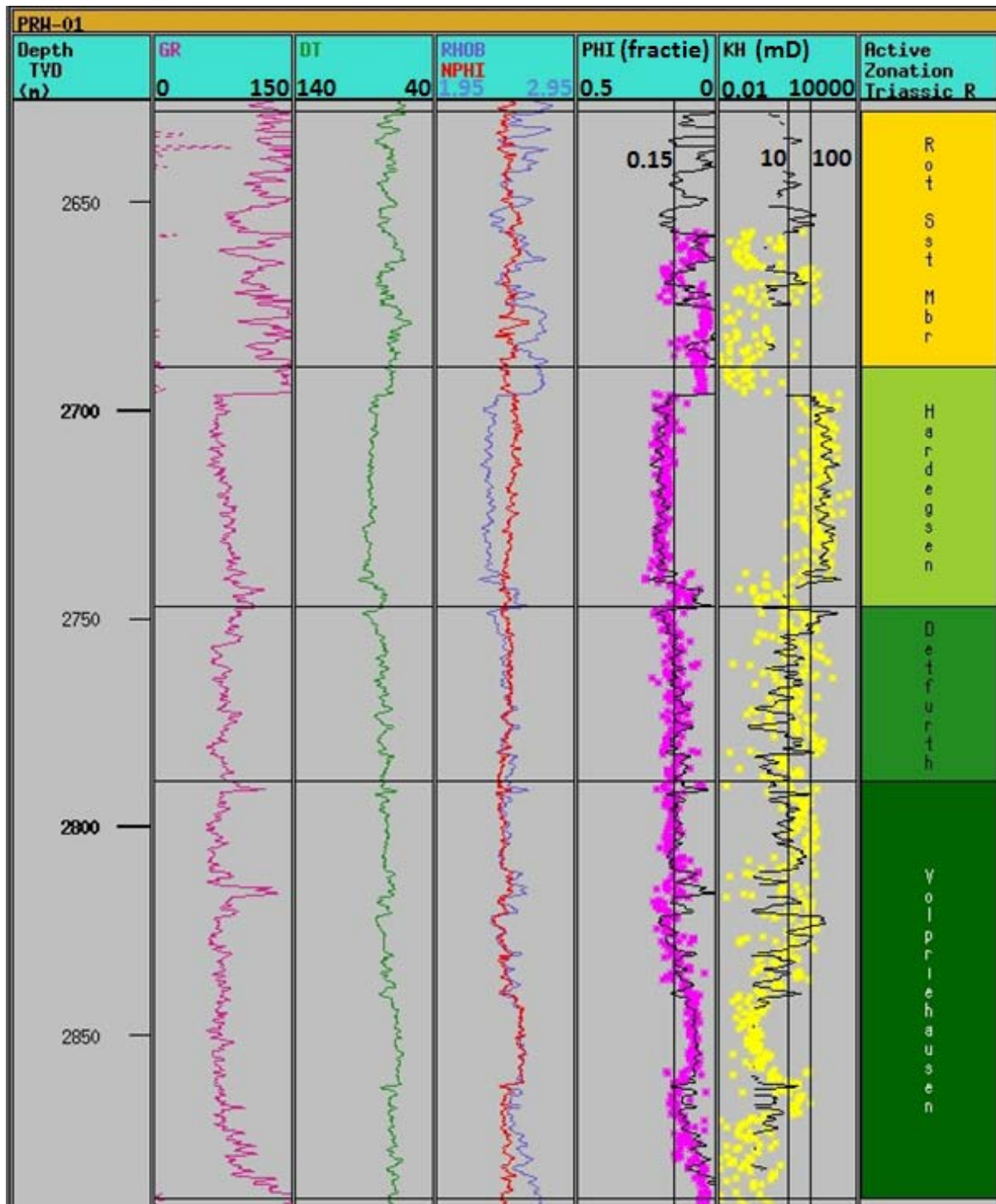


Figure 4-6 Wireline logs, calculated logs and core measurements over the Triassic interval in the well PRW-01. Column 1 shows true vertical depth in meters. GR = Gamma-Ray log, DT = Sonic log, RHOB = Density log, NPHI = Neutron density log, PHI(fractie) = calculated porosity in fractions, KH = calculated permeability in milliDarcy. The pink dots show the porosity measurements in the core, the yellow dots show the permeability measurements in the core. The Röt clay (low permeability) and the Solling Formation sands are included in the evaluated interval.

4.2.4 Averages

A cut-off of $V_{cl} < 50\%$ and a cut-off of $\phi > 8\%$ have been applied to calculate the average Net/Gross ratio and average porosity. The arithmetic averages of the results of the petrophysical evaluation are shown in Table 4-1. The transmissivity (in Darcy*meter, Dm) is calculated by multiplying the net thickness with the average permeability. The HVS-01 well is a positive exception with an average porosity of 21.6% in the Main Buntsandstein. The average permeability calculated for HVS-01 is high, in particular compared to expected permeability values in other wells.

Table 4-1 Average porosity (%), Net/Gross (%), permeability (milli Darcy mD) and transmissivity (Darcy*meter, Dm) for each sandstone interval and for the entire Main Buntsandstein Subgroup. A cut-off of $V_{cl} < 50\%$ and a cut-off of $\phi > 8\%$ have been applied to calculate average N/G, average porosity and average permeability. Thickness is based on tops as proposed by Matev (2011). Averages shown are arithmetic averages. *Hardeggen partly eroded; in HVS-01 the average is calculated from base Solling to base Hardeggen.

	Rot Sst Mbr					Main Buntsandstein Subgroup				
Well	Thickness	Porosity	N/G	Permeability	Transmissivity	Thickness	Porosity	N/G	Permeability	Transmissivity
BTL-01	58.2	21.3	69.9	3810.0	155.0	236.6	17.2	90.9	1767.9	380.2
GAG-02-S1	37.8	10.3	5.6	1.8	0.0	199.3	12	79.9	10.4	1.7
GAG-05	44.1	8.7	1.4	0.4	0.0	179.4	10.2	24	3.7	0.2
GAG-05 Deep			0			not complete interval				
HVS-01*	Eroded					148.5	21.6	93.9	3554.9	495.7
MSG-01	24.2	11.4	7.9	5.0	0.0	183.2	12.5	76.6	47.7	6.7
PRW-01	73.6	14	39.2	53.1	1.5	199.6	15.4	76.9	339.6	52.1
RZB-01	47.4	12.5	53.9	12.6	0.3	213.1	12.3	79.3	19.7	3.3
SGZ-01-S1	72.8	9.4	1.1	0.9	0.0	203.8	14.4	75.6	384.1	59.2
SPKO-01	81.7	20.6	60.7	2753.2	136.6	206.2	14	85.5	21.1	3.7
STW-01	81.2	20.9	44.7	3712.7	134.7	183.8	16.4	92.9	313.4	53.5
	Hardeggen Fm (=Low Rot+Solling+Hardeggen)					Detfurth Fm				
Well	Thickness	Porosity	N/G	Permeability	Transmissivity	Thickness	Porosity	N/G	Permeability	Transmissivity
BTL-01	76.0	22.7	93.8	5031.6	358.7	36.2	15.3	98.6	457.2	16.3
GAG-02-S1	64.7	12.6	81.4	22.8	1.2	39.7	11.6	75.8	3.1	0.1
GAG-05	62.2	10.7	56.9	9.9	0.4	29.6	8.7	22	0.2	0.0
GAG-05 Deep	79.9	10.5	37	121.8	3.6	Not penetrated				
HVS-01*	33.5	20.5	86.7	3297.5	95.8	38.0	20.6	99.6	2662.3	100.7
MSG-01	78.5	13.9	88.5	106.0	7.4	26.7	12.6	89.7	10.1	0.2
PRW-01	57.4	19.3	82.3	1089.0	51.5	42.0	14.3	99.4	48.8	2.0
RZB-01	57.4	14	91.4	57.0	3.0	39.9	12.1	95.1	7.9	0.3
SGZ-01-S1	63.9	19	83.6	1213.1	64.8	38.7	12.2	58.8	4.7	0.1
SPKO-01-S1	70.6	16.6	88.9	8.2	0.5	31.8	12.2	93	8.2	0.2
STW-01	41.2	18.6	89.1	1006.7	37.0	27.3	15.2	96.2	68.7	1.8
	Volpriehausen Fm									
Well	Thickness	Porosity	N/G	Permeability	Transmissivity					
BTL-01	124.4	14.5	87.2	155.4	16.9					
GAG-02-S1	94.9	11.7	78.9	5.0	0.4					
GAG-05	87.5	8.9	5.2	0.4	0.0					
GAG-05 Deep	Not penetrated									
HVS-01*	77.0	22.6	94.3	4107.5	298.2					
MSG-01	77.9	10.4	60.5	1.9	0.1					
PRW-01	100.2	13.2	64.4	31.8	2.1					
RZB-01	96.3	10.4	63.1	6.4	0.4					
SGZ-01-S1	101.2	11.8	77.1	6.1	0.5					
SPKO-01-S1	103.9	12.6	80.9	33.9	2.8					
STW-01	115.2	15.9	93.5	123.4	13.3					

4.3 Salinity

The salinity of the formation water depends on the type of rock, temperature of the water and the presence of salt layers. The salinity of the formation water is calculated using resistivity logs. This has been carried out for the wells PRW-01, RTD-01 and RZB-01. Calculations show a salinity of 140,000 ppm NaCl for the Detfurth and Volpriehausen sandstone layers. Water at room temperature can contain up to 320,000 ppm NaCl in solution, so the formation water salinity should not pose any problems in a geothermal doublet installation.

It must be noted however, that the chemical composition of the formation water is important as other chemical components can cause scaling problems in the installation. It is strongly recommended to take a water sample at reservoir conditions during the drilling of the first well.

4.4 Temperature

The local temperature at depth in the study area can be estimated by applying an appropriate temperature gradient of the area. The general average gradient for the Netherlands is $T = 10 + 0.031 * D$, where T = temperature in °C and D = depths in meters. As is evident from the estimated temperatures at 2500 m depth as calculated by TNO and shown in Figure 4-7, considerable variation is seen between the wells. In order to investigate possible differences between the general average Dutch temperature gradient and the local temperature gradient in the study area, the borehole temperature data (BHT) of several nearby wells have been investigated.

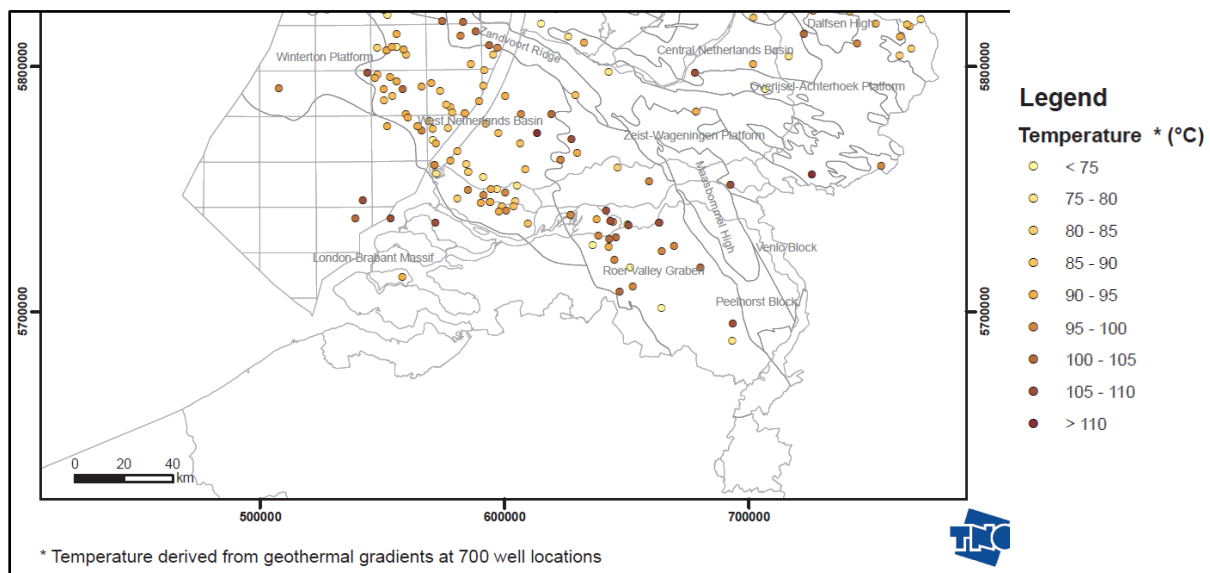


Figure 4-7 Temperature at 2500 m, derived from geothermal gradients at 700 well locations (by TNO, www.nlog.nl).

BHT data is from measurements of the temperatures of the mud in the borehole. BHT data are always lower than the true formation temperature away from the borehole, due to the cooling effect of the mud during drilling. Cooling effects can be corrected using the Horner plot (Fertl and Timko, 1972). To correct BHT circulation times and time since circulation must be known. The estimated formation temperatures were calculated from the BHT data from log headers. Corrections of the BHT are based on the CTRM method. Temperatures were calculated for the wells HVS-01, RZB-01 and SPKW-01. Well MSV-01 (+sidetracks) has BHT data but no circulation time, so this well was not used. For all gradients a surface temperature of 10 °C was applied. The resulting temperature gradients are shown in Table 4-2. The input data for the calculations and the results are given in Appendix 8.5.

For the HVS-01 well, a temperature log is available as well. However, log measurements from 2250 m and deeper are erratic and considered unreliable. This is shown in Figure 8-11 in Appendix 8.5. The temperature log has therefore not been used to determine a suitable temperature-gradient for the Brielle area.

Table 4-2 Temperature gradients deduced from BHT data evaluation.

Well	Temperature gradient
HVS-01	$T = 0.0288 * D + 10$
RZB-01	$T = 0.0332 * D + 10$
SPKW-01	$T = 0.0337 * D + 10$
General gradient of The Netherlands	$T = 0.031 * D + 10$

The HVS-01 BHT evaluation yields a relatively low temperature gradient. The temperature gradients in the West Netherlands Basin mainly depend on the capacity of the rock sequence to conduct heat. This means that rocks sequences with a higher thermal conductivity will have a lower gradient. Variations in local temperature gradients are therefore the result of variations in the rock types of the various geological formations. The HVS-01 well was drilled near the southern margin of the West Netherlands Basin on a relatively high fault block. It is possible that the geological setting is the reason for the lower temperature gradient as the Late Jurassic – Lower Cretaceous sequence has largely been eroded or not deposited at HVS-01. The possibility that the temperature data for this well are less reliable due to the use of relatively older tools can also not be excluded. The HVS-01 well was drilled in 1969. However, this possibility is considered less likely. Some other wells drilled in the sixties record high temperatures, so it cannot be assumed that all tools used in that period underestimate the temperature.

The uncertainty is large and therefore the preferred method is to use a combination of the BHT data from wells HVS-01, SPKW-01 and RZB-01 (Figure 4-8). These wells are closest to the study area. This gives a gradient of:

$$T = 0.0314 * D + 10$$

This gradient, which is very similar to the general Dutch temperature gradient, will be applied during this study. The resulting temperature map for the mid of the Main Buntsandstein in the study area is shown in Figure 4-9.

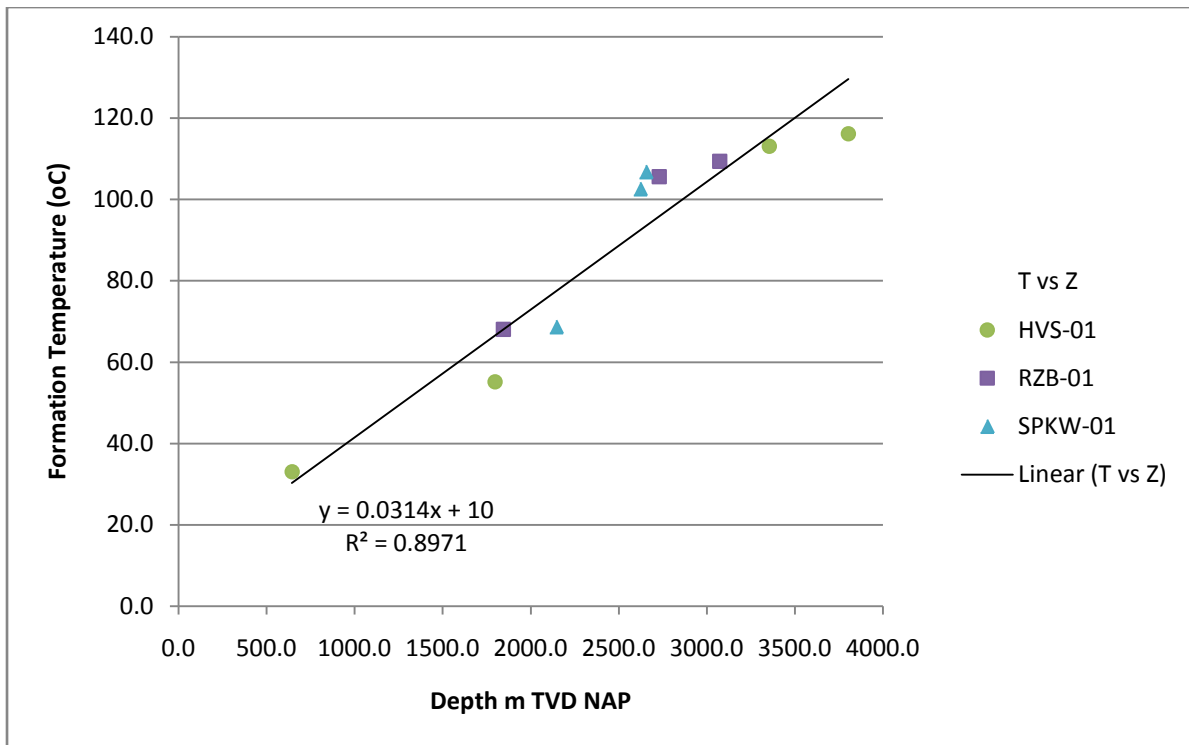


Figure 4-8 Temperature gradient based on combined BHT data (corrected for time since circulation) from the HVS-01, RZB-01 and SPKZ-01 wells. The black line is the gradient based on all temperature data. The input for this graph is shown in Appendix 8.5.

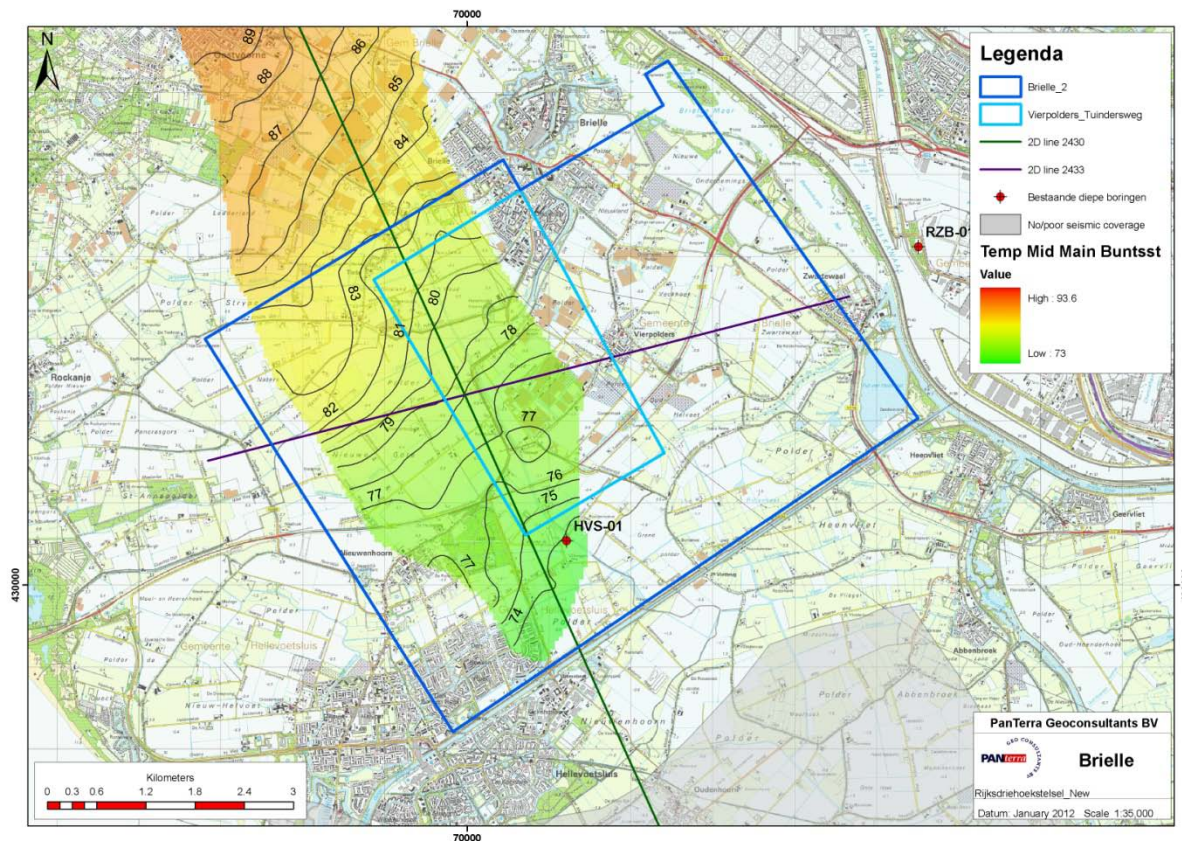


Figure 4-9 Temperature map of the middle of the Main Buntsandstein in the study fault block, based on the temperature gradient $T = 0.0314 * D + 10$.

5 Geothermal doublet

5.1 Proposed well configuration

Two wells are proposed for the geothermal doublet, one producer and one injector. The following criteria were taken into account in the planning of the doublet:

- Distance between producer and injector > 1500 m at mid aquifer level.
- Minimum distance to faults > 750 m.
- Proper seismic control along the proposed well path.
- Wells are not drilled into closed structures in order to minimize the risk of encountering accumulation of hydrocarbons in small stratigraphic traps.
- Highest temperature that can be reached from the surface location within the constraints of technical and financial feasibility and the license boundaries. The distance between the point where the producer penetrates the base of the reservoir and the license boundary is about 1480 m.
- The possibility to place an additional producer in the future. Space for an additional producer is defined as follows: a second producer in the same fault block would have to be at least 1500 m away from the currently planned producer at mid aquifer level and should also be at least 750 m away from faults.

The proposed doublet is shown on the map in Figure 5-7.

- **Producer**

The proposed well BRI-GT-01 is the producer and will be drilled from surface location:

X = 70444 and Y = 432190 (RD)

The kick-off point will be at 450 m depth from where the inclination will be built up to the maximum of 46° with an increase of 5° per 50 m and a constant azimuth of 278°. The deviation table is given in Appendix 8.7. The geological TD (Total Depth) is planned just below the base of the Main Buntsandstein. The expected depths of the main lithostratigraphic layers are shown in Table 5-1.

The 2D line 852117 provides good seismic control on the well trajectory of the proposed producer, as shown in the seismic cross-section in Figure 5-2. The proposed producer is also projected onto the 2D seismic lines 2033 (Figure 5-3) and 2030 (Figure 5-4). The location of the seismic cross-sections is shown on the maps in Figure 5-1 and Figure 5-6.

Table 5-1 Expected formation tops for the proposed well BRI-GT-01 (producer). The reference point for the drilling distance MD is taken at 0 m NAP. The highlighted surfaces are interpreted on seismic. Based on the interpretation, depth maps are created from which the expected depth in the proposed wells is determined. The depth of the other surfaces is estimated based on the expected thicknesses as deduced from existing wells.

Surface	MD (m)	TVD (m)	X	Y	Depth margin
Top Houthem Fm	1297	1132	69996.64	432252.87	± 75
Base Tertiary	1426	1222	69904.07	432265.88	± 75
Base Chalk	2407	1903	69205.79	432364.02	± 75
Base Cretaceous = Top Triassic	2642	2067	69037.85	432387.62	± 100
Top Röt Fringe Sandstone	2723	2123	68980.21	432395.72	± 100
Top Main Buntsandstein	2820	2191	68911.17	432405.43	± 100
Base Main Buntsandstein (TD)	3111	2393	68703.81	432434.57	± 100

- **Injector**

The proposed well BRI-GT-02 is the injector and will be drilled from the same surface location as the producer:

X = 70444 and Y = 432190 (RD)

The kick-off point will be at 1300 m depth from where the inclination will be built up to the maximum of 15° with an increase of 5° per 50 m and a constant azimuth of 230°. The deviation table is given in Appendix 8.7. The injector has not been planned vertical in order to avoid possible closure that is contoured on the depth maps directly northeast of the doublet surface location (discussed in Chapter 5.4 and shown in Figure 5-11). The seismic coverage here is poor and the closure may well be an artefact of the relative positioning of the 2D seismic lines. However, to be on the safe side the injector well is deviated away from the possible structure. The geological TD (Total Depth) is planned just below the base of the Main Buntsandstein. The expected depths of the main lithostratigraphic layers are shown in Table 5-2.

The 2D lines 2033 and 2030 provide good seismic control on the well trajectory of the proposed injector, as shown in the seismic cross-sections in Figure 5-3 and Figure 5-4. The proposed injector is also projected onto the 2D seismic line 852117 (Figure 5-2), which is located relatively far from the well. The location of the seismic cross-sections is shown on the maps in Figure 5-1 and Figure 5-6.

Table 5-2 Expected formation tops for the proposed well BRI-GT-02 (injector). The reference point for the drilling distance MD is taken at 0 m NAP. The highlighted surfaces are interpreted on seismic. Based on the interpretation, depth maps are created from which the expected depth in the proposed wells is determined. The depth of the other surfaces is estimated based on the nearby HVS-01 well.

Surface	MD (m)	TVD (m)	X	Y	Depth margin
Top Houthem Fm	1132	1132	70444.00	432190.00	± 75
Base Tertiary	1222	1222	70444.00	432190.00	± 75
Base Chalk	1895	1878	70340.86	432103.45	± 75
Base Cretaceous = Top Triassic = Top Main Buntsandstein	2067	2044	70306.76	432074.85	± 100
Base Main Buntsandstein	2260	2230	70268.53	432042.76	± 100

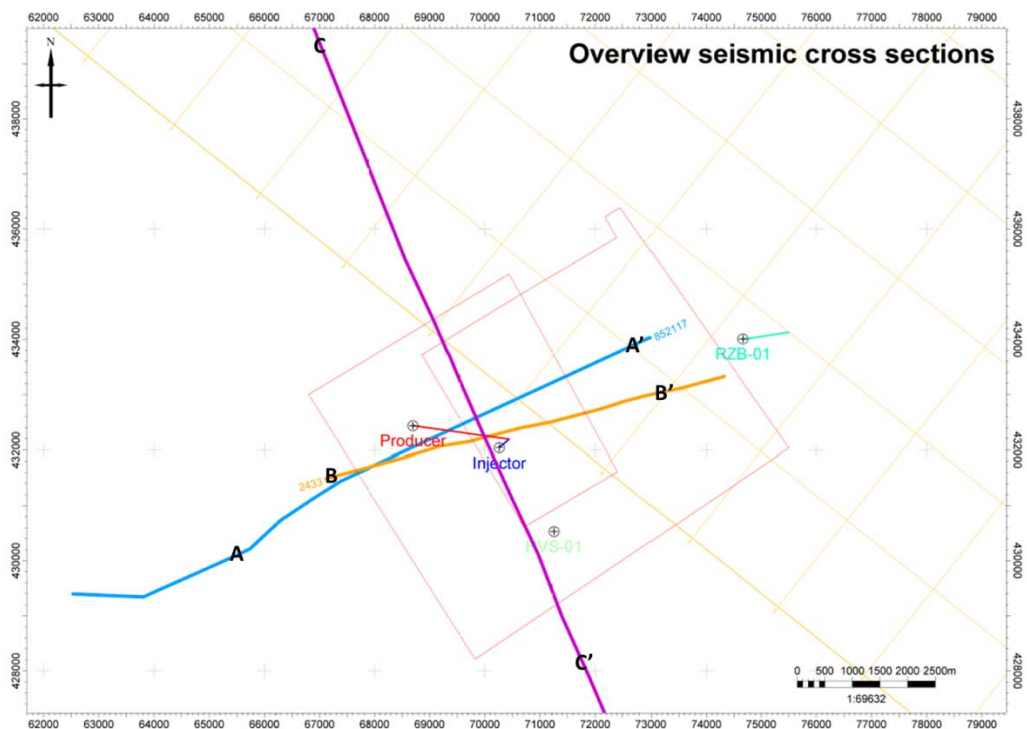


Figure 5-1 Overview map of the seismic cross-sections shown in Figure 5-2, Figure 5-3 and Figure 5-4.

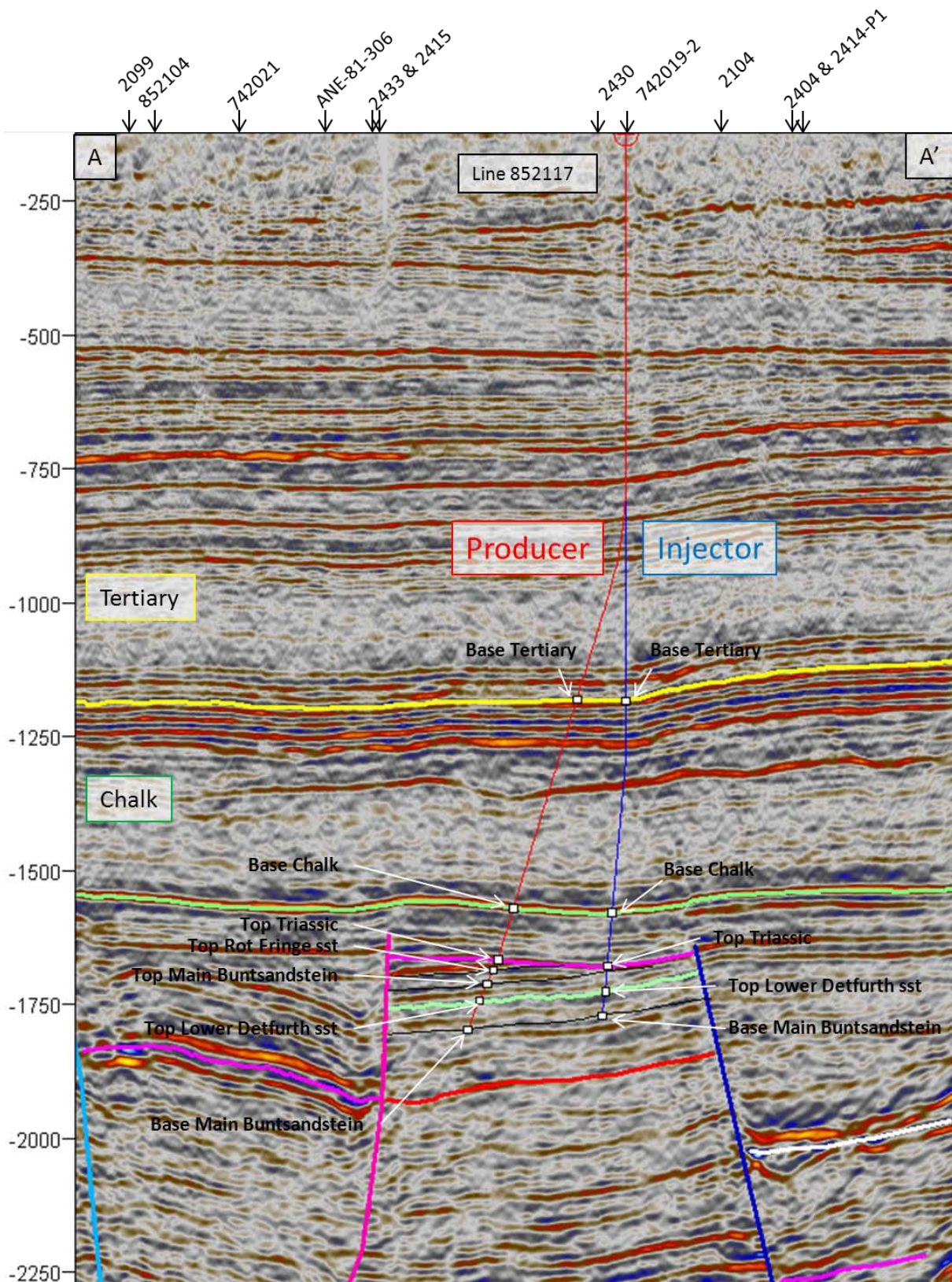


Figure 5-2 Seismic cross-section along 2D line 852117, showing the proposed producer (BRI-GT-01) and injector (BRI-GT-01). No major faults cut through the proposed well trajectories at reservoir level. The position of this cross-section, A-A', is shown in Figure 5-1. The red line = Base Permian Unconformity. Cross-section of this line with other 2D lines is indicated by the arrows at the top.

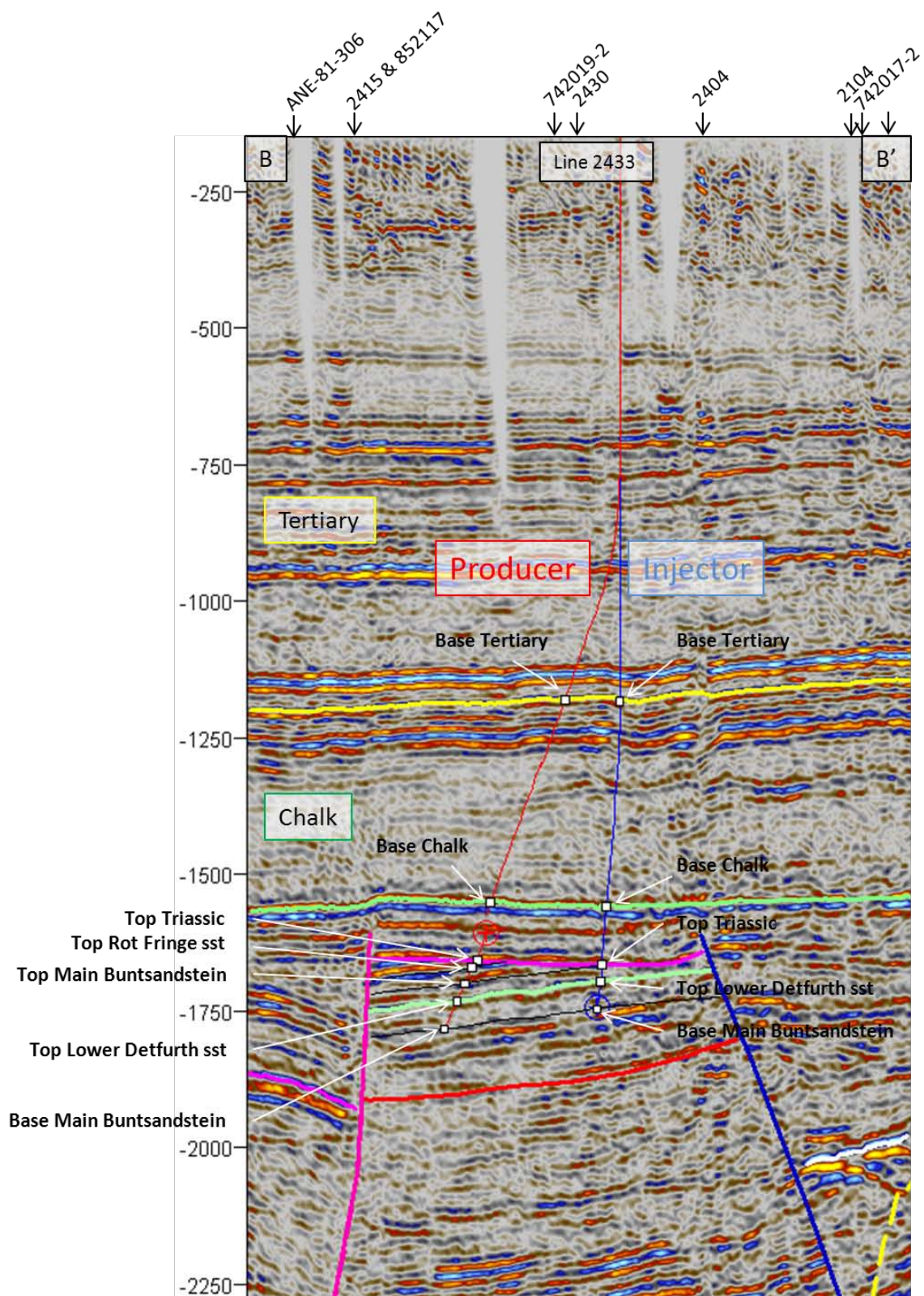


Figure 5-3 Seismic cross-section along 2D line 2433, showing the proposed producer (BRI-GT-01) and injector (BRI-GT-01). No major faults cut through the proposed well trajectories at reservoir level. The position of this cross-section, B-B', is shown in Figure 5-1. The red line = Base Permian Unconformity. The apparent kink in the well path of the producer is due to the distance of the well to line 2033. Cross-section of this line with other 2D lines is indicated by the arrows at the top.

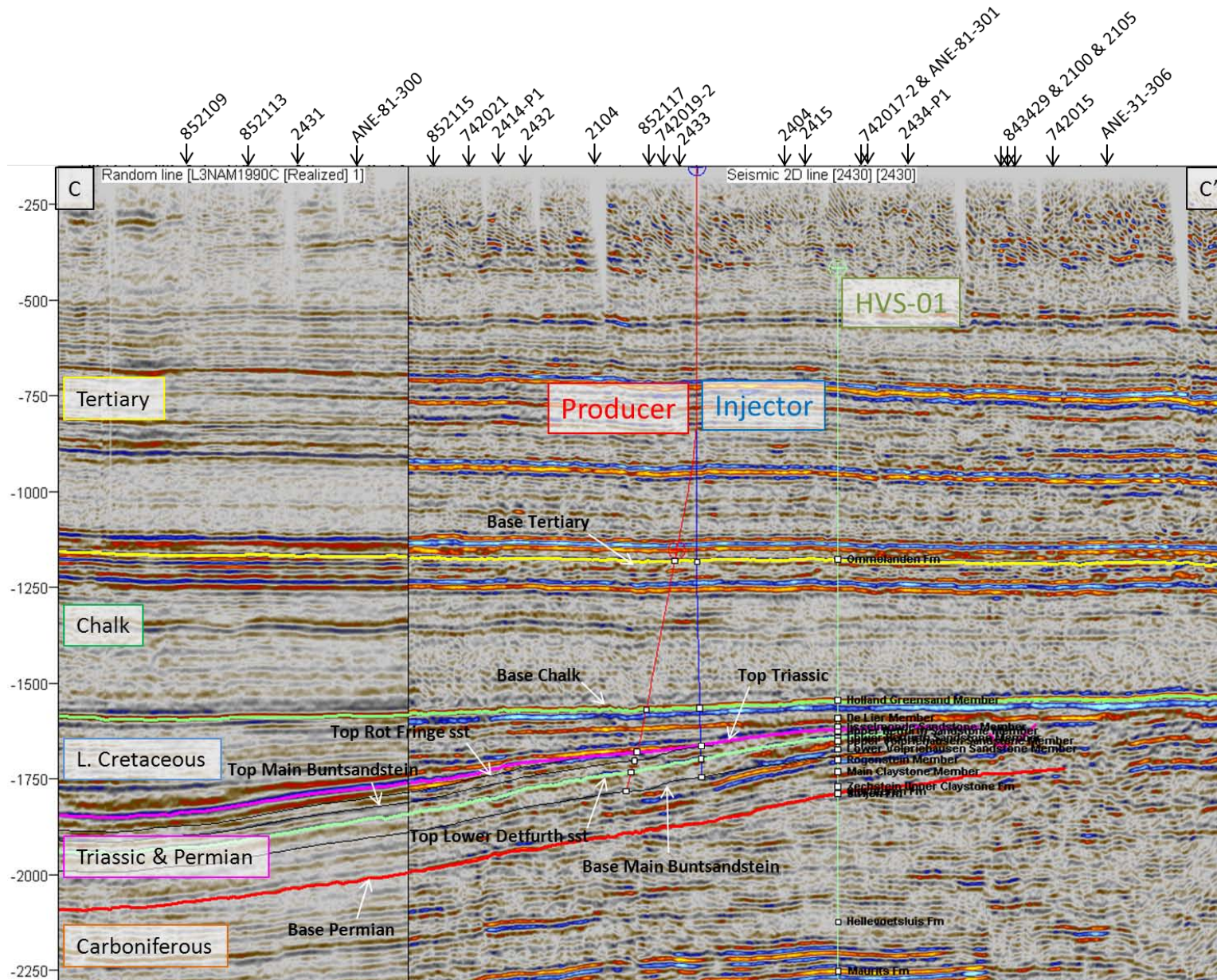


Figure 5-4 Seismic cross-section along composite line of the L3NAM1990C survey and 2D line 2430, showing the proposed producer (BRI-GT-01) and injector (BRI-GT-01). No major faults cut through the proposed well trajectories at reservoir level. The position of this cross-section, C-C', is shown in Figure 5-1. Cross-section of this line with other 2D lines is indicated by the arrows at the top.

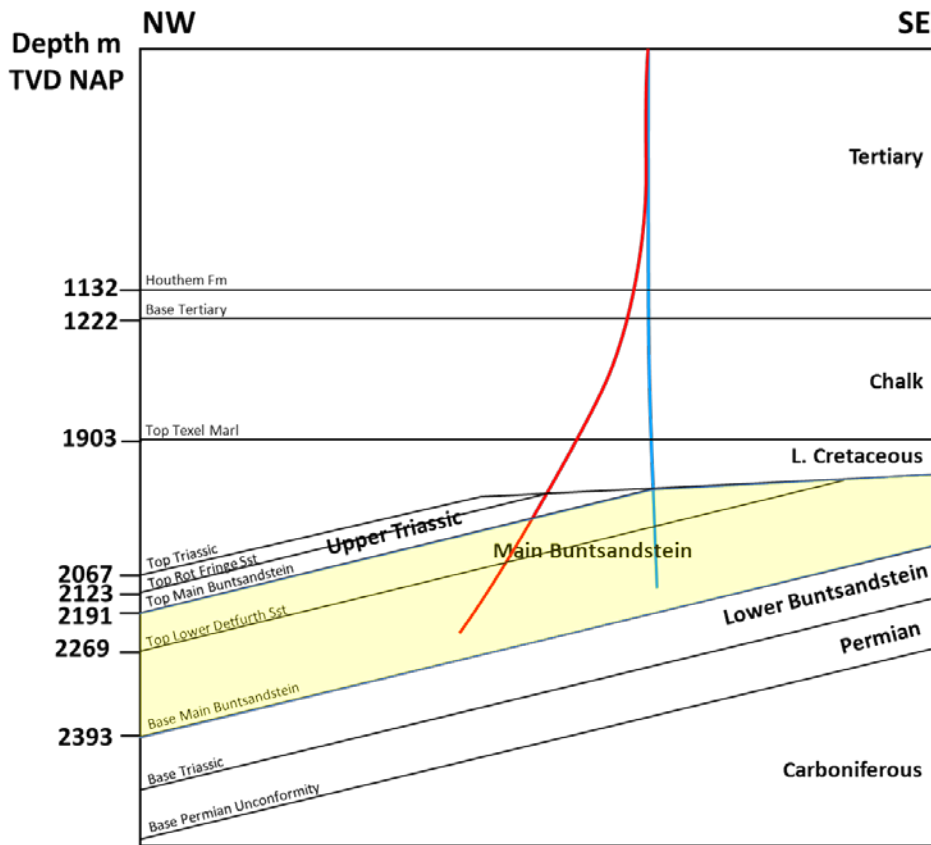


Figure 5-5 Schematic cross section through the geothermal doublet. The producer is shown in red and the injector is shown in blue. Shown depths are the depths in the producer. NB This image is strongly simplified and not to scale.

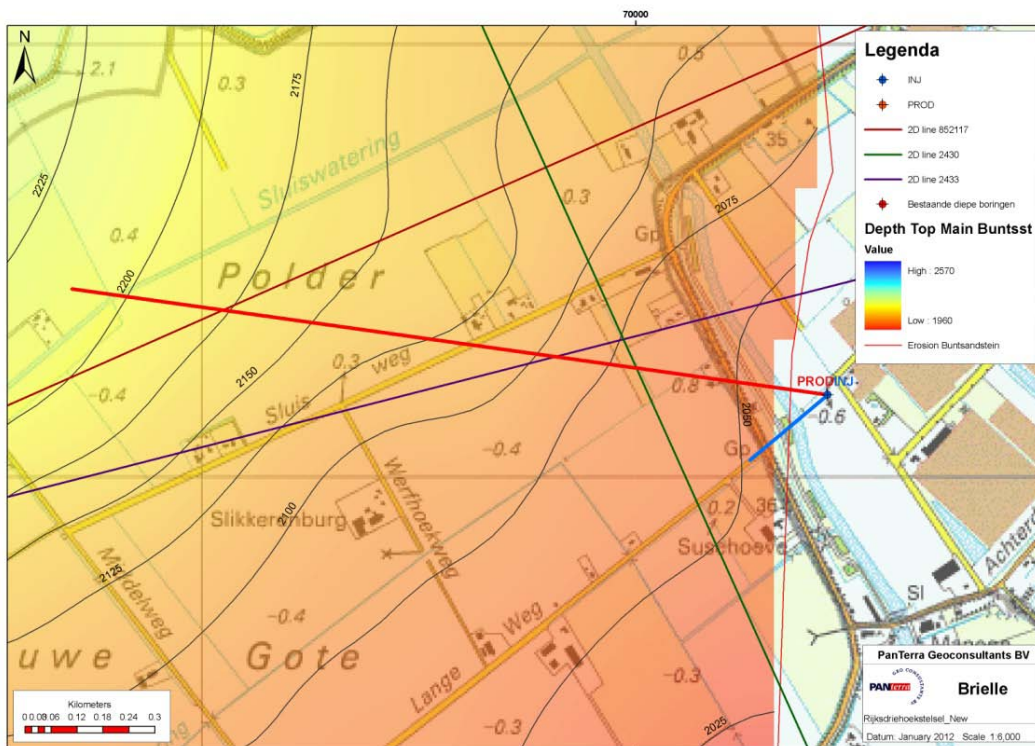


Figure 5-6 Depth map of the top of the Main Buntsandstein with the proposed producer and injector. The 2D lines from Figure 5-2 to Figure 5-4 are shown for reference.

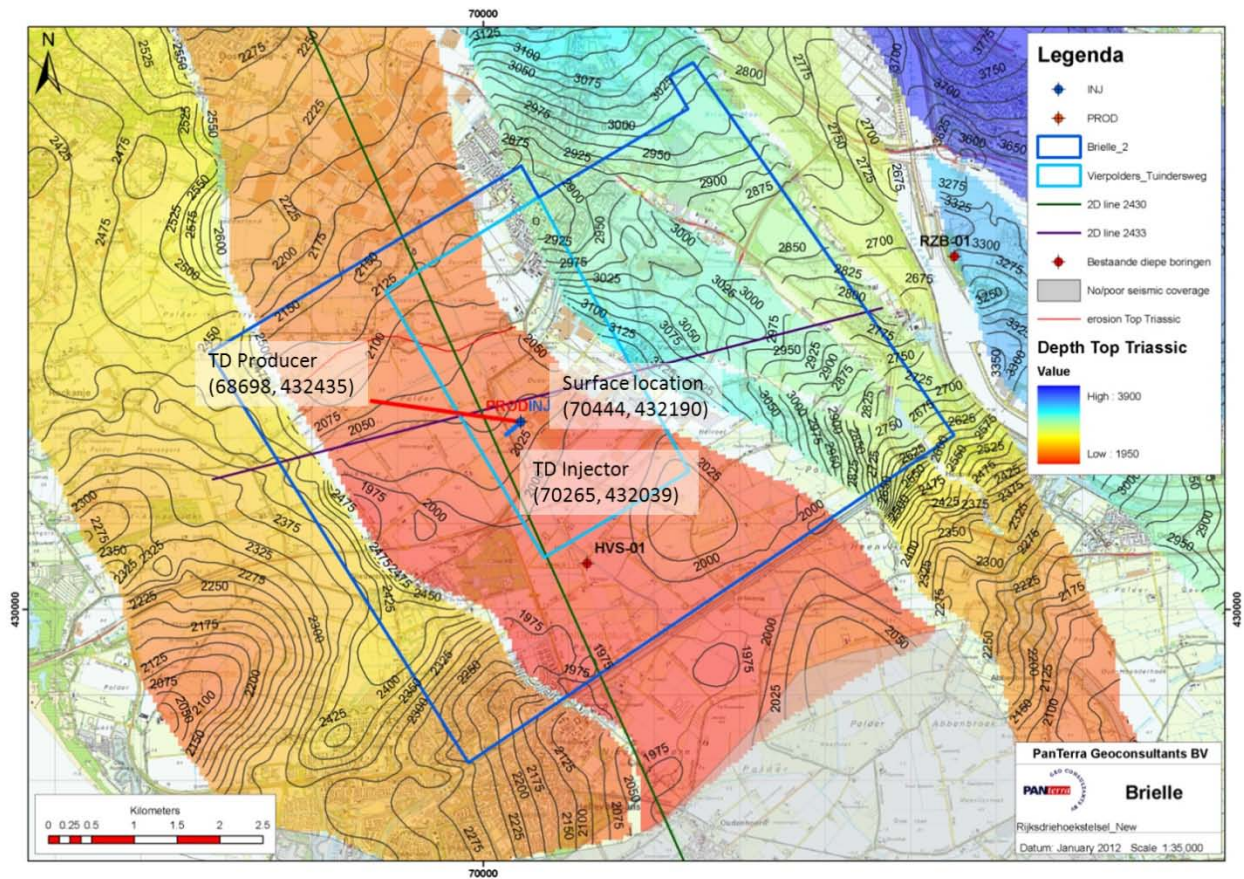


Figure 5-7 Position of the proposed doublet with respect to the Triassic fault blocks. Shown is the depth map of the top of the Triassic (identical to Figure 3-13) with the location of the proposed doublet. The coordinates of the surface location and the TD of the proposed producer and injector are shown.

5.2 Flowrate calculation

The expected flowrate is calculated according to TNO standards by using the *Doublet Calculator* software developed by TNO (*Mijnlieff et al, 2009*). The input for this probabilistic software is realistic estimates and assumptions that are based on the depth, thickness and temperature and reservoir quality as described in this report. Petrophysics, thickness and depth evaluations have been carried out for the Main Buntsandstein and the Röt formation. The Röt formation however, is not expected to be present at the planned injector due to erosion of the upper Triassic. The doublet construction of producer and injector is such that injector and producer are in the same reservoir in order to maintain reservoir pressure. Therefore, the flowrate is calculated over the Main Buntsandstein sequence in the proposed doublet, excluding the Röt formation. The input for the flow rate calculation and the results are discussed below.

A) Aquifer properties

The top of the aquifer in the producer is at 2191 m depth and in the injector at 2045 m depth. The average gross thickness is estimated to be 182 m ± 15 m. The aquifer water salinity is discussed in Chapter 4.3 and the applied geothermal gradient is discussed in Chapter 4.4.

The petrophysical results as described in Chapter 4 and the porosity-depth relation as shown in Figure 4-4 are used to determine the range of permeability and net-to-gross (N/G) values suitable for the flow rate calculations. From the general geology (described in Chapter 1.3) it is known that the reservoir quality of the Main Buntsandstein is very good in the basin fringe area of the West Netherlands Basin. Towards the northeast, the clay content increases and the reservoir quality decreases.

- **Maximum permeability & N/G**

The producer is planned in the basin fringe of the West Netherlands Basin, about 3 km northwest of the HVS-01 well. The reservoir quality is expected to decrease towards the northeast. The petrophysical results for the HVS-01 well are therefore used as maximum input values for the permeability and N/G (set at 3555 mD and 94% respectively).

- **Minimum permeability & N/G**

The porosity-depth relation described in Figure 4-4 can be used to apply a depth correction to the permeability measured in shallower reservoirs. However, the lateral variation of reservoir quality must be taken into account as well. Lateral variation is the result of two processes:

- Depositional environment: higher clay content towards the northeast
- Tectonic movements: the basin was inverted during late Cretaceous and Tertiary times. The fault blocks near the centre of the basin have been buried deeper than their current position, which has reduced the reservoir quality.

The relation of Figure 4-4 is based on nine wells. Most of these wells are located further north/northeast of the target area in parts of the basin that were strongly influenced by inversion. The calculated porosity from the porosity-depth relation from these wells is therefore considered a minimum. This porosity is determined by calculating the porosity at the depth of the middle of the reservoir using the porosity-depth relation. The result is shown on the map in Figure 5-8.

The resulting porosity at the middle of the reservoir in the producer is ~18.1%. This yields a minimum permeability of 210 mD by applying the general porosity-permeability relation for the Main Buntsandstein from Figure 4-1.

The calculated average N/G values for RZB-01 and SPKO-01 are 79.3% and 85.5% respectively. These two wells are located further away from the basin fringe than the planned producer. The minimum N/G ratio input for the doublet is therefore set at 88%.

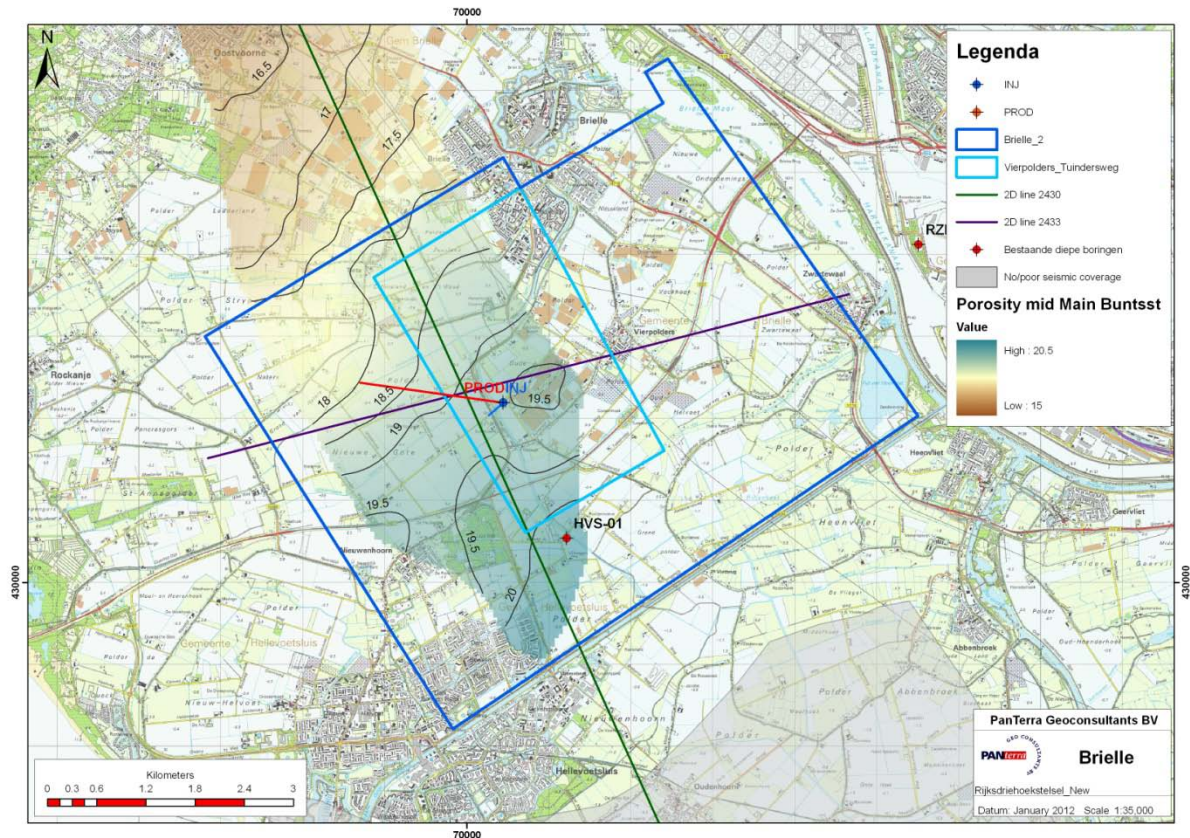


Figure 5-8 Porosity map of the target fault block at mid Main Buntsandstein level. This map has been created by applying the porosity-depth relation from Figure 4-4 to the depth map of the middle of the Main Buntsandstein. The resulting porosities are pessimistic; the calculated porosity for the HVS-01 well is higher than shown on this map.

- Median permeability & N/G

The median aquifer permeability is determined by averaging the minimum calculated porosity (18.1%) and the HVS-01 porosity (21.6%) and applying the porosity-permeability relation for the Main Buntsandstein. The resulting value of 730 mD is used as median permeability input for the planned doublet. The median N/G ratio is set at 91% (the average between the established minimum and maximum).

B) Doublet and well properties

The skin of the wells is used to correct for the fact that the wells cross the reservoir at an angle and has been calculated based on the reservoir thickness, the proposed well inclination and the well bore radius. The calculated skin for the producer is -0.6. The calculated skin for the injector is 0, as this well is almost vertical. The average well bore diameter is 9.625 inch with average 8.679 inch tubing. The horizontal distance between the centre of the aquifer in the producer and the injector is 1524 m. The planned horizontal outstep of the producer is 1547 m at the top of the aquifer and for the injector 179 m. The tubing roughness is assumed to be the same as for the first geothermal doublet in the Netherlands: 1.19 milli-inch. The planned heat exchanger has an exit temperature of 35 °C.

C) Pump properties

The pump system efficiency is set at 0.61. The production pump, with a maximum pump capacity of 450 m³/h will be positioned at 500 m depth. The pump pressure difference is set at 17 bar.

The expected temperature in the middle of the reservoir in the producer (2292 m) is expected to be 82°C. Uncertainty in the depth maps is set at 10%. Minimum temperature in the middle of the reservoir in the producer is therefore 75°C and maximum temperature is 89°C.

An overview of all input for the flow rate calculation is given in Table 5-3 and the results are summarized in Table 5-4 and in Appendix 8.8.

Table 5-3 Input for the flow rate calculation in Doublet Calc.

	min	median	max
aquifer gross thickness (m)	167.0	182.0	197.0
aquifer net to gross (-)	0.88	0.91	0.94
aquifer permeability (mD)	210.0	730.0	3555.0
aquifer top at producer (m)	1972.0	2191.0	2410.0
aquifer top at injector (m)	1841.0	2045.0	2250.0
[aquifer pressure at producer (bar)]		0.0	
[aquifer pressure at injector (bar)]		0.0	
surface temperature (°C)		10.0	
geothermal gradient (°C/m)		0.0314	
aquifer water salinity (ppm)		140000.0	
producer well deviation (m)		1547.0	
injector well deviation (m)		179.0	
distance wells at aquifer level (m)		1524.0	
tubings inner diameter (inch)		8.68	
wells outer diameter (inch)		9.63	
tubings roughness (milli-inch)		1.19	
skin producer (-)		-0.6	
skin injector (-)		0.0	
production pump depth (m)		500.0	
pump system efficiency (-)		0.61	
pump pressure difference (bar)		17.0	
exit temperature heat exchanger (°C)		35.0	
number of simulation runs (-)		1000.0	

Table 5-4 Results of the flow rate calculation for the planned doublet with a pump pressure difference of 17 bar. P90 stands for a probability of 90%, P50 for 50% and P10 for 10%. The base case scenario is close to the P50 values.

	P90	P50	P10	
Pump volume flow	201.4	282.7	411.5	m ³ /h
Required pump power	155.9	218.8	318.6	kW
Geothermal power	9.35	13.94	20.33	MW
COP	57.4	62.5	67.5	kW/kW

The breakthrough time is modelled with the software package Petrasim. The breakthrough time is the calculated time the injected water will take to reach the production well. In this model warming up of injected water was neglected. Logically the temperature of the produced water will go down with time, but it does not mean the geothermal doublet is at the end of its lifetime when breakthrough of the injected water occurs. For this model it was neglected that the water warms up by the existing natural heat flux.

For modelling purposes, the geological model has been simplified. The Petrasim results represent a rough estimate of the breakthrough time. The simplified model is shown in Figure 5-9. This model assumes vertical wells 1500 m apart and a flow rate of 260 m³/hr. Figure 5-10 shows the resulting temperature graph for the production well at the middle of the reservoir. After 30 years the temperature will have decreased 0.05 °C. After 50 years the temperature will decrease with an average of 0.07 °C/yr.

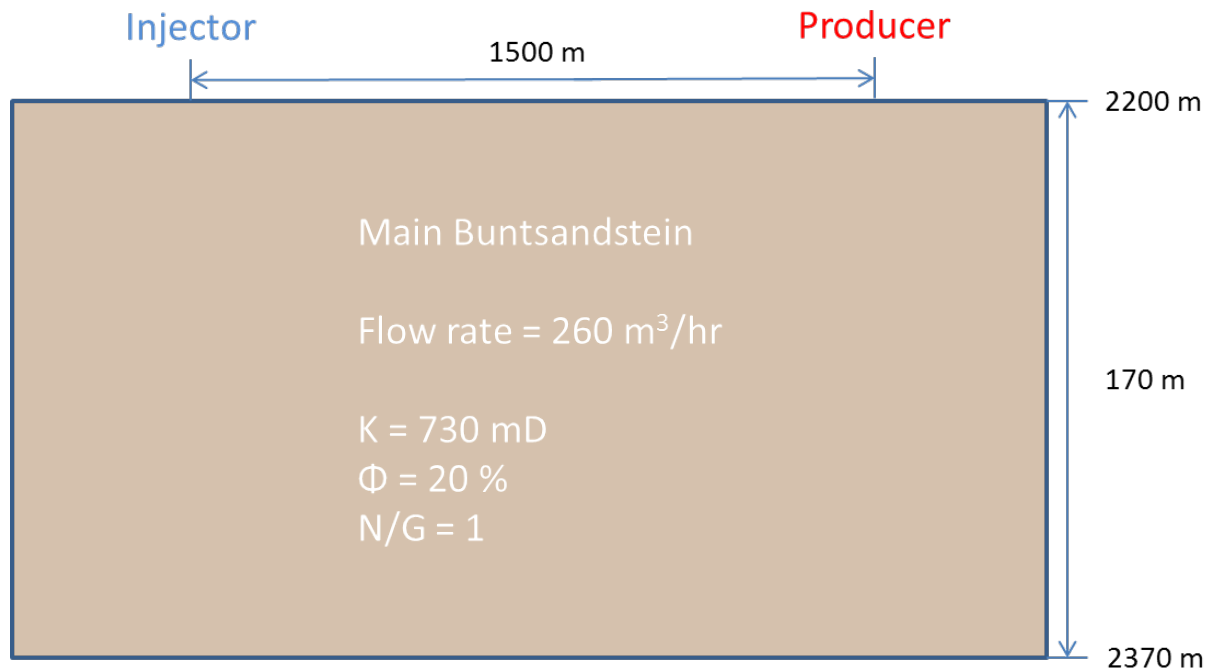


Figure 5-9 Schematic image of the static model that was used to model the temperatures in the reservoir over time. Grid cells size is 50x50x25 m (length x width x height).

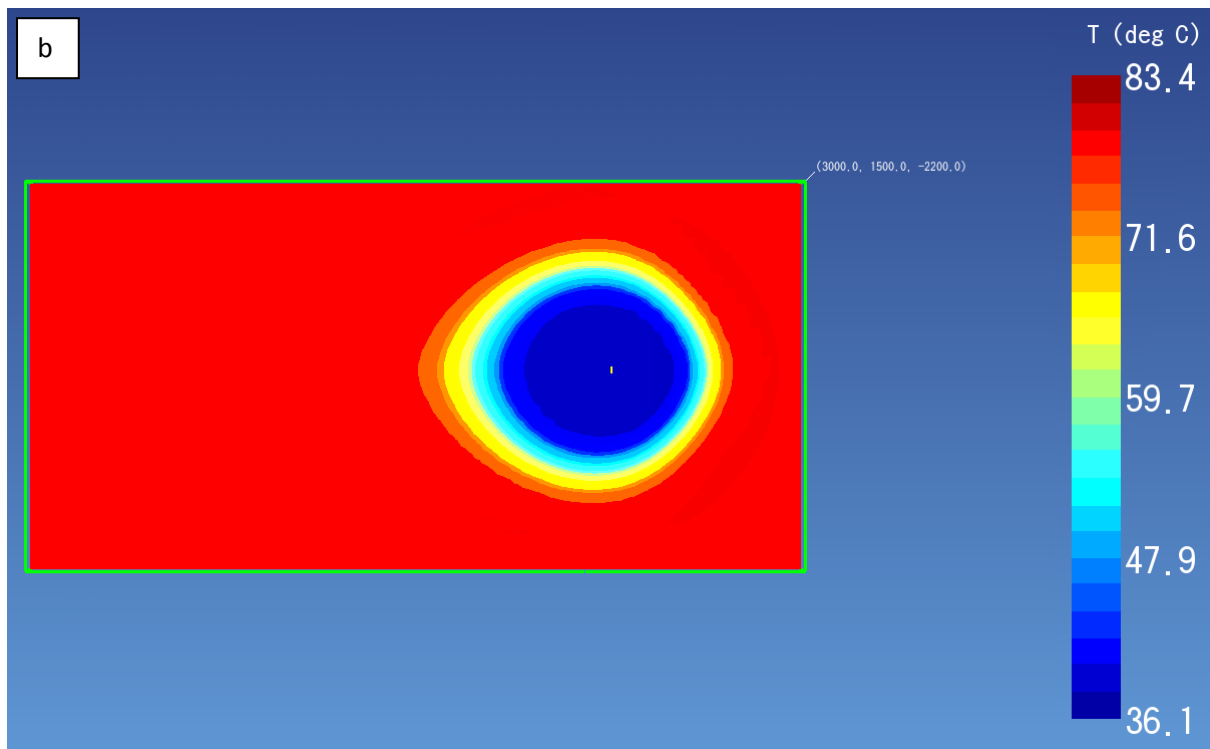
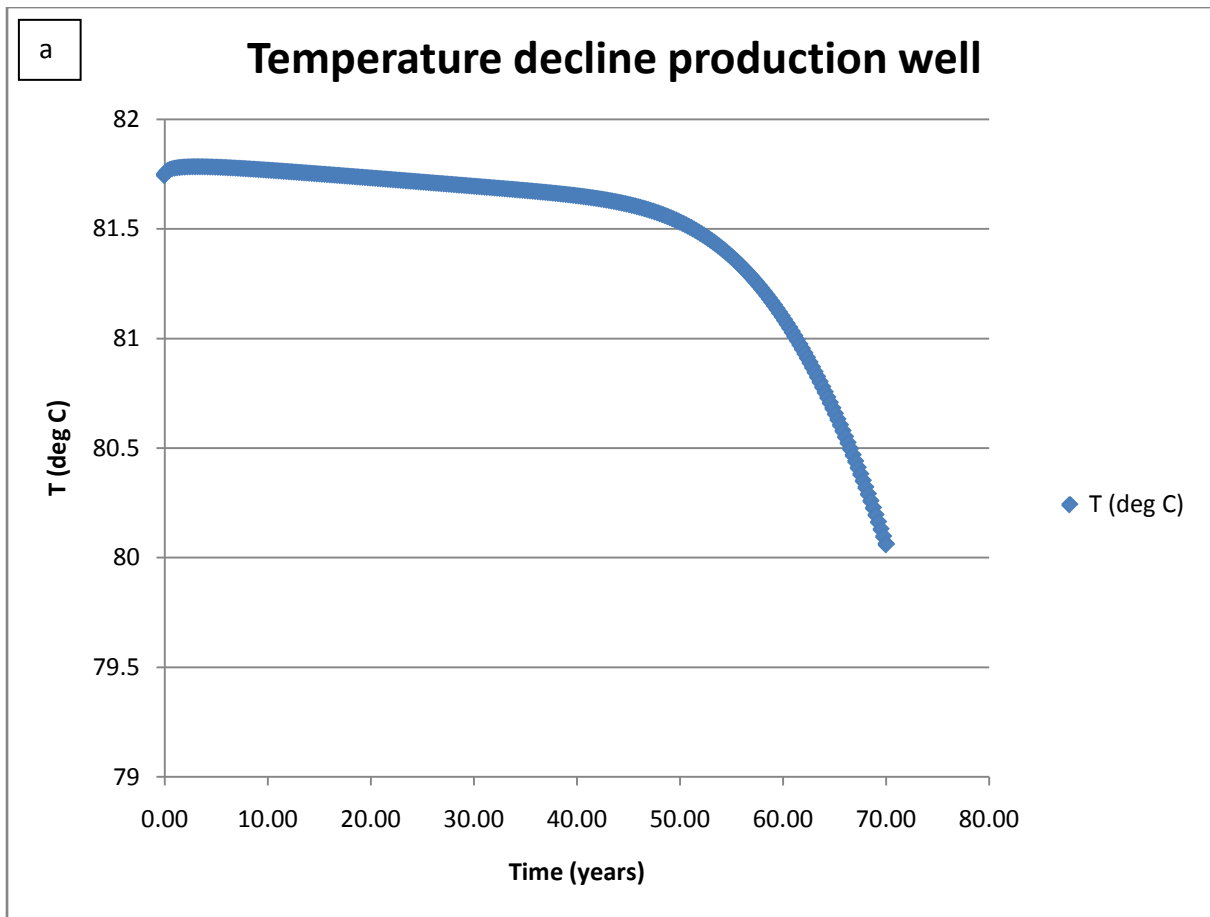


Figure 5-10 a) Temperature decline in the production well. The simulation was run over 70 years. b) Flow model results at 2275 m depth with the temperature situation after 30 years.

5.3 Geological uncertainties

- **Depth and thickness**

The uncertainty with respect to the depth and the thickness of the reservoir depends on:

- The available seismic data
- Time-depth conversion
- Distance to existing wells
- Lateral continuity of the reservoir sandstones

Seismic coverage by the 2D lines is good and the fact that the area is close to the 3D survey L3NAM1990C allows a reliable interpretation and reduces the uncertainty of the seismic interpretation. The uncertainty in the depth maps due to time-depth conversion was evaluated by comparing well tops in existing wells with the depth maps based on the seismic interpretation. The maximum error in these wells is less than 1%. The uncertainty away from the wells that were used for the velocity model is larger. A depth uncertainty of 10% is applied in the flow rate calculations.

The proposed injector is planned close to HVS-01 and the producer is planned 3050 m from HVS-01. Most of the Detfurth formation and the entire Volpriehausen sequence are encountered by HVS-01. The lateral continuity of the Main Buntsandstein sediments is expected to be good, based on regional geological information and the seismic on which no thickness variations can be seen. The uncertainty with regard to the presence and the thickness of the sandstones in the proposed wells is therefore considered low. A thickness range of ± 15 m is applied.

Uncertainty in the mapping of major faults is low due to the use of 3D seismic and migrated 2D seismic. The wells are planned > 750 m from the major faults. Faults with throws smaller than 20 m are not visible on seismic and can therefore be present. Such faults may form a barrier, but fluid flow across small faults can be possible. It is assumed that the major faults are not open, probably cemented and hampering fluid flow.

- **Reservoir quality**

The quality of the reservoir is the main parameter that defines how much water can be pumped up and therefore defines the total geothermal power of the doublet. The uncertainty with respect to reservoir quality depends on:

- Availability of wireline logs and core data from existing wells
- Distance to these existing wells
- The calculation methods

Wireline logs are available for ten wells and core data are available for eleven wells in the southern part of the basin. For two wells, HVS-01 and SGZ-01-S1, only wireline data are available. The number of existing wells that were drilled into the Triassic sequence is not large and most wells are not located close to the target area. However, the vicinity of the planned wells to the HVS-01 well significantly reduces the uncertainty. In addition, the information from the other wells provides essential insight in the reservoir quality and solid ground to extrapolate the reservoir quality of the HVS-01 well to the proposed doublet.

The methods used to calculate the volume of clay and the porosity are proven petrophysical methods that yield reliable results that match the available core data. The uncertainty in the calculated volume of clay and the calculated porosity is low. The method chosen to calculate the permeability is in general use. However, it may result in much uncertainty. One reason is that it is dependent on the choice of trend line through the permeability and porosity core data. A second reason is that the core data have not been corrected because no special core analysis is available. A range of 210 mD to 3555 mD is used in the flow rate calculation. The range of Net/Gross values is 88-93%.

- **Temperature**

In previous geothermal projects in the West Netherlands Basin, the general geothermal gradient of the Netherlands has proven to yield acceptable estimates of the temperature of the formation water. The geothermal gradient can however, vary throughout the basin due to variation in thermal conductivity of the various layers in the subsurface. Uncertainty in the temperature estimate in the study area is related to availability of temperature data from existing wells and corrections applied to borehole temperature data. The method used to correct borehole temperature data (Horner plot) is proven and widely applied. The borehole temperature data from wells close to the target area (HVS-01, RZB-01 and SPKW-01) however, suggest different geothermal gradients (Chapter 4.4). This increases the uncertainty. The preferred method in this

report is to use a combination of the BHT data from wells HVS-01, SPKW-01 and RZB-01. This yields a gradient that is similar to the general temperature gradient in the subsurface of the Netherlands. The uncertainty in the depth maps of 10% indicates a minimum temperature in the middle of the reservoir in the proposed producer of 75°C and maximum temperature of 89°C.

5.4 Risk assessment

Due to many wells in this part of the Netherlands most of the drilling risks can be estimated and mitigated. Some of these risks are:

- In the Tertiary swelling clays may occur, causing the pipe to get stuck.
- In the Ommelanden en Texel Chalk (total) mud losses may occur. One of the reasons of these mud losses are incised valleys in the Chalk with a higher quartz content and thus higher permeability. Beneath the GeoMEC-4P Brielle area these incised valleys are not visible on seismic, but local higher permeabilities can still occur throughout the Chalk Group.
- Clays in the Holland and Vlieland can swell. Thick clay intervals are not expected to be present.
- The wells are planned > 750 m from the major faults. Major faults are assumed not to be open, probably cemented and hampering fluid flow. No major faults cut the planned well trajectories, but sub-seismic faults can be present.
- Hydrocarbon risk

The Hydrocarbon risk in the Brielle Vierpolders area has been assessed by PanTerra for GeoMEC-4P in September 2011. This study is carried out by modelling the maturation of source rocks in the vicinity of Brielle using a basin modelling software package (Petromod). The results were reported in PanTerra report G920 and a short summary of the results is given below:

- *The chance of finding a hydrocarbon accumulation is considered small and estimated at 1%.*
- *Experience in the Westland area combined with the knowledge of presence of active source rocks below Vierpolders shows that the chance of finding residual and/or dissolved gas in the formation water of the sandy intervals is large, estimated by PanTerra at 80%. However, the amounts are difficult to estimate. Reliable but short-term tests in the Westland area suggest a gas-water ratio between 0.5 and 1.5 Nm³/m³ methane in formation water. These amounts could be up to 2.2 Nm³/m³ based on solubility of methane.*
- *Up to 2% oil may be present in the formation water but the chance that this occurs is relatively low, estimated by PanTerra at 5-10%.*
- *Hydrocarbons if present will have a composition similar to fields in the area. In case hydrocarbons are present it is expected that it is gas, but presence of some oil cannot be excluded. H₂S will be absent. CO₂ and N₂ may be present with amounts <1.5 % each.*

In the current study the Posidonia shale was mapped. The resulting depths maps of the Posidonia shale versus the target reservoir are given in Chapter 3.4. The Posidonia shale is absent (eroded) in the target fault block, but present in the neighbouring fault block. This is shown in Figure 5-11. All formations in the neighbouring fault block dip towards the southwest and therefore hydrocarbon migration would be expected towards the northeast, away from the project area. This will reduce the risk of presence of oil from the earlier estimate of 5-10% to a lower level, assume 1-2%.

A closure is visible directly northeast of the doublet surface location on the depth maps. The seismic coverage here is poor and the closure maybe an artefact of the relative positioning of the 2D seismic lines. The 2D seismic profiles have been shifted relative to the 3D seismic survey in such a way that horizons from the 3D seismic and the 2D seismic are in line. Further away from the 3D survey, the lines may be slightly off vertically. However, to avoid the possible closure the injector well has been planned away from this possible structure.

The HVS-01 well, which is very close to the proposed doublet, was drilled in 1969 and found to be dry.

The results of the current study do not change the outcome of the hydrocarbon risk assessment (*Panterra G920*) with the exception of the reduction in risk of encountering Posidonia oil.

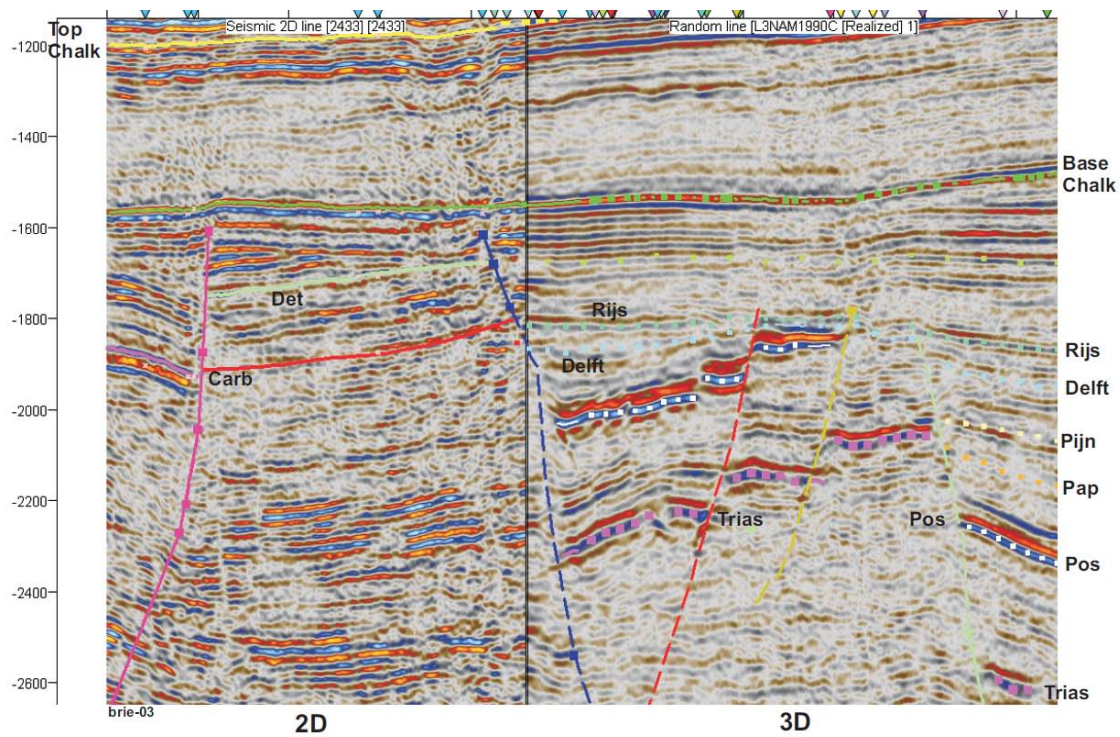
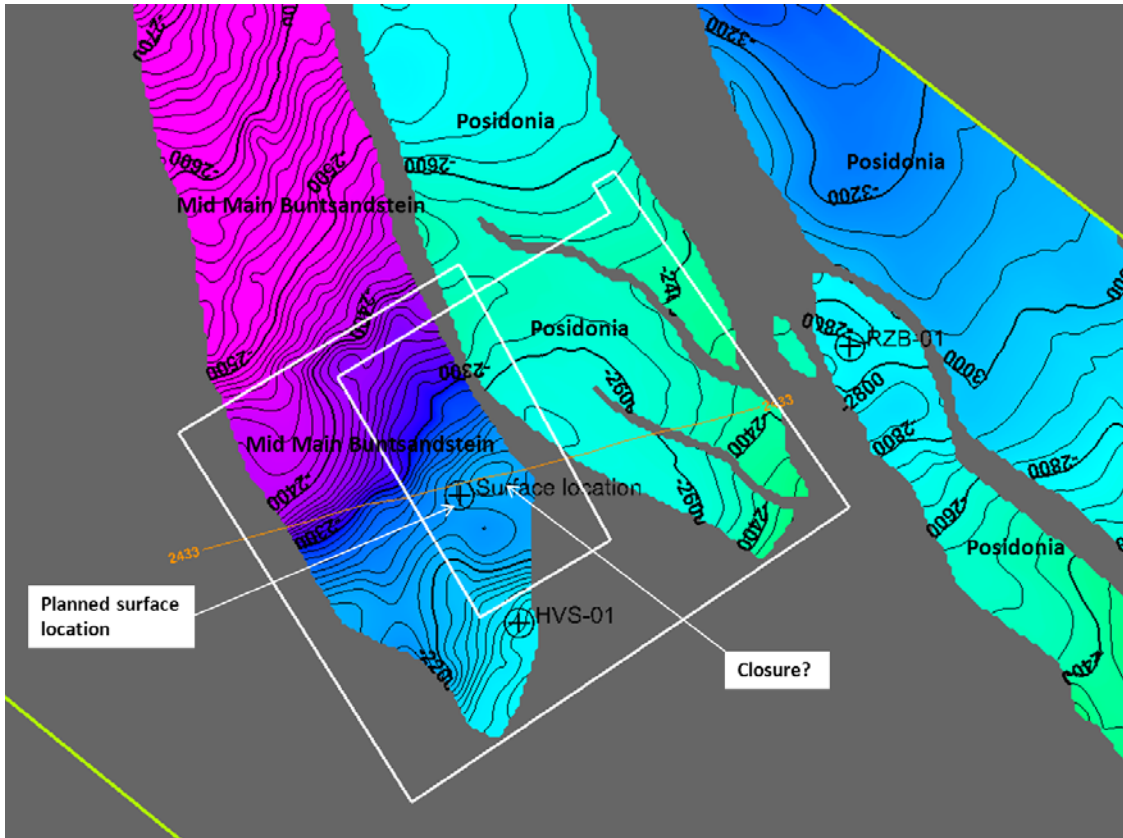


Figure 5-11 Overview map of the depth of the middle of the Main Buntsandstein versus the depth of the Posidonia Shale. The Posidonia shale does not occur in the same fault block as the target area, but does occur in the neighbouring fault block. As visible on the map and on the seismic section of 2D line 2433, all formations in the neighbouring fault block dip towards the southwest. Any hydrocarbon migration is therefore expected to occur towards the northeast, away from the project area.

- Overpressure

In many wells pressure data are available from Drill Stem Tests (DST) and Repeat Formation Testers (RFT). The wells for which pressure data were available are BTL-01, GAG-02-S1, GAG-03, GAG-04, LIR-48, LIR-49, MON-02, MON-02-S1, MON-03, MSG-01, MSG-02, PRN-01, PRN-01-S1, PRW-01, PRW-02, RTD-01, SGZ-01, SGZ-01-S1, SPKO-01-S1, SPKO-02-S1 and SPKW-01. Figure 5-12 shows these tests plotted against the depth. Apart from lower pressures due to production from the De Lier field and the Gaag field, no anomalies are observed. The formations that will be encountered by the proposed producer and injector are thus not expected to be overpressured.

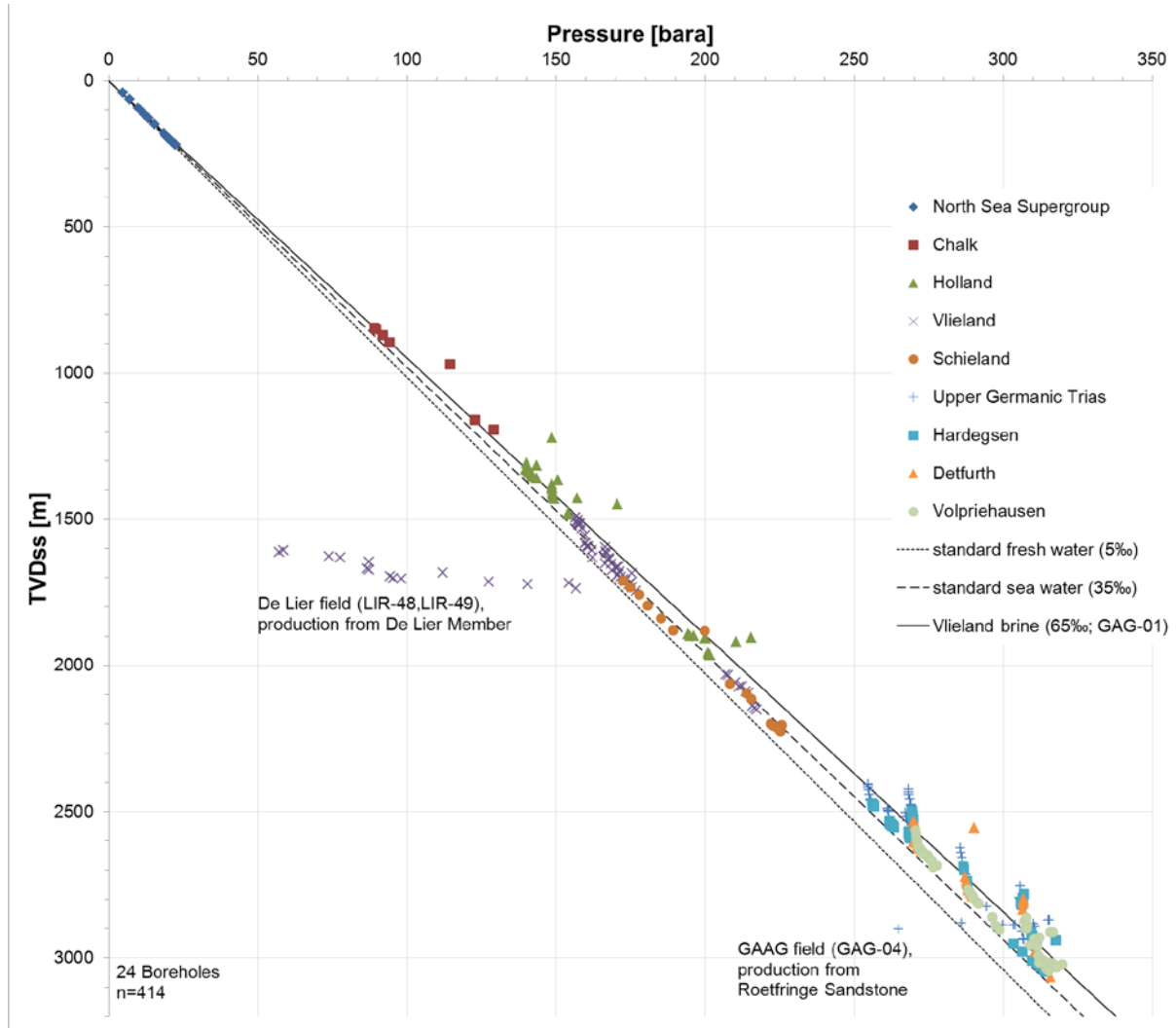


Figure 5-12 Pressure versus depth graph of measurements in 24 wells. The colouring is based on the lithostratigraphic groups. The line shows the hydrostatic gradient.

6 Conclusions

- The HVS-01 well is located within the geothermal licenses and is of key importance for this geological study. Other important wells are RZB-01, SPKW-01, BTL-01 and MSV-01 due to their vicinity to the study area.
- For the seismic interpretation one 3D survey and 30 2D lines have been used. In order to obtain optimal results, only migrated 2D seismic data has been used because migration is important for the correct identification and location of faults and dipping horizons.
- The 3D seismic was interpreted first. The solid interpretation on the 3D seismic significantly contributes to a good interpretation on the 2D seismic.
- The sound interpretation of the Base Permian unconformity in combination with the mapped top of the Lower Detfurth Sandstone provides a strong base for the delineation and thickness estimate of the Main Buntsandstein reservoir.
- The depth of the top of the Main Buntsandstein reservoir within the geothermal licenses Vierpolders and Brielle-2 varies between 1975 and 2275 m. The top of the aquifer in the proposed producer is at 2191 m depth and in the proposed injector at 2045 m depth.
- The determined total thickness of the Main Buntsandstein in the Brielle area is 182 m.
- In the study area, the Houthem Formation occurs on top of the Ommelanden Chalk. The Houthem formation consists of chalk as well and is important for the casing scheme.
- A combination of Borehole temperature data (BHT) from HVS-01, RZB-01 and SPKW-01 corrected for circulation time is used to determine a suitable temperature gradient for the Brielle area. The resulting gradient is: $T = 0.0314 * D + 10$ (T = temperature in °C and D = depths in meters). The expected temperature in the middle of the reservoir in the proposed producer (2292 m) is expected to be 82°C.
- Porosity, permeability and Net/Gross ratio of the reservoir have been calculated for ten existing wells. The results are used to determine the reservoir quality in the study area. The reservoir quality in the planned doublet is expected to be good, with a median estimated porosity of 19.8%, permeability of 730 mD and N/G of 91%.
- A geothermal doublet, with a producer (BRI-GT-01) and an injector (BRI-GT-01) has been planned. The Röt Fringe sandstone is not expected to be present in the planned injector. Flow rate calculations have therefore been performed over the Main Buntsandstein interval only. Doublet Calculator was used for the calculations. The resulting P50 flow rate is 282.7 m³/h resulting in a return of 9.35 MW geothermal power.
- The breakthrough time is modelled with the software package Petrasim. After 30 years the temperature will have decreased 0.05 °C.
- Uncertainties with respect to depth, thickness, temperature and reservoir quality are evaluated.
 - Seismic coverage by 2D lines is good and the fact that the area is close to the 3D survey L3NAM1990C allows a reliable interpretation and reduces the uncertainty of the seismic interpretation. A depth uncertainty of 10% is applied.
 - The uncertainty with regard to the presence and the thickness of the sandstones in the proposed wells is considered low due to the short distance from the HVS-01 well and the continuous character of the Main Buntsandstein sediments. A thickness range of ± 15 m is applied.
 - Uncertainty in the mapping of major faults is low due to the use of 3D seismic and migrated 2D seismic.
 - The vicinity of the planned wells to the HVS-01 well significantly reduces the uncertainty in reservoir quality. The range of Net/Gross values is 88-93%. Uncertainty of the calculated permeability is high. A range of 210 mD to 3555 mD is used in the flow rate calculation.

- Uncertainty in the temperature estimate in the study area is related to availability of temperature data from existing wells and corrections applied to borehole temperature data. Uncertainty in the depth maps is set at 10%. Minimum temperature in the middle of the reservoir in the proposed producer is 75°C and maximum temperature is 89°C
- The risks associated with the planned doublet have been assessed.
 - Risk of swelling clays exists in the Tertiary and the Vlieland.
 - Mud losses may occur in the Chalk formation.
 - The wells are planned > 750 m from the major faults. Major faults are assumed not to be open, probably cemented and hampering fluid flow.
 - Sub seismic faults may be present.
 - The chance of finding a hydrocarbon accumulation is considered small and estimated at 1%. The chance of finding residual and/or dissolved gas in the formation water of the sandy intervals is large, estimated at 80%. However, the amounts are difficult to estimate. The risk of presence of oil is estimated at 1-2%. H₂S will be absent. CO₂ and N₂ may be present with amounts <1.5 % each.
 - The formations that will be encountered by the proposed producer and injector are not expected to be overpressured.

7 References

Van Adrichem Boogaert, H.A. and W.F.P. Kouwe [1994]. *Stratigraphic Nomenclature of the Netherlands; revision and update by the RGD and NOGEPa*. Mededelingen Rijks Geologische Dienst, No. 50.

Van Balen, R.T., Van Bergen, F., De Leeuw, C., Pagnier, H., Simmelink, H., Van Wees, J.D., Verweij, J.M. [2000]. *Modelling the Hydrocarbon generation and migration in the West Netherlands Basin, the Netherlands*, Geologie en Mijnbouw/Netherlands Journal of Geosciences, v. 79 (1), p. 29-44.

Duin, E.J.T., J.C. Doornenbal, R.H.B. Rijkers, J.W. Verbeek and Th.E. Wong [2006]. *Subsurface structure of the Netherlands – results of recent onshore and offshore mapping*. Netherlands Journal of Geosciences. Geologie en Mijnbouw, 85-4, p. 245-276.

Fertl, W.H. and Timko, D.J., [1972]. *How downhole temperature pressures affect drilling*. World Oil, 7382 (10 parts). June 1972-March 1973.

Geluk, M.C., Plomp, A., Van Doorn, Th.H.M. [1996]. *Development of the Permo-Triassic succession in the basin fringe area, southern Netherlands*. In: *Geology of Gas and Oil under the Netherlands*, Rondeel, H.E., Batjes, D.A.J., Nieuwenhuijs, W.H. (Editors), KNGMG, p 57-78.

Geluk, M.C. [2007], *Triassic*. In: *Geology of the Netherlands*, Wong, T.E., Batjes, D.A.J., en de Jager, J. (Editors), Koninklijke Nederlands Akademie van Wetenschappen, p. 85-106.

Matev, P. [2011]. *Comprehensive reservoir quality assessment including static and dynamic modelling of Buntsandstein sandstone reservoirs in the West Netherlands Basin for Geothermal applications in Zuid Holland province area*. Master thesis, Delft University of Technology.

Mijnlieff, H., A. Obdam, A. Kronimus, J-D. van Wees [2009]. *Voorstel rapportagevereisten geologische evaluatie aardwarmte project*. TNO-034-UT-2009-02002/B.

De Mulder, E.F.J., Geluk, M.C., Ritsema, I.L., Westerhoff, W.E., Wong, T.E. (editors) [2003]. *De Ondergrond van Nederland*.

PanTerra study, carried out for GeoMEC-4P, September 2011. *An evaluation of the Hydrocarbon risks in the Brielle Vierpolders area*. PanTerra report G920.

Rondeel, H.E., Batjes, D.A.J. and Nieuwenhuijs, W.H. [1996]. *Geology of gas and oil under the Netherlands*. KNGMG.

Yuhasz, I. [1986]. *Conversion of routine air-permeability data into stressed brine-permeability data*. Society of Professional Well Log Analysts.

8 Appendices

8.1 Appendix 1: Seismic surveys

A summary of the processing parameters of the 3D survey L3NAM1990C is given in Figure 8-1. An overview of the 2D seismic lines that have been used and the applied polarity shifts and static shift is given in Table 8-1 and the location of the 2D lines and the 3D survey w.r.t. the study area is shown in Figure 8-1.

DATA_TYPE	LAND
SURVEY_TYPE	3D
COORD_SYSTEM	RD
POINT_TYPE	BIN-POINTS
AREA	Monster
Navigation file: L3NAM1990C.hdr.sgn	
NAV_SEPARATION_CDP	20.00
NAV_SEPARATION_LINE	20.00
NAV_AZIMUTH_INLINE	51.411
NAV_AZIMUTH_CROSSLINE	-38.589
NAV_MINIMUM_CDP	110
NAV_MAXIMUM_CDP	1140
NAV_MINIMUM_LINE	580
NAV_MAXIMUM_LINE	2500
NAV_XORIGIN_0	44549.58
NAV_YORIGIN_0	450899.04
NAV_XORIGIN_1	44577.69
NAV_YORIGIN_1	450902.20
X_minCDP_minLINE	54988.00
Y_minCDP_minLINE	445384.00
X_minCDP_maxLINE	85000.27
Y_minCDP_maxLINE	421434.84
X_maxCDP_minLINE	67836.87
Y_maxCDP_minLINE	461485.76
X_maxCDP_maxLINE	97849.13
Y_maxCDP_maxLINE	437536.59
Velocity file: L3NAM1990C.ivl	
VELOCITY_TYPE	stacking
VEL_MINIMUM_CDP	122
VEL_MAXIMUM_CDP	942
VEL_MINIMUM_LINE	780
VEL_MAXIMUM_LINE	2200
VEL_SCAN_COUNT	2346
Signal Data	
SIG_MINIMUM_CDP	110
SIG_MAXIMUM_CDP	1140
SIG_MINIMUM_LINE	580
SIG_MAXIMUM_LINE	2500
SIG_CDP_INTERVAL	1
SIG_LINE_INTERVAL	1
SIG_NUMBER_OF_SAMPLES	1250
SIG_SAMPLE_INTERVAL	4000
SIG_TOTAL_SIZE	8535109920 bytes = 8139 Mb
Standard byte locations in trace- and binaryheaders of SegY-output created by QC of TNO-NITG. The other bytelocations are unchanged.	
Line number (trace)	189 - 192
CDP number (trace)	193 - 196
Number of samples (binary)	21 - 22
Number of samples (trace)	115 - 116
Sample interval (binary)	17 - 18
Sample interval (trace)	117 - 118
X, easting (trace)	181 - 184
Y, northing (trace)	185 - 188

Figure 8-1 Processing parameters L3NAM1990C.

Table 8-1 Overview of the 30 2D seismic lines used for the study and the applied time and phase shifts. Colouring matches the colours used in Figure 8-1.

Seismic survey	Seismic line	Length	Digital	Migrated (by Fugro)	Navigation	Static shift (ms)	Polarity shift (°)
L2AMC1981A	ANE81-300	7408	Y	Y	Y	0	-
L2AMC1981A	ANE81-301	9420	y	Y	Y	+252	180
L2AMC1981A	ANE81-306	14384	Y	Y	Y	0	-
L2NAM1957A	2099	10497	Y	Y	Y	0	180
L2NAM1958A	2100	9060	Y	Y	Y	0	180
L2NAM1958A	2104	20470	Y	Y	Y	+10	180
L2NAM1958A	2105	20208	Y	Y	Y	0	180
L2NAM1964A	2404	8927	Y	Y	Y	-12	-
L2NAM1964A	2414	43365	Y	Y	Y	P1: +14 P2: 0	180
L2NAM1964A	2415	20594	Y	Y	Y	+22	180
L2NAM1964A	2430	13905	Y	Y	Y	+6	180
L2NAM1964A	2431	11132	Y	Y	Y	+2	180
L2NAM1964A	2432	8601	Y	Y	Y	0	180
L2NAM1964A	2433	8072	Y	Y	Y	0	180
L2NAM1964A	2434	18163	Y	Y	Y	P1: -192 P2: 0	180
L2NAM1973H	903084B	10913	Y	Y	Y	+72	-
L2NAM1974D	742015	7308	Y	Y	Y	-14	180
L2NAM1974D	742017	21795	Y	Y	Y	0	180
L2NAM1974D	742019	21353	Y	Y	Y	0	180
L2NAM1974D	742021	10770	Y	Y	Y	0	180
L2NAM1974D	742025	5151	Y	Y	Y	-16	180
L2NAM1984K	843429	19283	Y	Y	Y	-44	-
L2NAM1985D	852102	12497	Y	Y	Y	-30	-
L2NAM1985D	852104	21331	Y	Y	Y	-22	-
L2NAM1985D	852106	8227	Y	Y	Y	-36	-
L2NAM1985D	852109	14172	Y	Y	Y	-20	-
L2NAM1985D	852111	9751	Y	Y	Y	-28	-
L2NAM1985D	852113	11871	Y	Y	Y	-24	-
L2NAM1985D	852115	26911	Y	Y	Y	-24	-
L2NAM1985D	852117	11527	Y	Y	Y	-26	-

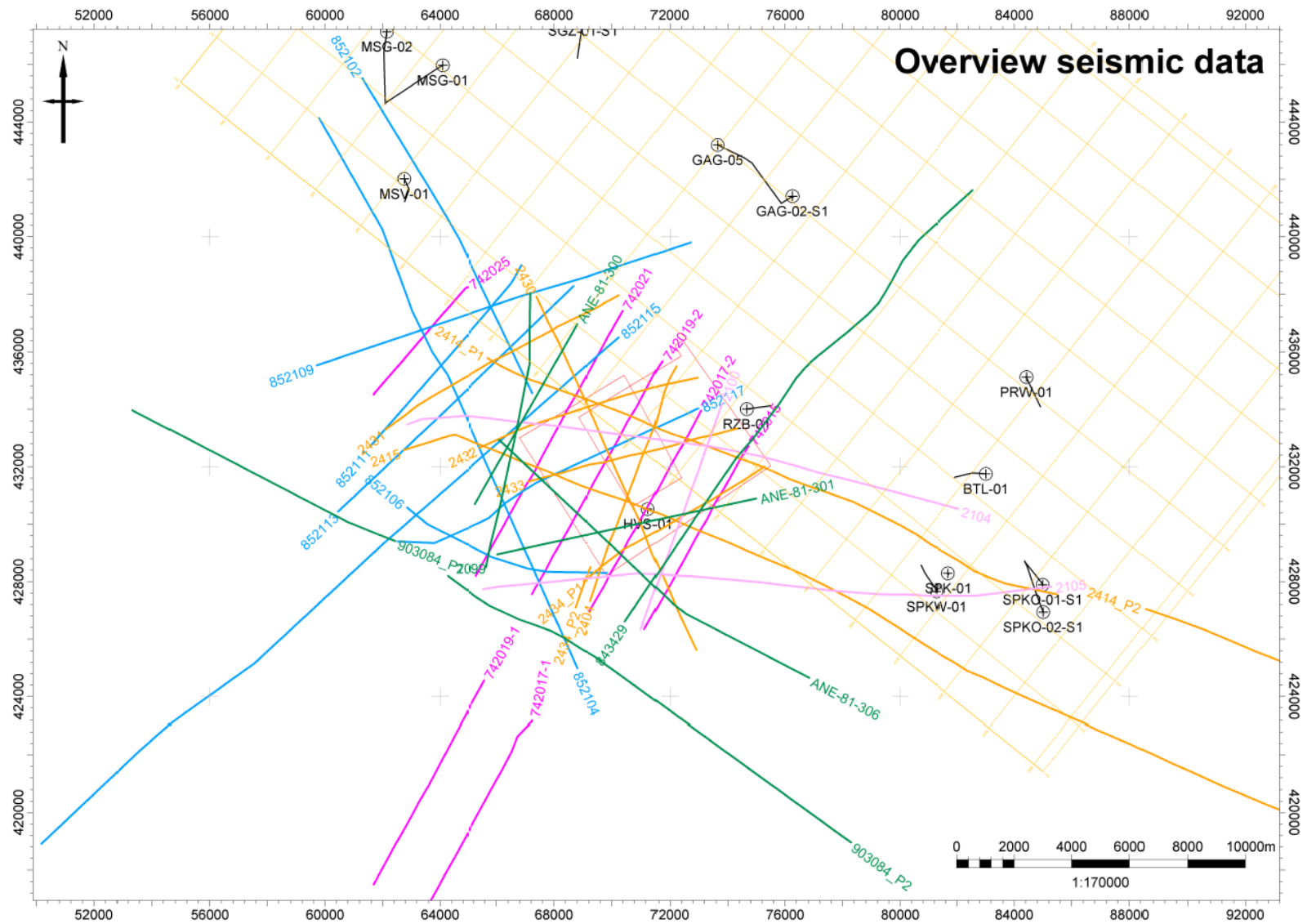


Figure 8-1 Overview of seismic data used for this study. The orange lined square is the L3NAM1990C 3D survey. The 2D lines are labelled. The outline of the Vierpolders and Brielle-2 geothermal exploration licenses is shown in red.

8.2 Appendix 2: Synthetic Seismograms

Synthetic seismograms were created for the BTL-01, RZB-01 and MSV-01 wells. These are shown in Figure 8-2, Figure 8-3 and Figure 8-4.

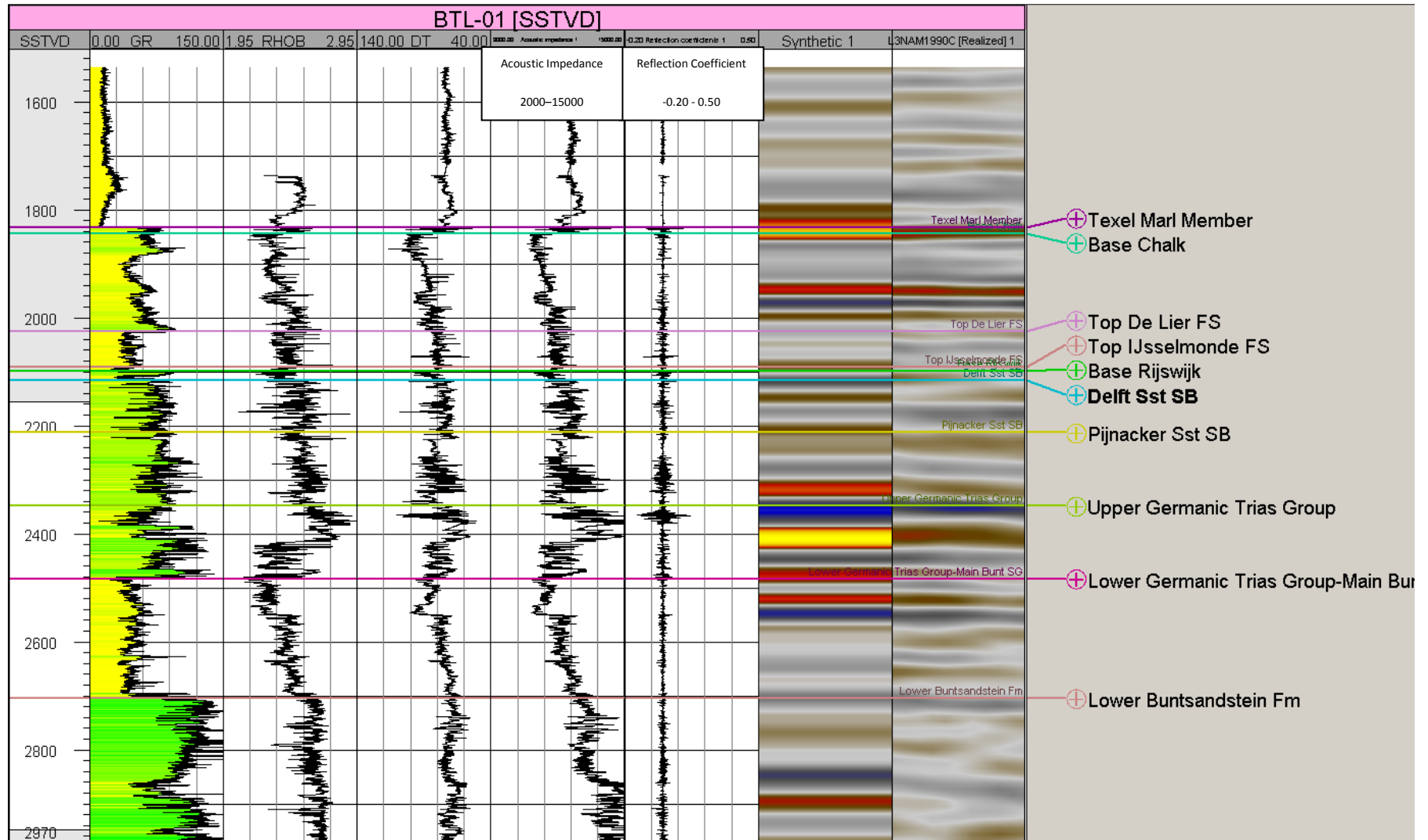


Figure 8-2 The gamma ray, density and sonic logs of BTL-01 are shown next to the results of the synthetic seismogram showing acoustic impedance, reflection coefficient and the synthetic seismic. At the right the seismic image from the L3NAM1990C survey is shown.

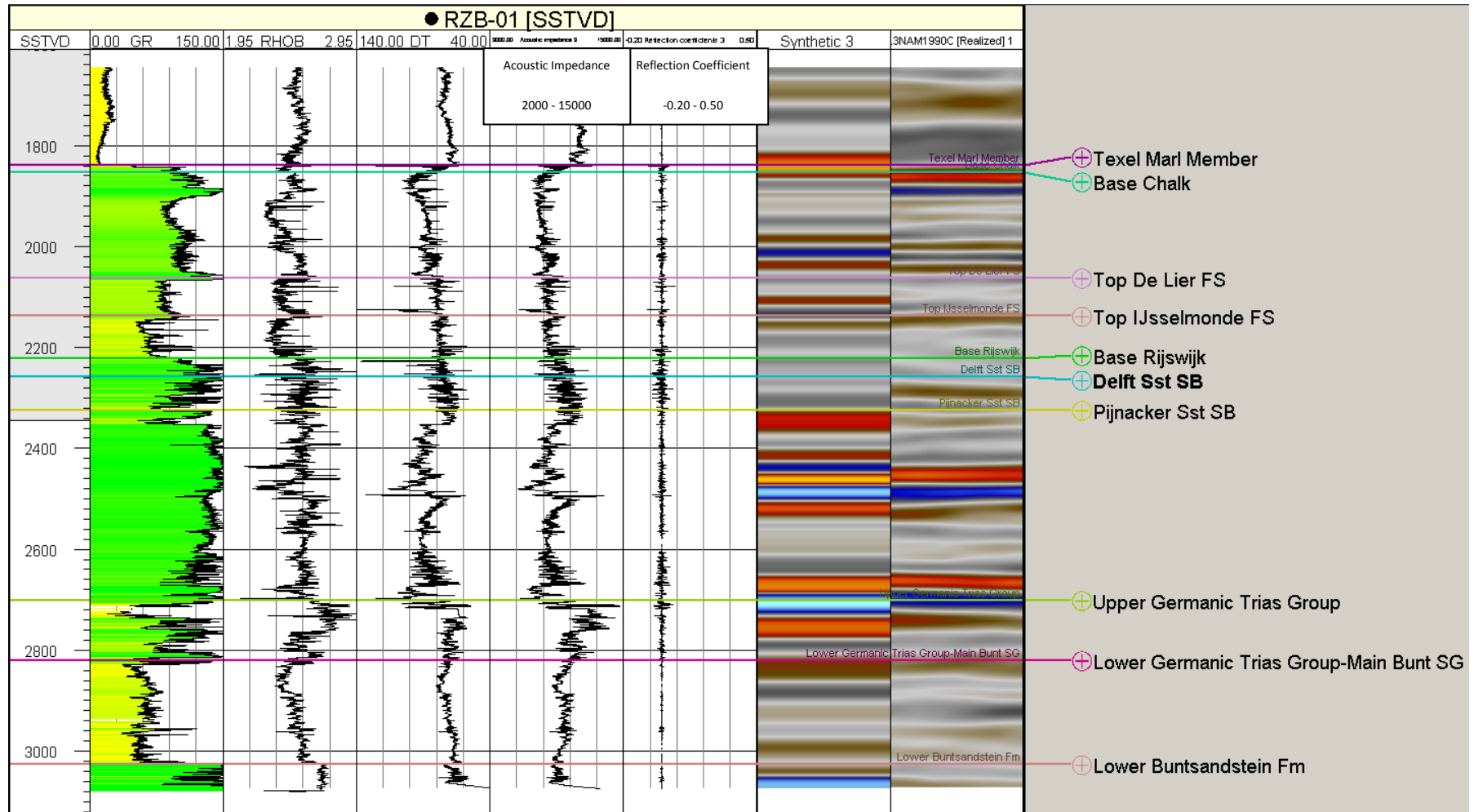


Figure 8-3 The gamma ray, density and sonic logs of RZB-01 are shown next to the results of the synthetic seismogram showing acoustic impedance, reflection coefficient and the synthetic seismic. At the right the seismic image from the L3NAM1990C survey is shown.

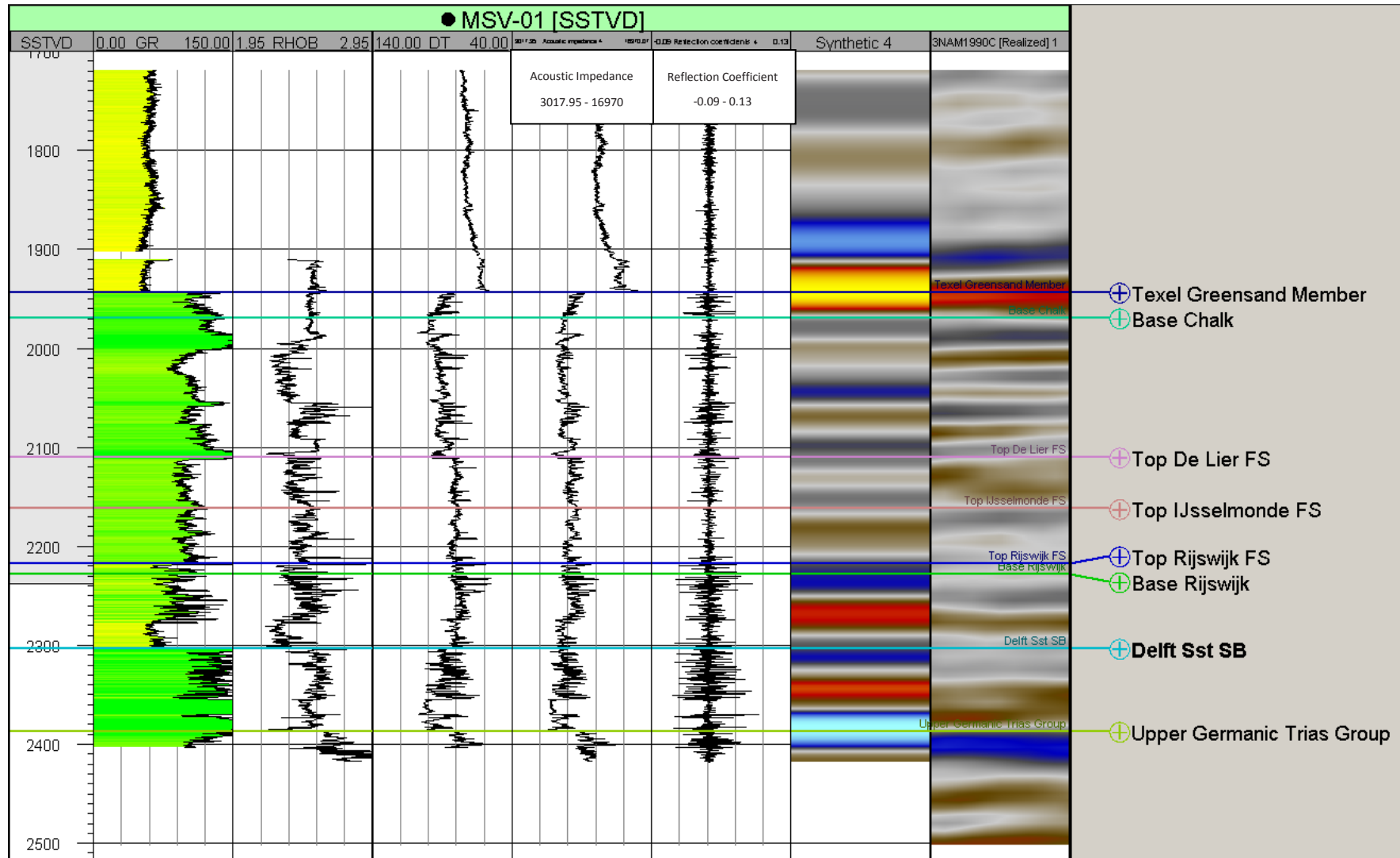


Figure 8-4 The gamma ray, density and sonic logs of MSV-01 are shown next to the results of the synthetic seismogram showing acoustic impedance, reflection coefficient and the synthetic seismic. At the right the seismic image from the L3NAM1990C survey is shown.

8.3 Appendix 3: Additional Time Maps

The time map for the Top Triassic interpretation is shown in Chapter 3.2. Time maps for the rest of the interpreted horizons are given below.

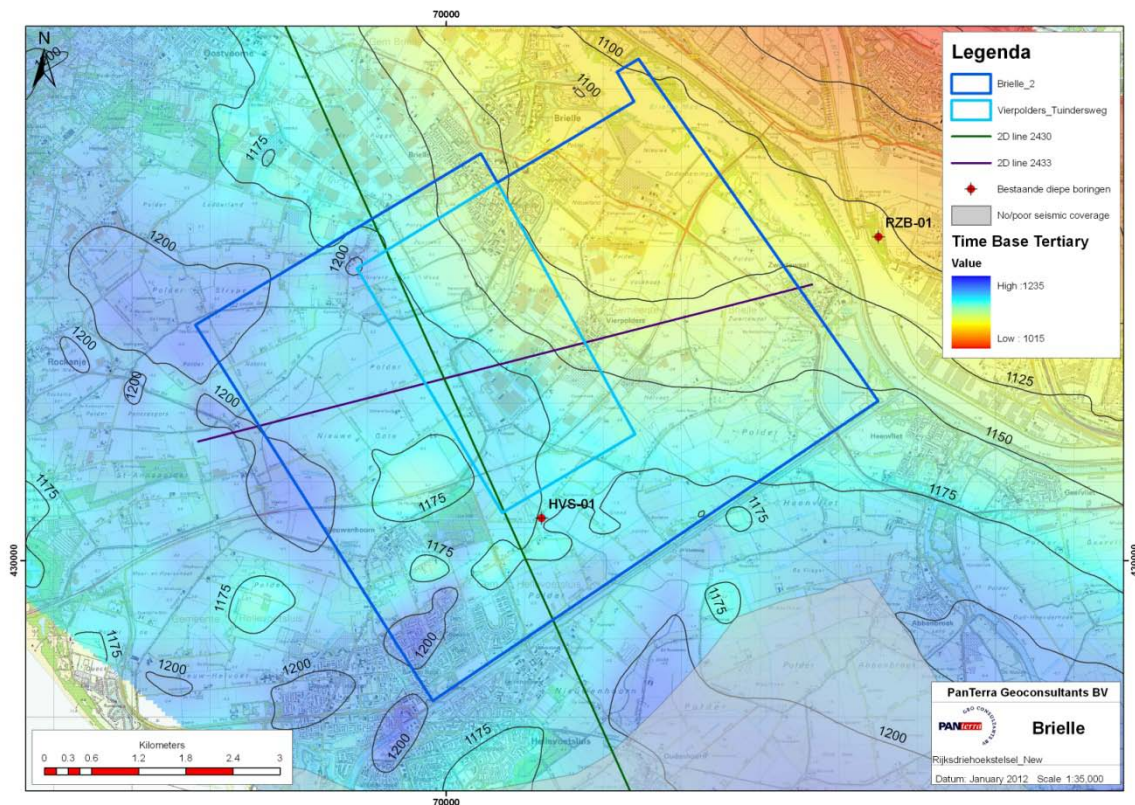


Figure 8-5 Time map of Base Tertiary in two way travel time (ms). The grey shade indicates an area of no or poor seismic coverage. The outline of the Vierpolders and Brielle-2 licenses is shown in blue. The 2D lines 2430 and 2433 are shown for reference.

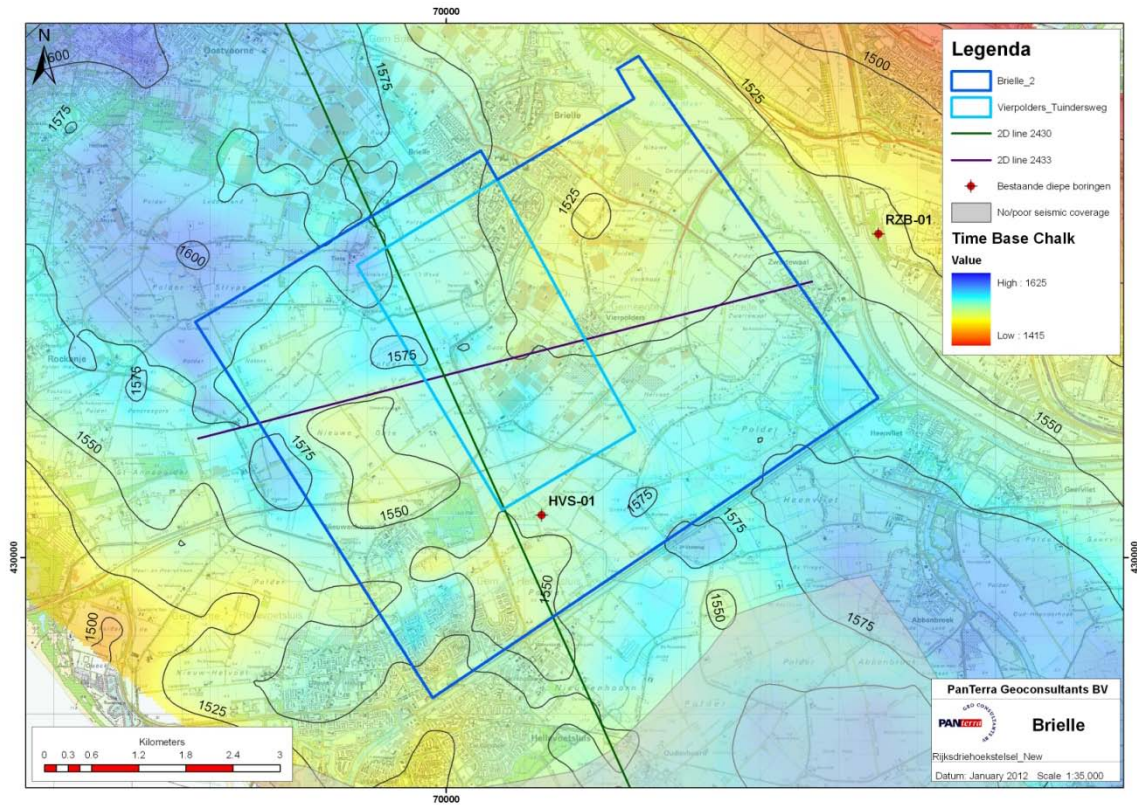


Figure 8-6 Time map of Base Chalk in two way travel time (ms). The grey shade indicates an area of no or poor seismic coverage. The outline of the Vierpolders and Brielle-2 licenses is shown in blue. The 2D lines 2430 and 2433 are shown for reference.

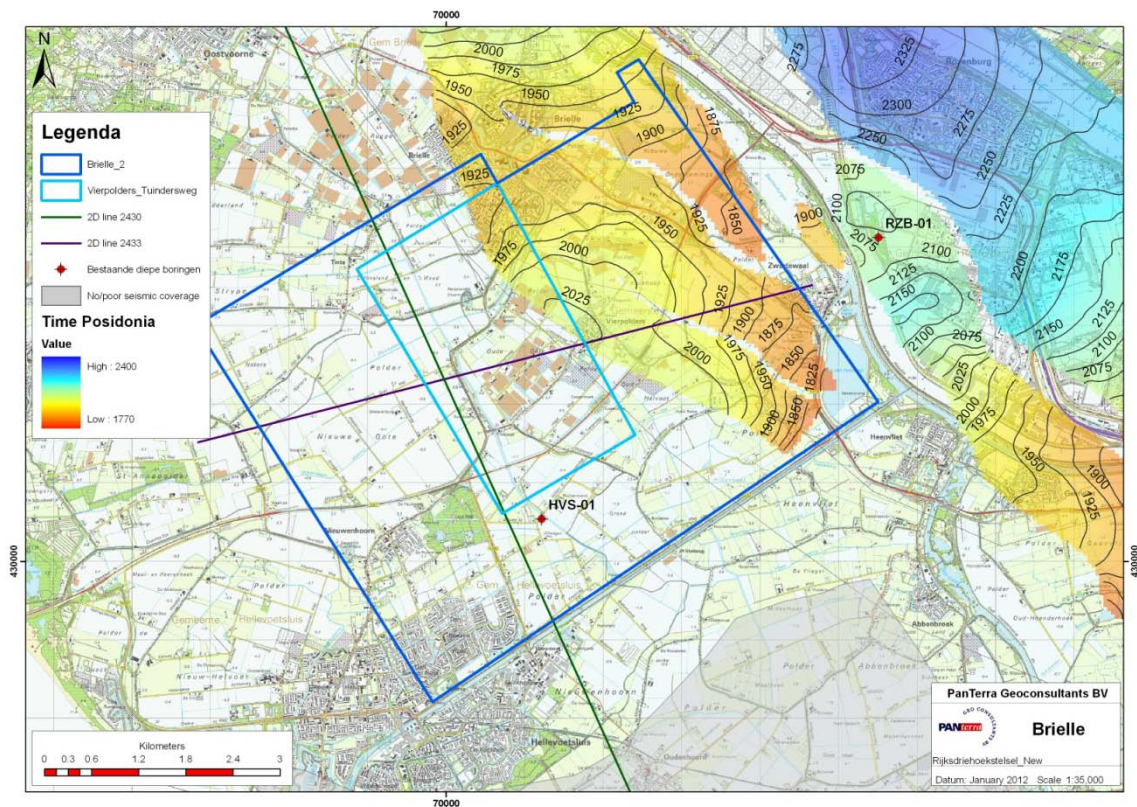


Figure 8-7 Time map of Posidonia Shale in two way travel time (ms). The grey shade indicates an area of no or poor seismic coverage. The outline of the Vierpolders and Brielle-2 licenses is shown in blue. The 2D lines 2430 and 2433 are shown for reference.

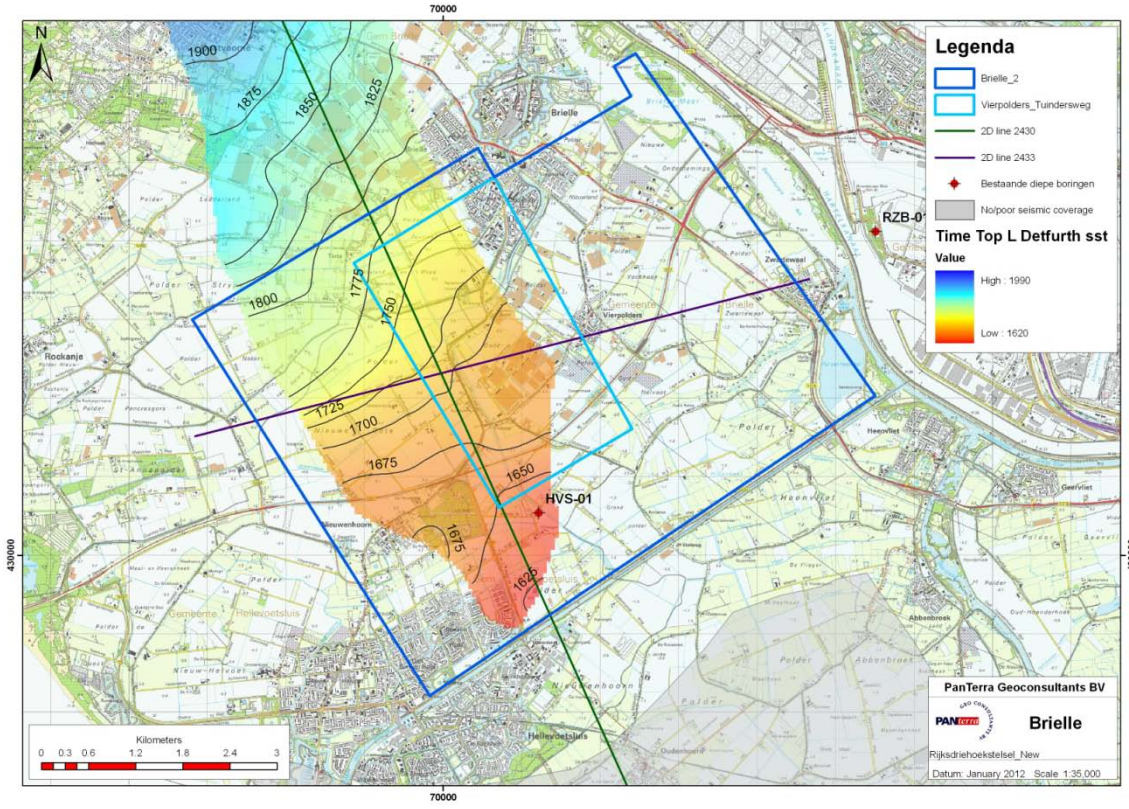


Figure 8-8 Time map of the top of the Lower Detfurth sandstone in two way travel time (ms). The grey shade indicates an area of no or poor seismic coverage. The outline of the Vierpolders and Brielle-2 licenses is shown in blue. This horizon has only been interpreted in the target fault block. The 2D lines 2430 and 2433 are shown for reference.

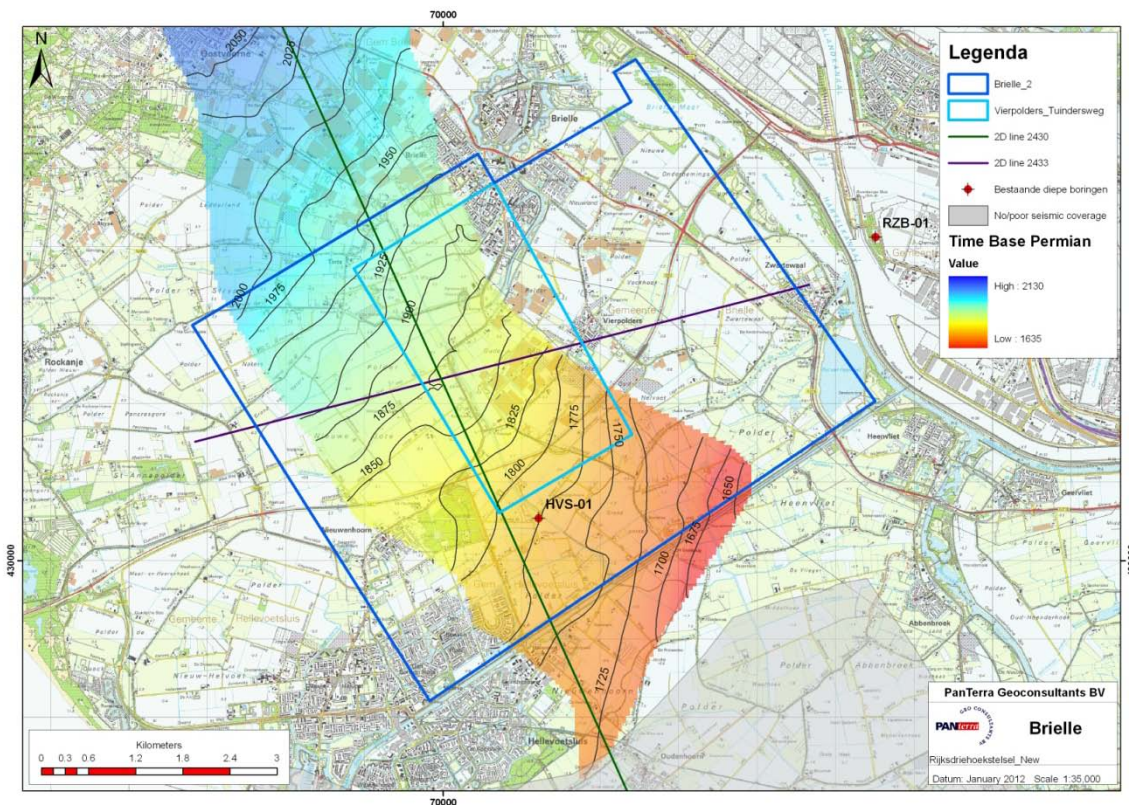


Figure 8-9 Time map of the top of the Base Permian unconformity in two way travel time (ms). The grey shade indicates an area of no or poor seismic coverage. The outline of the Vierpolders and Brielle-2 licenses is shown in blue. This horizon has only been interpreted in the target fault block. The 2D lines 2430 and 2433 are shown for reference.

8.4 Appendix 4: Petrophysics

Well_ID	Number of plug measurements in Triassic
BTL-01	300
GAG-02-S1	83
GAG-03	104
GAG-05	53
MSG-01	108
MSG-02	52
MSV-01	40
PRW-01	781
RZB-01	109
SPKW-01	122

Figure 8-10 Overview of available core plug measurement data from the Triassic.

Table 8-2 Overview of formation tops as used during the petrophysical calculations. These tops are proposed by Matev (2011) as discussed in Chapter 2.4.

Well	Formation	MD	TVD	Well	Formation	MD	TVD
BTL-01	Top Rot	2611	2429.3	PRW-01	Top Rot	2939	2615.88
BTL-01	Top Hardeggen	2662.1	2487.5	PRW-01	Top Hardeggen	3000.6	2689.5
BTL-01	Top Detfurth	2748.2	2563.5	PRW-01	Top Detfurth	3058.0	2746.9
BTL-01	Top Volpriehausen	2789.9	2599.7	PRW-01	Top Volpriehausen	3100.1	2788.9
BTL-01	Base Main Buntsandstein	2943.0	2724.1	PRW-01	Base Main Buntsandstein	3200.3	2889.1
GAG-02-S1	Top Rot	3011.0	2952.8	RZB-01	Top Rot	2944	2776.46
GAG-02-S1	Top Hardeggen	3049.0	2990.7	RZB-01	Top Hardeggen	2981.4	2823.9
GAG-02-S1	Top Detfurth	3114.0	3055.3	RZB-01	Top Detfurth	3059.1	2900.9
GAG-02-S1	Top Volpriehausen	3154.0	3095.0	RZB-01	Top Volpriehausen	3099.3	2940.7
GAG-02-S1	Base Main Buntsandstein	3251.0	3189.9	RZB-01	Base Main Buntsandstein	3196.0	3037.0
GAG-05	Top Rot	4033.0	3490.1	SGZ-01-S1	Top Rot	3102.0	2711.5
GAG-05	Top Hardeggen	4077.9	3534.2	SGZ-01-S1	Top Hardeggen	3172.6	2784.3
GAG-05	Top Detfurth	4158.0	3596.4	SGZ-01-S1	Top Detfurth	3243.0	2848.1
GAG-05	Top Volpriehausen	4198.9	3626.1	SGZ-01-S1	Top Volpriehausen	3285.2	2886.8
GAG-05	Base Main Buntsandstein	4335.7	3713.6	SGZ-01-S1	Base Main Buntsandstein	3392.3	2988.0
GAG-05 Deep	Top Rot			SPKO-01	Top Rot	2634	2411.33
GAG-05 Deep	Top Hardeggen	5160.92	3863.67	SPKO-01	Top Hardeggen	2708.4	2493.1
GAG-05 Deep	Top Detfurth	5363.89	3943.52	SPKO-01	Top Detfurth	2788.3	2563.6
HVS-01	Top Rot			SPKO-01	Top Volpriehausen	2824.2	2595.4
HVS-01	Top Hardeggen	1965	1959.96	SPKO-01	Base Main Buntsandstein	2941.8	2699.3
HVS-01	Top Detfurth	1999.3	1993.48	STW-01	Top Rot	2428.3	1992.1
HVS-01	Top Volpriehausen	2037.2	2031.47	STW-01	Top Hardeggen	2526.8	2073.3
HVS-01	Base Main Buntsandstein	2114.2	2108.46	STW-01	Top Detfurth	2573.1	2114.5
MSG-01	Top Rot	3718.0	2920.7	STW-01	Top Volpriehausen	2604.8	2141.9
MSG-01	Top Hardeggen	3747.0	2944.9	STW-01	Base Main Buntsandstein	2730.6	2257.1
MSG-01	Top Detfurth	3840.0	3023.4				
MSG-01	Top Volpriehausen	3817.0	3050.2				
MSG-01	Base Main Buntsandstein	3965.0	3128.1				

8.5 Appendix 5: Temperature

Table 8-3 shows the input data from log headers that were used to calculate corrected BHT in order to determine a suitable temperature gradient for the Brielle area. The white columns show raw data from the log headers. The grey column was calculated from the input data. The yellow column shows the corrected temperatures.

A temperature log taken in HVS-01 is shown in Figure 8-11.

Table 8-3 Input data and results for the correction of BHT temperature data from HVS-01, RZB-01 and SPKW-01.

HVS-01												
Tif	Run	bitsize	date	Depth Driller	Depth Logger	Bottom logged interval	TVD NAP	BHT (oC)	Circulation Time (hrs)	Time since circulation (hrs)	Average TVD (NAP)	Estimated Formation Temperature (oC)
bhc_01	1	18.5	3/4/1969	651.0	651.0	649.5	649.5	33	2.0	3	650.0	33
ies_01	1	18.5	3/4/1969	651.0	651.0	650.5	650.5	33	2.0	6		
bhc_02	2	12.25	3/11/1969	1804.0	1803.8	1801.5	1801.5	52	1.5	7	1802.8	55.1
ies_02	2	12.25	3/11/1969	1804.0	1804.3	1804.0	1804.0	50	1.5	4		
bhc_03	3	8.5	4/2/1969	3370.0	3362.0	3358.0	3358.0	108	1.0	17	3360.2	113
ies_03	3	8.5	4/2/1969	3370.0	3362.5	3362.3	3362.3	106	1.0	12		
bhc_04	4	8.5	4/20/1969	3841.0	3811.5	3811.0	3810.0	112	2.5	11	3810.0	116.1
ies_04	4	8.5	4/20/1969	3841.00	3811.3	3811.0	3810.0	110	2.5	7		
RZB-01												
Tif	Run	bitsize	date	Depth Driller	Depth Logger	Bottom logged interval	TVD NAP	BHT (oC)	Circulation Time (hrs)	Time since circulation (hrs)	Average TVD (NAP)	Estimated Formation Temperature (oC)
corgun_01	1	12.25	8/13/1987	1956.0	1945.0	1945.0	1847.0	68		20.5		
fdc_01	1	12.25	8/12/1987	1956.00	1955.0	1953.7	1855.7	68		15.5	1853.0	68
difl_01	1	12.25	8/12/1987	1956.0	1955.0	1954.3	1856.3	68		15.5		
fdc_02	2	8.375	8/30/1987	2901.00	2899.4	2899.0	2738.4	93		13.5		
difl_iss_bhca_01	2	8.375	8/30/1987	2901.0	2898.4	2896.6	2736.0	88		8.5	2737.2	105.6
4ac_01	2	8.375	8/30/1987	2901	2899	2898.7	2738.1	98		18.5		
dil_mil_01	2	8.375	8/31/1987	2901.0	2897.6	2897.0	2736.4	98		22.5		
fdc_cn1_01	1	5.875	9/11/1987	3244.0	3245.8	3245.5	3083.1	105		12		
dip1_01	1	5.875	9/11/1987	3244.0	3244.0	3243.8	3081.4	106		16	3081.3	109.4
difl_iss_bhca_02	1	5.875	9/11/1987	3244.0	3243.8	3241.8	3079.4	103		8		
cad_01	1	5.875	9/11/1987	3244.0	3244.0	3243.8	3081.4	106		16		
SPKW-01												
Tif	Run	bitsize	date	Depth Driller	Depth Logger	Bottom logged interval	TVD NAP	BHT (oC)	Circulation Time (hrs)	Time since circulation (hrs)	Average TVD (NAP)	Estimated Formation Temperature (oC)
ldl_ams_01	A-2	12.25	8/6/1992	2366.0	2358.8	2358.0	2147.0	65		12.67	2147.3	68.7
lssl_ams_01	A-1	12.25	8/5/1992	2366.0	2360.7	2358.8	2147.5	62.5		7		
cbl_vdl_01	D-1	8.375	8/27/1992	2912.0	2869.0	2868.0	2617.0	93		6.67	2624.5	102.6
ft_01	C-3	8.375	8/21/1992	2911	2912	2883	2632.0	99.4		23		
dil_msl_01	C-1	8.375	8/21/1992	2911.00	2912.0	2907.5	2655.0	93		7	2657.0	106.8
shdt_01	C-4	8.375	8/21/1992	2911.0	2912.0	2911.0	2658.0	100		13.5		
isl_cn1_01	C-2	8.375	8/21/1992	2911.00	2912.0	2911.0	2658.0	95		10.67		

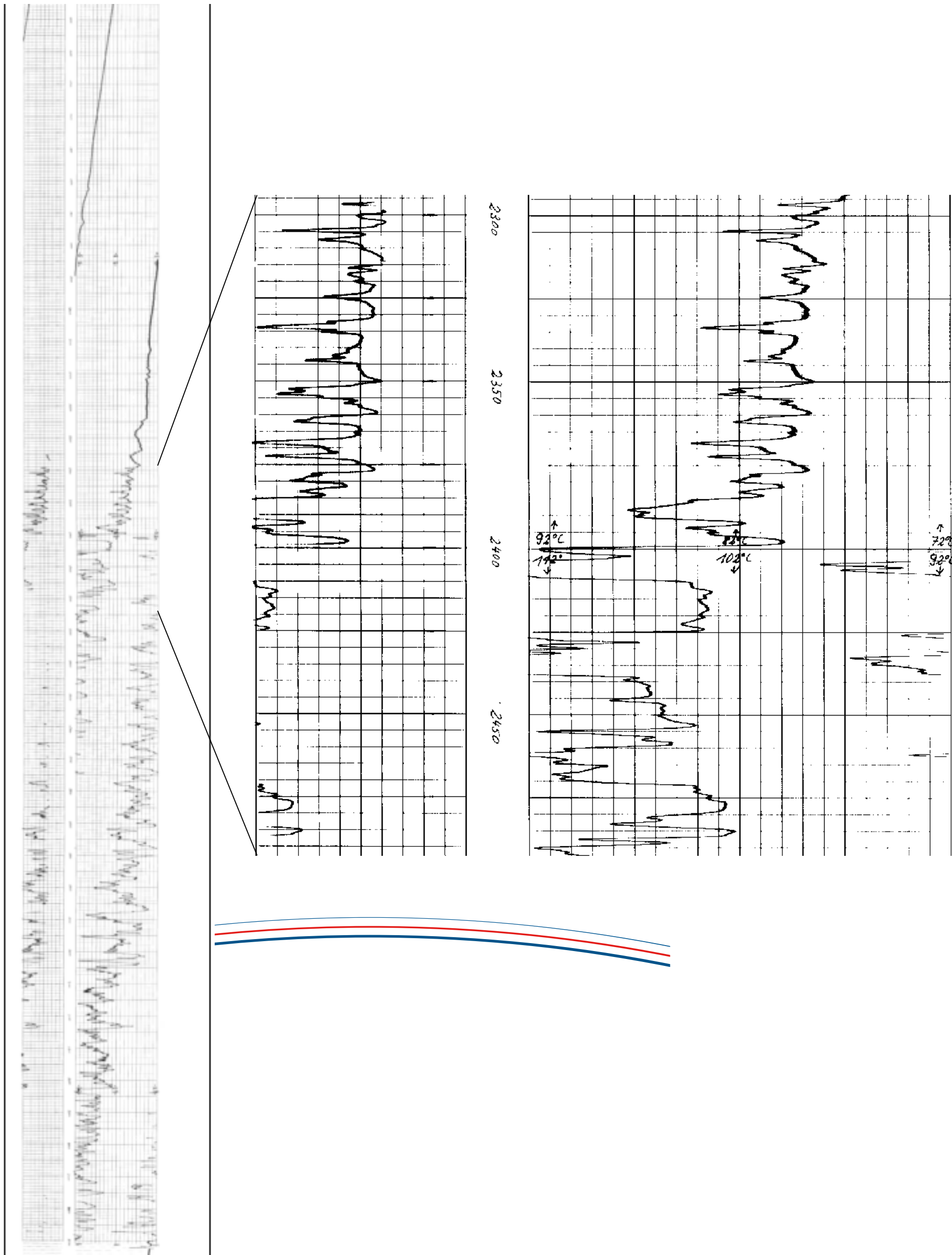


Figure 8-11 Temperature log from the HVS-01 well. The left image shows the log from 1450 m to 3500 m depth. From the top of the well, the temperature increases linearly with depth. However, at a depth of 2250 meters the logs starts to spike with a deviation of up to 10 °C as is shown in the blow-up image on the right. These measurements are considered unreliable and therefore have not been used to determine a suitable temperature-gradient for the Brielle area.

8.6 Appendix 6: Well correlation panel

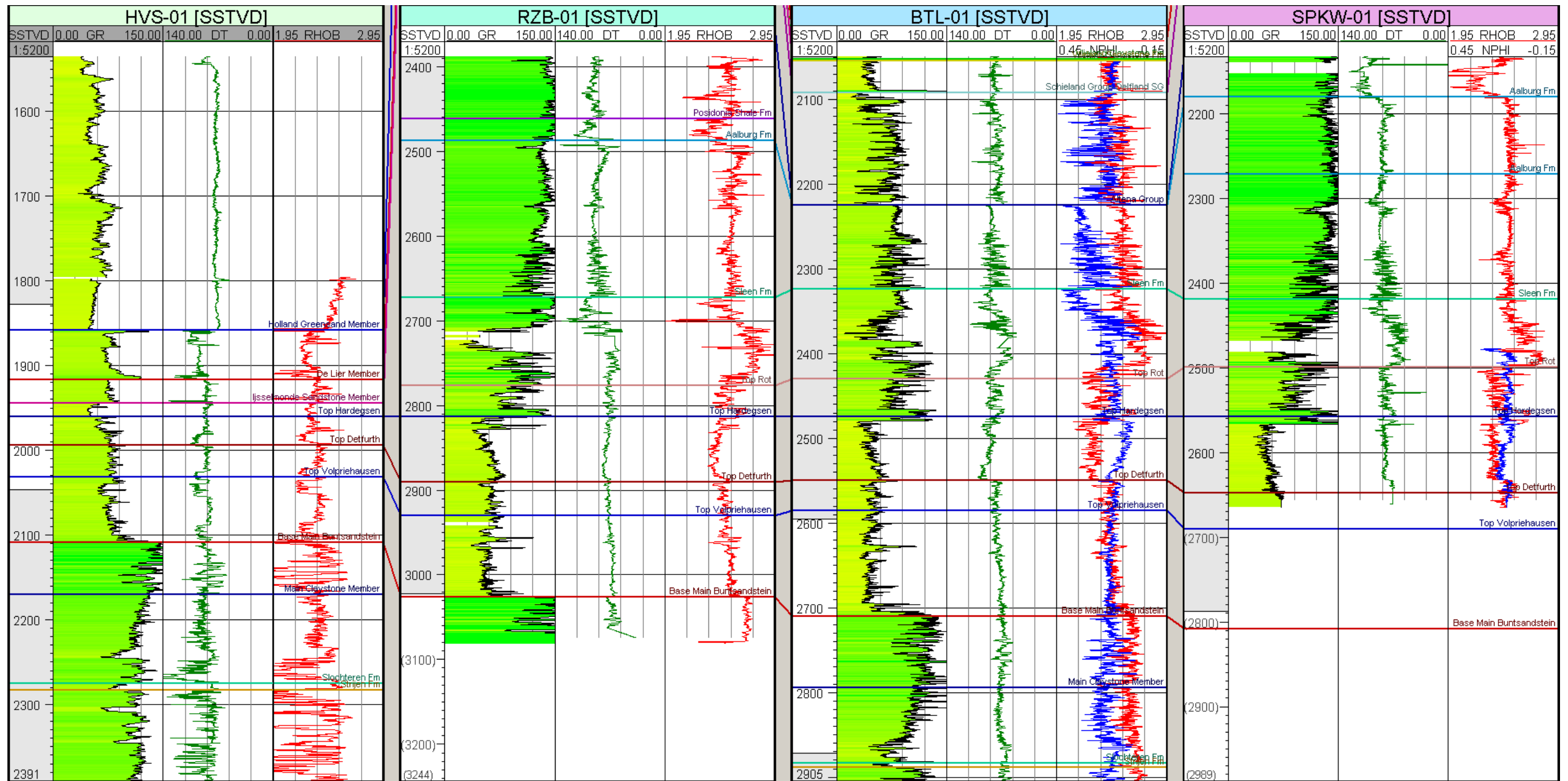


Figure 8-12 Well correlation panel through HVS-01, RZB-01, BTL-01 and SPKW-01, showing the Gamma Ray, Sonic, Density and Neutron logs and the well tops as applied for the petrophysics.

8.7 Appendix 7: Well configuration

The well configuration of the proposed producer and injector are given in Table 8-4 and Table 8-5. The well summary is given in Table 8-6.

Table 8-4 Deviation file of BRI-GT-01 (producer).

X- coordinate (RD)	Y-coordinate (RD)	TVD (m NAP)	MD (m RT)	Inclination	Azimuth	DX	DY	Calc DLS
70444	432190	0	0	0	0	0	0	0
70444	432190	450	450	0	0	0	0	0
70441.84	432190.3	499.94	500	5	278	-2.16	0.3	3
70435.38	432191.21	549.49	550	10	278	-8.62	1.21	3
70424.67	432192.72	598.29	600	15	278	-19.33	2.72	3
70409.78	432194.81	645.96	650	20	278	-34.22	4.81	3
70390.84	432197.47	692.14	700	25	278	-53.16	7.47	3
70367.99	432200.68	736.48	750	30	278	-76.01	10.68	3
70341.39	432204.42	778.64	800	35	278	-102.61	14.42	3
70311.26	432208.65	818.29	850	40	278	-132.74	18.65	3
70278.46	432213.27	855.73	900	43	278	-165.54	23.27	1.8
70243.76	432218.14	891.39	950	46	278	-200.24	28.14	1.8
68698.05	432435.38	2398.8	3120	46	278	-1745.95	245.38	0

Table 8-5 Deviation file of BRI-GT-02 (injector).

X- coordinate (RD)	Y-coordinate (RD)	TVD (m NAP)	MD (m RT)	Inclination	Azimuthh	DX	DY	Calc DLS
70444	432190	0	0	0	0	0	0	0
70444	432190	1300	1300	0	0	0	0	0
70442.33	432188.6	1349.94	1350	5	230	-1.67	-1.4	3
70437.33	432184.41	1399.49	1400	10	230	-6.67	-5.59	3
70429.05	432177.45	1448.29	1450	15	230	-14.95	-12.55	3
70264.49	432039.37	2250.01	2280	15	230	-179.51	-150.63	0

Table 8-6 Summary of the proposed doublet.

License	:	Vierpolders and Brielle-2
License holder	:	GeoMEC-4P
Location name	:	BRI
Type of wells	:	Geothermal wells (producer and injector)
Planned spud date	:	2012

BRI-GT-01	
Surface coordinates	X= 70444 E, Y= 432190N (RD)
Type of well	Producer
Target information	Main Buntsandstein Subgroup
Coordinates top reservoir	X= 68911.17 E , Y= 432405.43 N (RD) at 2191 m TVD NAP
Hor. displacement at top reservoir	1548 m at 278° azimuth from surface location
Max. Deviation	46° and kick-off point at 450 m TVD NAP
Planned TD	m TVD NAP and m MD at m horizontal displacement
Potential hazards	<ul style="list-style-type: none"> - Swelling clays (Tertiary, Vlieland) - (Total) mud losses in the Chalk Group - Residual and/or dissolved gas in the formation water of the sandy intervals (Holland formation, Delfland Group, Röt Formation and Main Buntsandstein Subgroup).

BRI-GT-02	
Surface coordinates	X= 70444 E, Y= 432190N (RD)
Type of well	Injector
Target information	Main Buntsandstein Subgroup
Coordinates top reservoir	X= 70306.76 E, Y= 432074.85 N (RD) at 2044 m TVD NAP
Hor. displacement at top reservoir	179 m at 230° azimuth from surface location
Max. Deviation	15° and kick-off point at 1300 m TVD NAP
Distance from BRI-GT-01	1434 m at top of aquifer and 1613 m at base of aquifer
Planned TD	m TVD NAP and m MD at m horizontal displacement
Potential hazards	<ul style="list-style-type: none"> - Swelling clays (Tertiary, Vlieland) - (Total) mud losses in the Chalk Group - Residual and/or dissolved gas in the formation water of the sandy intervals (Holland formation, Delfland Group and Main Buntsandstein Subgroup).

8.8 Appendix 8: Flow rate results

Figure 8-13 to Figure 8-17 show screenshots of Doublet Calculator with the input and output parameters of the flow rate calculation as discussed in Chapter 5.2.

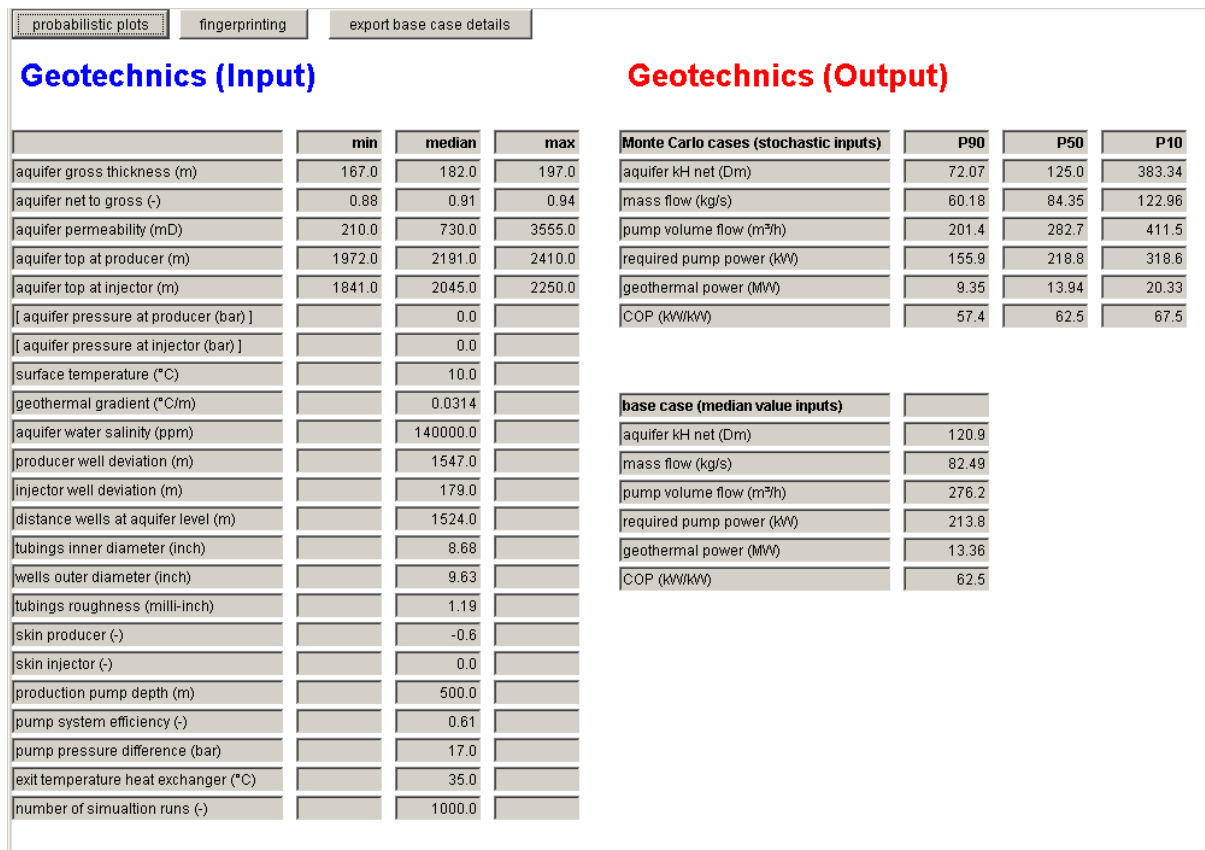


Figure 8-13 Input parameters and results of the flow rate calculation for the proposed geothermal doublet.

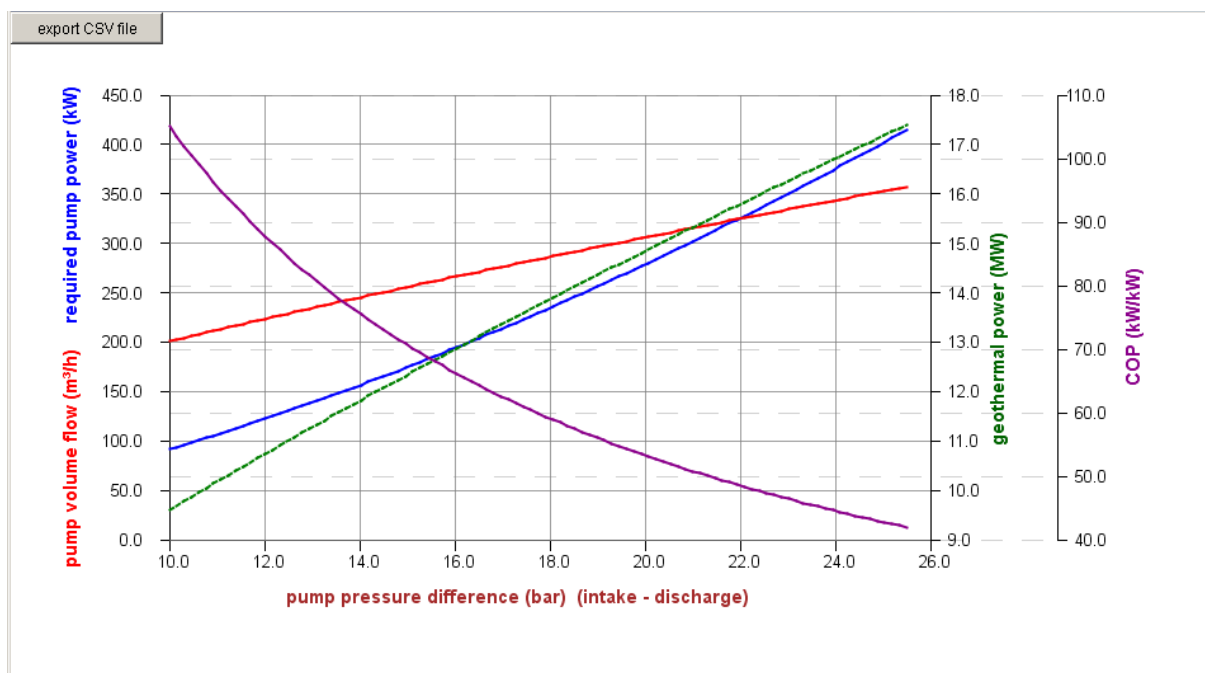


Figure 8-14 Resulting 'Fingerprint' graph for the base case scenario. If the pump pressure difference is increased, the flow rate, required pump power and geothermal power will increase and the COP will drop.

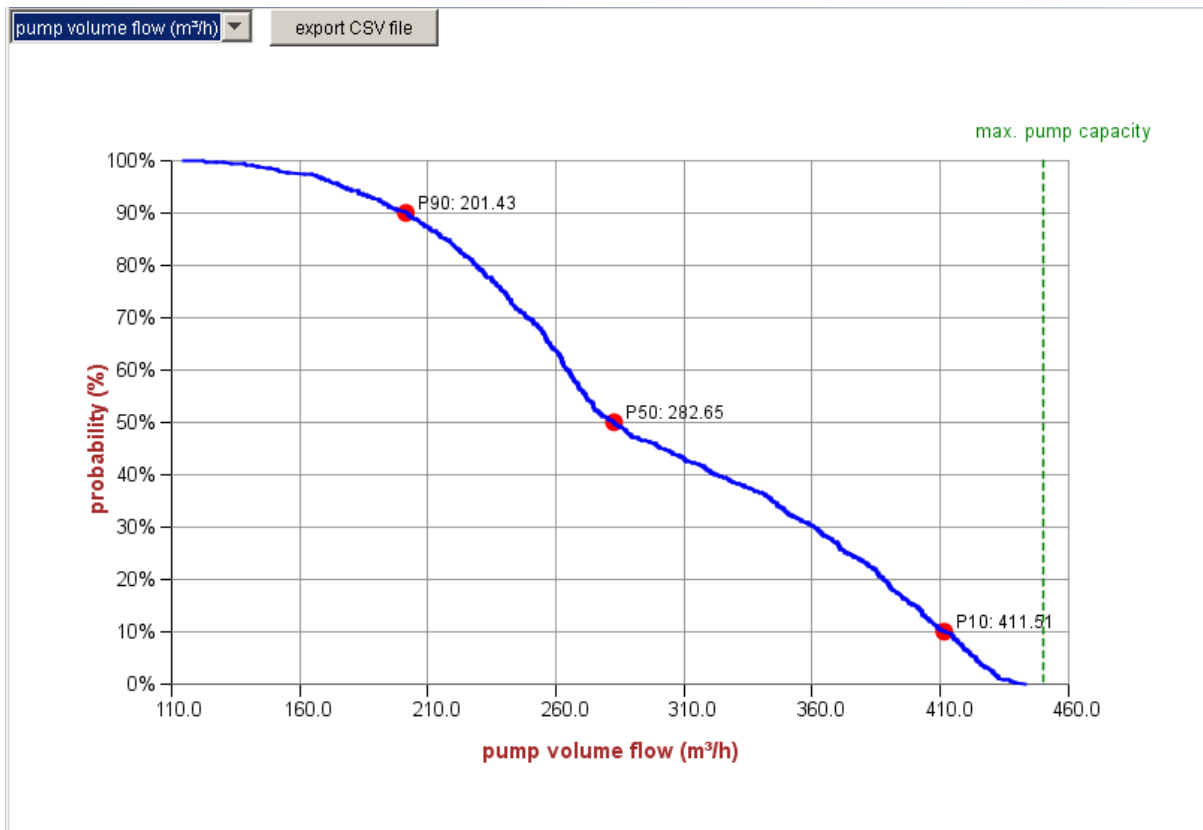


Figure 8-15 Resulting graph of the calculated flow rate.

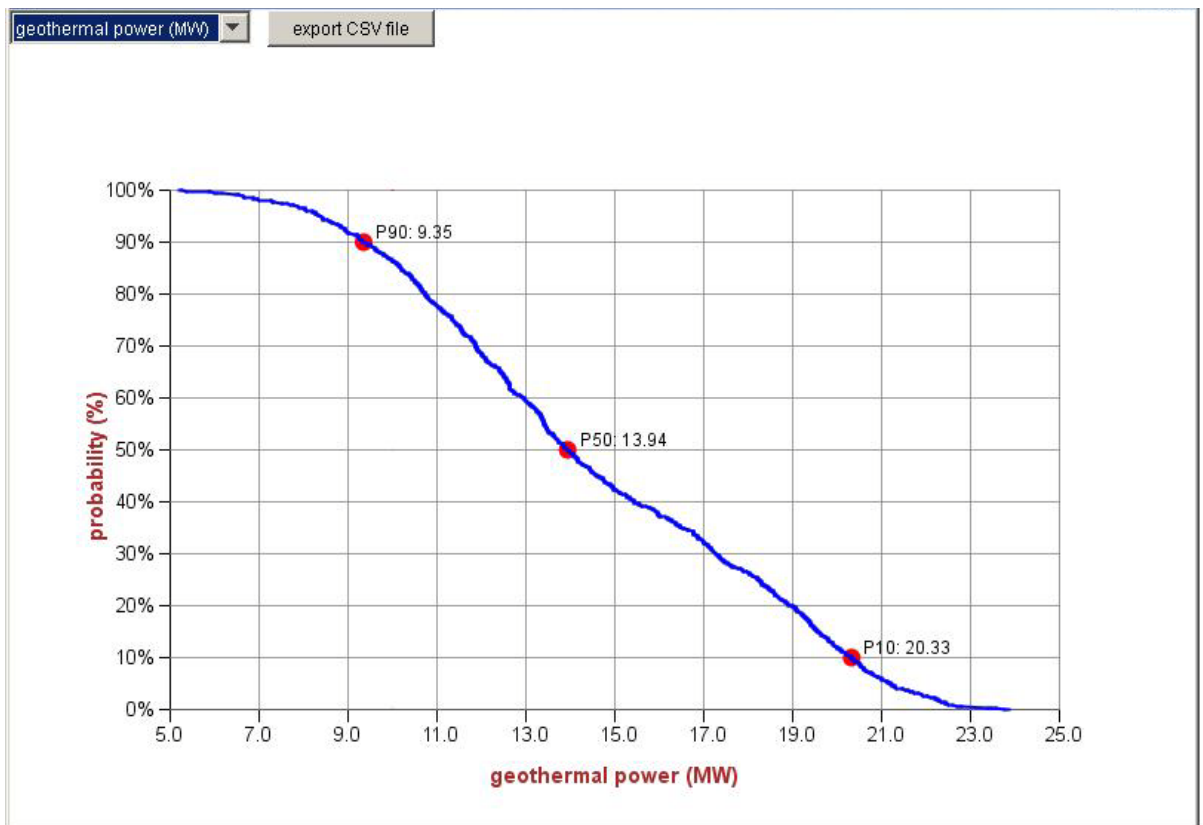


Figure 8-16 Resulting graph of the geothermal power.

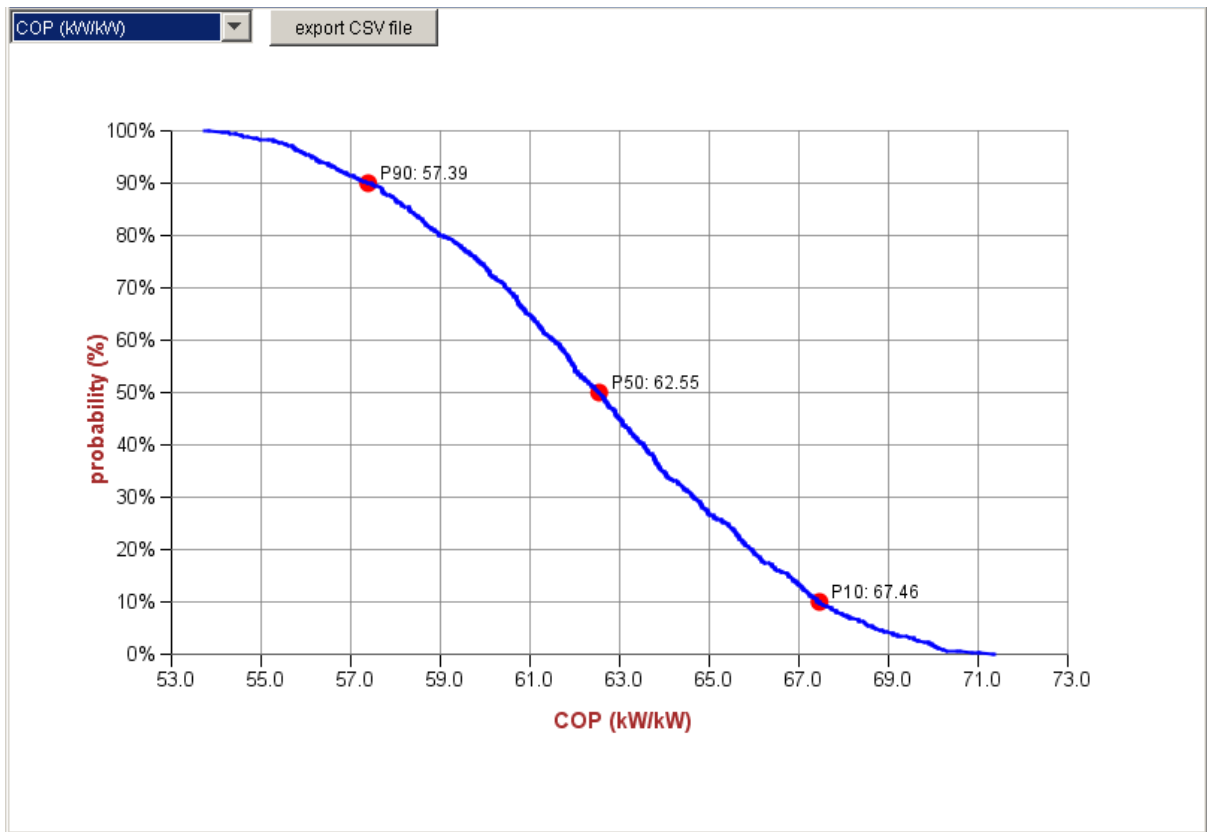


Figure 8-17 Resulting COP graph.

8.9 Appendix 9: Schematic sketch of the proposed doublet by Well Engineering Partners

A preliminary schematic sketch of the proposed doublet has been provided by Well Engineering Partners (WEP). The well diagram and deviation images for the injector and the producer are shown below.

9.625-in liner Inj

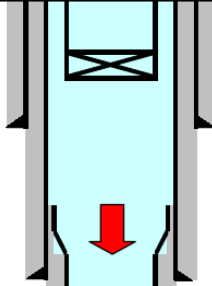
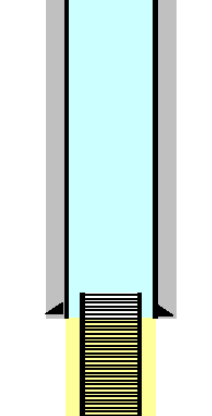
Nr.	Item Description	Wellhead and Xmastree	Depth	Depth	Hole ID	Pipe	Collar	Pipe ID
			m tvd	m ah	in drift	in	in	in Drift
1	30" welded conductor		60	60	30	30,000	30,000	26,000
2	Regulator valve in landing nipple on 13 3/8" pipe		250	250	22			
3	18 5/8" 96.5 ppf K55 BTC		450	450	20	18,625	20,125	17,468
4	Liner hanger 13 3/8" x 9 5/8"		1150	1150				
5	13 3/8" 68 ppf L80 VAM TOP		1250	1250	16	13,375	14,230	12,259
	Kick Off Point (KOP)		1300	1300				
	End Of Build (EOB) to 15°		1450	1453				
6	9 5/8" 47 ppf L80 liner VAM TOP		2050	2074	12 1/4	9,625	10,451	8,525
	Trias							
7	7" wire wrapped screen		2250	2280	8 1/2"	7,000	7,800	

Figure 8-18 Well diagram for the proposed injector. Provided by WEP.

TVD	2.250	m				
AHD	2282	m	Hor. Section	0	m	
HD	234	m				0
Open Hole	0	m	deg/100m		deg	
KOP1	1.300	DLS1	10	Angle1	15	
KOP2		DLS2	0	Angle2	0	

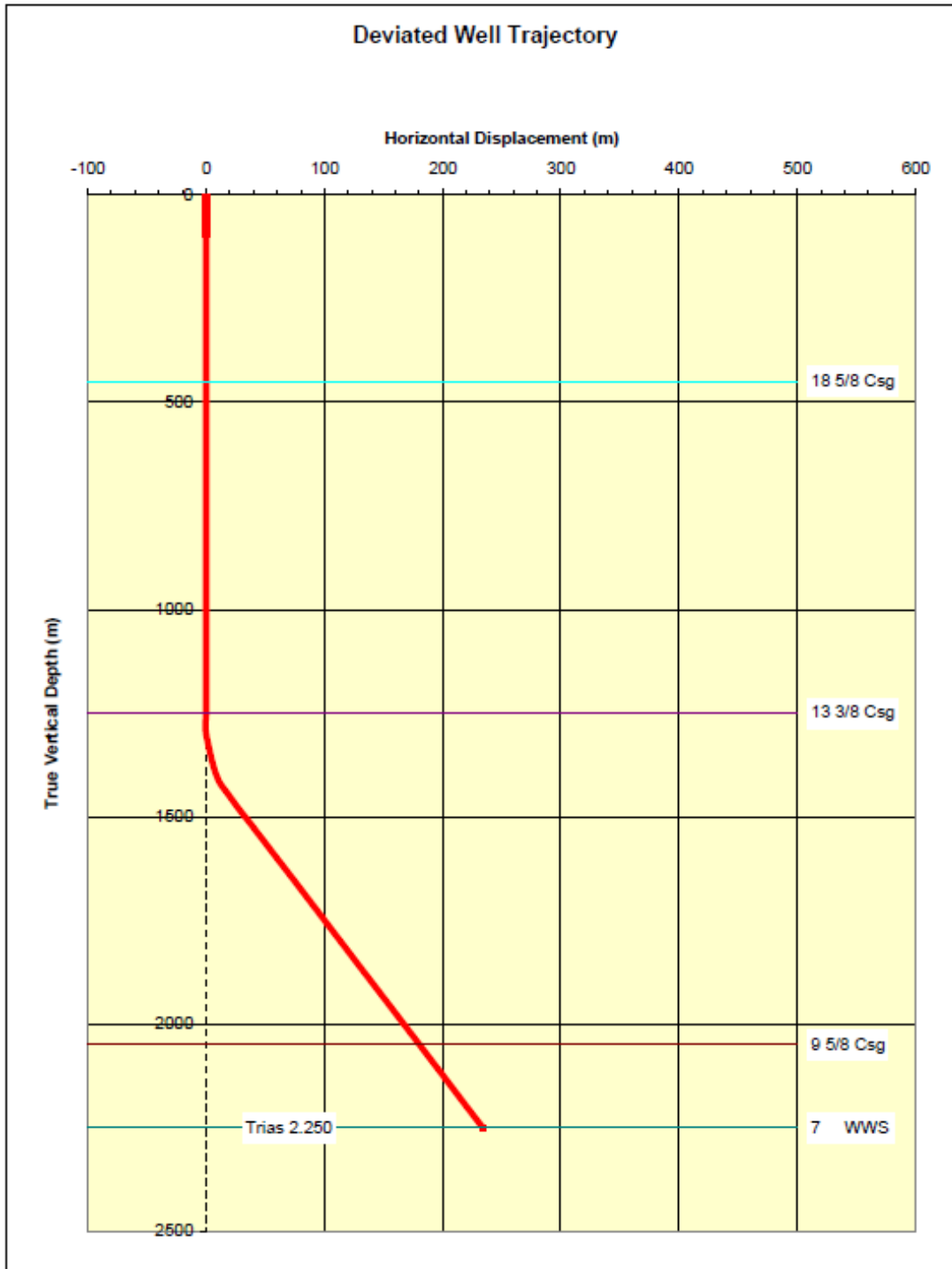


Figure 8-19 Deviation of the proposed injector. Provided by WEP.

9.625-in liner Prod

Nr.	Item Description	Wellhead and Xmastree	Depth	Depth	Hole ID	Pipe	Collar	Pipe ID
			m tvd	m ah	in drift	in in	in in	in Drift
1	30" welded conductor		60	60	30	30,000	30,000	26,000
2	18 5/8" 96.5 ppf K55 Kick Off Point (KOP)		450	450	22	18,625	20,125	17,468
3	ESP		450	450				
	End Of Build (EOB) to 46°		500	500				
4	Liner hanger 13 3/8" x 9 5/8"		950	1044				
5	13 3/8" 68 ppf L80		1050	1232				
			1150	1332	16	13,375	14,230	12,259
6	9 5/8" 47 ppf L80 liner VAM TOP	2200	2843	12 1/4	9,625	10,451	8,525	
7	7" wire wrapped screen	2399	3130	8 1/2	7,000	7,800		

Figure 8-20 Well diagram for the proposed producer. Provided by WEP.

TVD	2.399	m			
AHD	3130	m	Hor.	0 m	
HD	1746	m			0
Open Hole	0	m	deg/100m		deg
KOP1	450	DLS1	10	Angle1	46
KOP2		DLS2	0	Angle2	0

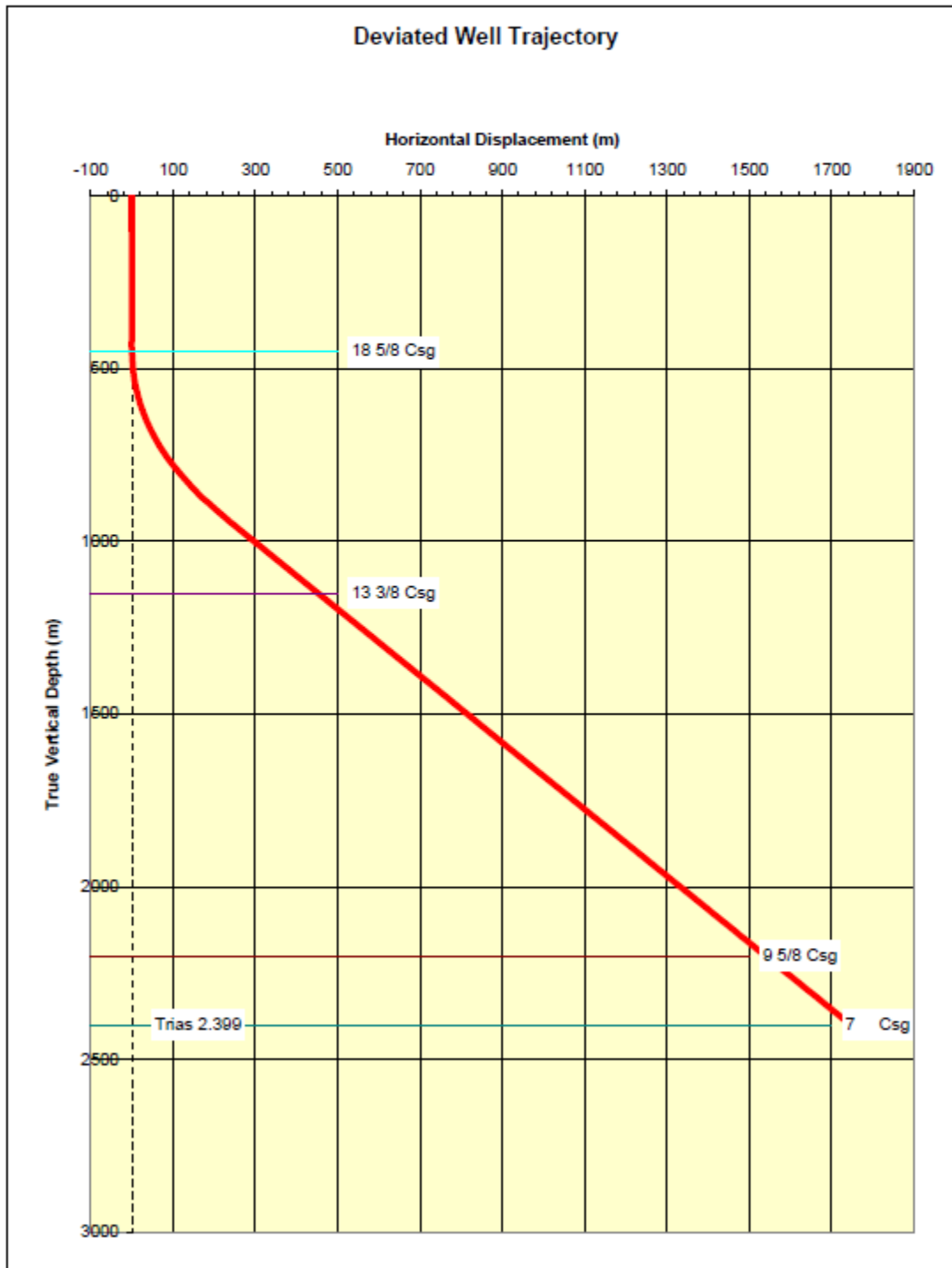


Figure 8-21 Deviation of the proposed producer. Provided by WEP.